The Phase Structure of Entanglement Measures and their Role in Holography and Quantum Gravity

Alexandre Belin

Doctor of Philosophy

Department of Physics - Faculty of Science

McGill University

Montréal

Québec, Canada

24th March 2015

A thesis submitted to McGill University in partial fulfillment of the requirements of the degree of Alexandre Belin

Abstract

AdS/CFT is today our best understanding of quantum gravity and its holographic nature. In the past decade, understanding the role of quantum entanglement in the emergence of a classical spacetime from a UV complete theory of quantum gravity has become a very important goal. Through the Ryu and Takayanagi formula relating complicated boundary quantum information measures to simple geometric objects in the bulk, we have refined the dictionary of the AdS/CFT correspondence and made several important steps towards deepening our understanding of the emergence of spacetime. The goal of this thesis is to study the importance of quantum information measures such as (charged) Rényi entropies in the AdS/CFT dictionary as well as understanding their phase structure and what it can teach us about entanglement.

Abrégé

La dualité AdS/CFT est aujourd'hui notre meilleur atout pour comprendre la gravité quantique et sa nature holographique. Depuis une dizaine d'années, l'importance de l'intrication dans l'émergence d'un espace-temps classique à partir d'une théorie de gravité quantique est devenue claire. Au travers de la formule proposée par Ryu et Takayanagi reliant une mesure compliquée d'intrication en théorie des champs à un objet géométrique simple dans la théorie gravitationelle, nous avons approfondi notre compréhension du dictionnaire d'AdS/CFT et avons franchi plusieurs étapes cruciales pour comprendre l'émergence de l'espace-temps. Le but de cette thèse est d'étudier l'importance de mesures d'information telles que les entropies (chargées) de Rényi dans le dictionnaire d'AdS/CFT ainsi que de comprendre leurs phases et ce qu'elles nous enseignent sur l'intrication.

To my beloved Sandra

Acknowledgments

I would like to sincerely thank my supervisor Alexander Maloney for his amazing guidance during the past three years, for the tolerance and patience for the numerous times where I stormed into his office screaming "I found the mistake, everything works now!" before he calmly explained to me that I had made yet another mistake, for his sincere help in making important decisions for my career in physics, and most of all, for sharing with me and teaching me his sharp perception and approach to physics. I would like to thank McGill University and the entire department of physics for the hospitality during my PhD thesis and for providing an exceptional work environment for scientific research. I would like to thank all the faculty members of the High Energy Group Robert Brandenberger, Jim Cline, Keshav Dasgupta, Johannes Walcher for great times spent discussing physics or other topics and for helping me during my PhD. I would especially like to thank Guy Moore for an extended amount of help on understanding various topics of physics and for accepting to answer my numerous questions with such great enthusiasm. I would like to thank the amazing postdoctoral fellows that I had the chance to interact with: Yifu Cai, Alejandra Castro, Josh Lapan, Shunji Matsuura, Ian Morrison and Jihye Seo. I would especially like to thank Alejandra Castro, Josh Lapan and Ian Morrison for taking so much time and effort into giving the graduate students in our group three high level and high quality graduate classes. I would also like to thank all the fellow graduate students with whom I overlapped and with whom I had interesting physics discussions, especially Arnaud Lepage-Jutier and Grant Salton. I would like to thank my collaborators on projects reported in this thesis: Ling-Yan Hung, Shunji Matsuura, Robert Myers and Todd Sierens. I would

also like to thank my collaborators on projects conducted during my PhD but not reported in this thesis: Shamik Banerjee, Simeon Hellerman, Christoph Keller, Arnaud Lepage-Jutier, Djordje Radicevic and Stephen Shenker. I would like to sincerely thank the David Stewart Memorial Fellowship foundation, the Schulich Graduate Fellowship foundation as well as the Swiss National Science Foundation for financial support during my PhD thesis. I would also like to thank Harvard University and the Center for the Fundamental Laws of Nature, where part of the research presented in this thesis was conducted, for their hospitality.

Preface

The work presented in this thesis is original work by my supervisor Alexander Maloney, my collaborators Ling-Yan Hung, Shunji Matsuura, Robert Myers, Todd Sierens and myself. Work presented in each paper was done equally by all authors. Chapters 1 and 5 were written explicitly for this thesis as an introduction to the goals of this research, a review of the literature relevant for the understanding of this thesis as well as a discussion of the results. Chapters 2, 3 and 4 are each composed of an article written by my collaborators and myself published in Journal of High Energy Physics. They are written as they appear in the journal and assembled here with the agreement both of the journal and of my collaborators.

Notation

This thesis will be using the mostly + convention for the metric, where for example the Minkowski metric is written as $\eta_{\mu\nu} = \text{diag}\,(-1, 1, 1, 1)$. Most of the text will also use natural units where $\hbar = c = 1$.

Contents

Chapter 1

Introduction

1.1 The puzzle of quantum gravity

Since the introduction of quantum mechanics in physics, understanding the fundamental interactions at the quantum level of all particles in our universe has been one of the most important goals of physics. For some time now, it has become clear that the Standard Model, a quantum field theory with matter and a $SU(3) \times SU(2) \times U(1)$ gauge group describes the electro-magnetic, strong and weak interactions admirably well at the quantum level [1]. The recent discovery of the Higgs boson at the LHC comforts our feeling of having a deep understanding of three of the four fundamental interactions in physics.

However, gravity remains a far more difficult beast to tame. As explained by Einstein almost a hundred years ago in his theory of General Relativity, gravity is geometry. The presence of matter deforms spacetime and this curved geometry *is* gravity. Indeed, Einstein's equations couple the stress tensor of matter $T_{\mu\nu}$ to the Einstein tensor $G_{\mu\nu}$, a tensor built from the Riemann tensor which encodes the curvature of spacetime:

$$G_{\mu\nu} = 8\pi G_N T_{\mu\nu} \,, \tag{1.1}$$

where G_N is Newton's constant. This theory generalizing Newton's law has been tested to extremely good accuracy and is used daily in a random person's life. Nowadays, rare are those who leave home without their smart phone and these electronic devices all have a built-

in GPS. But GPS technology could never work to such great accuracy without accounting for corrections coming from General Relativity.

It is perhaps shocking to admit that although we understand classical gravity very well, we know very little about the way it must be embedded in its quantum counterpart. If quantum mechanics is correct, which is believed by the vast majority of the community, one must be able to merge General Relativity and quantum mechanics. In fact quantum corrections are somehow *needed* in General Relativity. Simple solutions of Einstein's equations such as black holes or cosmologies admit curvature singularities, for instance the Schwarzschild metric

$$ds^2 = -\left(1 - \frac{2G_N M}{r}\right) dt^2 + \frac{dr^2}{1 - \frac{2G_N M}{r}} + r^2 d\Omega_2^2 \,, \tag{1.2}$$

has a curvature singularity at $r = 0$. But singularities are not physical, they merely indicate that the theory we are considering breaks down and some new theory comes into play. Typically, quantum gravity effects are expected to appear at length scales of order the Planck length

$$\ell_p = \sqrt{\hbar G_N / c^3} \sim 10^{-35} \text{ m} \,. \tag{1.3}$$

At this scale, we expect quantum gravity effects to become important and (hopefully) cure the singularity problem. Such scales are however hard to experiment in a lab as the energy scale one would need to achieve to probe such degrees of freedom is roughly the Planck mass $m_P \sim 10^{19}$ GeV, many orders of magnitude above the energy present in the LHC collisions.

But quantum field theory has been the object of so much study over the past decades, why not use the path integral formulation that works so well for the Standard Model and apply it to General Relativity? Indeed, Einstein's equations (1.1) can be derived by the variational method from the Einstein-Hilbert action:

$$S = \frac{1}{16\pi G_N} \int d^4x \sqrt{-g} R + S_{matter} \,. \tag{1.4}$$

Is it not possible to write the partition function as a path integral over the degrees of freedom of gravity, namely the metric $g_{\mu\nu}$? Indeed, one can formally write

$$Z = \int \mathcal{D}g \mathcal{D}\phi \exp \frac{i}{\hbar} S \,. \tag{1.5}$$

However, we do not know how to perform this path integral over metrics in full generality[1]. It would for one probably require dividing the integration over metrics in a sum over topologies, which are not classified in a general dimension. Furthermore, even a perturbative approach to quantum gravity fails: simple dimensional analysis shows that General Relativity is a non-renormalizable theory. These rather dramatic issues were quite discouraging for understanding quantum gravity, which remains today without doubt one of the greatest challenges of modern physics.

Nonetheless, the 1970s saw some great breakthroughs in the field. First in 1972, Bekenstein proposed that black holes should have entropy given by the area measured in Planck units [3, 4, 5]. This was confirmed by Hawking's calculation of the radiation emitted by a black hole: Hawking radiation [6, 7]. These results strongly suggested the relation between black holes and thermodynamics, where the black hole is seen as a finite temperature object whose entropy is given by the Bekenstein-Hawking formula:

$$S_{BH} = \frac{k_B c^3 A}{4\hbar G_N}\,, \tag{1.6}$$

This formula is without doubt one of the most remarkable equations in physics. First of all, it involves many different fields of physics: c is the ambassador of special relativity, $\hbar$ its quantum mechanics counterpart, k_B represents statistical mechanics and G_N of course involves gravity. More surprisingly, the entropy scales with the area of the black hole, not its volume. This was a quite dramatic result as any undergraduate in physics is taught that entropy is an extensive quantity that must scale with the volume of a system. This was the first clue that gravity is holographic and that somehow its degrees of freedom live not in the volume of a region but on the boundary that encloses it.

The Bekenstein-Hawking entropy should be counting microstates of the quantum gravity degrees of freedom of the black hole. The Bekenstein-Hawking entropy of Sagittarius A*, the supermassive black hole at the center of the Milky Way is

$$S_{Sag.A^*} \sim 2.69 \times 10^{67}\ [\mathrm{J/K}] \tag{1.7}$$

[1] In a particular simple setting, this has been studied in [2]

which is more than twenty orders of magnitude bigger than the thermodynamical entropy of the sun. Black holes should thus have an enormous degeneracy of quantum states. This is quite surprising as from a classical point of view, uniqueness theorems stipulate that a black hole is uniquely determined by its mass and charges. Finally, another puzzle coming from the merger of quantum mechanics and gravity was formulated by Hawking in the information loss paradox. A black hole formed from collapse of a pure state should evaporate in an essentially thermal state violating the unitarity of quantum mechanics.

String Theory has brought much insight in the previously stated puzzles of quantum gravity. First of all, string theory is a great candidate for a theory of quantum gravity as it is a quantum theory that contains, amongst other ingredients, gravity in its spectrum. Furthermore, singularities such as orbifold singularities can be resolved in String Theory and quantum stringy corrections to classically singular gravitational solutions were shown to play an important role in [8]. But perhaps the biggest breakthrough came from Strominger and Vafa's result on the matching of black hole entropy and a counting of BPS states [9]. This was the first understanding of the nature of black hole microstates and was in fact the first signs of a much deeper connection involving quantum gravity and holography, which will be the subject of the following section. We should however emphasize that the black hole information paradox and related questions are still the object of much debate today [10, 11, 12, 13, 14, 15]. A fully consistent merger of quantum mechanics and General Relativity consistent with a semi-classical limit remains to be found.

1.2 Holography and the AdS/CFT correspondence

Our best understanding today of quantum gravity is through the AdS/CFT correspondence, conjectured by Maldacena in 1997 [16]. Although unproven, this conjecture has passed a great number of non-trivial checks in the extensive literature that followed after Maldacena's original proposal, see for instance [17, 18]. Maldacena's original conjecture was that the partition function of $\mathcal{N} = 4$ SYM with $SU(N)$ gauge group, a superconformal field theory in 4 spacetime dimensions was dual - in the sense that it has an equivalent description - to

that of type IIB string theory on $AdS_5 \times S^5$:

$$Z_{\text{AdS}} = Z_{\text{CFT}} \,. \tag{1.8}$$

From the point of view of the conformal field theory, the partition function is viewed as the generating function for all correlators of the theory. This remarkable conjecture was the first precise proposal of the holographic nature of gravity: a theory of quantum gravity is dual to a standard quantum field theory (i.e. *without* gravity) in one *less* dimension: the field theory lives on the boundary of the space described by the gravitational theory.

Anti-de Sitter space is a negatively curved manifold satisfying Einstein's equation with a negative cosmological constant

$$G_{\mu\nu} + \Lambda g_{\mu\nu} = 0 \,, \tag{1.9}$$

with $\Lambda < 0$. The metric on global AdS_{d+1} is given by

$$\frac{ds^2}{\ell_{AdS}^2} = -\cosh^2\rho dt^2 + d\rho^2 + \sinh^2\rho d\Omega_{d-1}^2 \,. \tag{1.10}$$

with $\Lambda = -\frac{(d-1)(d-2)}{2\ell_{AdS}^2}$. Note that we will in fact consider the universal cover of AdS space where we have unwrapped the time cycle do avoid having closed timelike curves. AdS space is often represented as a solid cylinder and the conformal boundary $\mathbb{R} \times S^{d-1}$ can be viewed as the space on which the dual conformal field theory "lives", as drawn in Fig. 1.1.

Maldacena's conjecture comes in various forms but one often refers to the "weak" form of the conjecture where the field theory is taken to have N large and the 't Hooft coupling $\lambda = g_{YM}^2 N$ large so it is strongly coupled. This theory is dual to classical supergravity on $AdS_5 \times S^5$, a rather simple theory with which one can compute quite easily complicated objects from the point of view of the strongly coupled field theory. In fact, one often refers to AdS/CFT as a dictionary: an object on the boundary has an interpretation in the bulk and vice versa. For example, correlations functions of the boundary theory can be calculated by Witten diagrams involving bulk interactions, as shown in Fig. 1.2. Other examples include for instance Wilson lines in the CFT given by bulk minimal surfaces who end on the boundary Wilson lines.

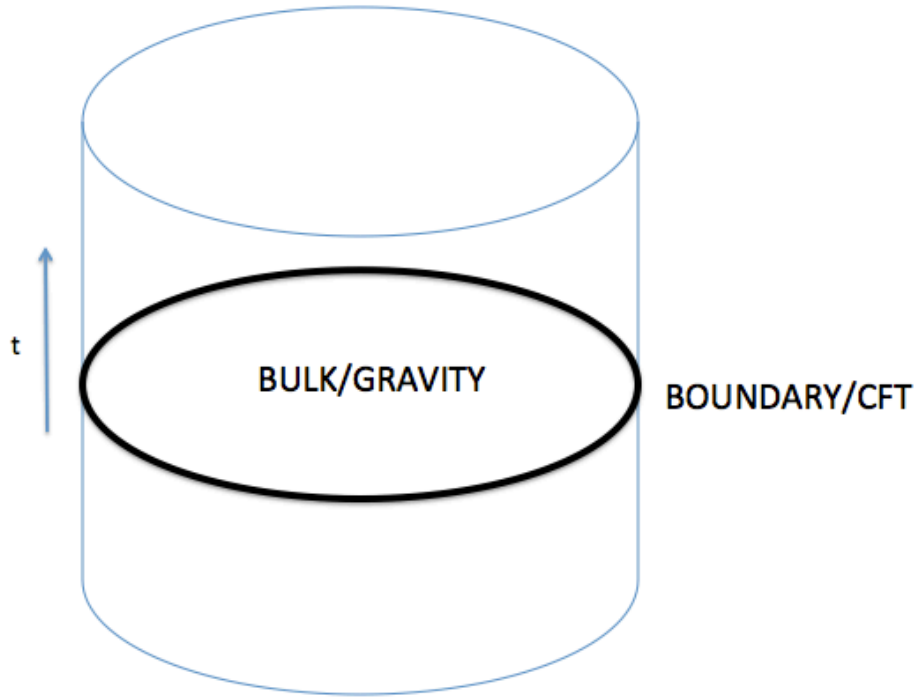

Figure 1.1: AdS_3 is represented as a solid cylinder with conformal boundary $S^1 \times \mathbb{R}_t$. The vertical direction is the time direction and the boundary cylinder is the space on which the CFT lives. The thick dark circle represents a fixed time slice of the boundary spacetime: a circle.

Naturally, black holes also play an important role in the AdS/CFT duality. At sufficiently high temperature, thermal states on the boundary are dual to AdS black holes. At low temperatures, the dominant geometry is thermal AdS and the Hawking-Page phase transition responsible for the switch of the dominant gravitational saddle also has a natural interpretation in the boundary theory: it is related to the confinement/deconfinement phase transition [19]. In this holographic setting, it is natural that the black hole entropy be proportional to the area as it is given by a thermal entropy of a local quantum field theory in one less dimension. For instance, modular invariance and the Cardy formula [20] for two-dimensional CFTs naturally reproduce the entropy of the BTZ black hole [21].

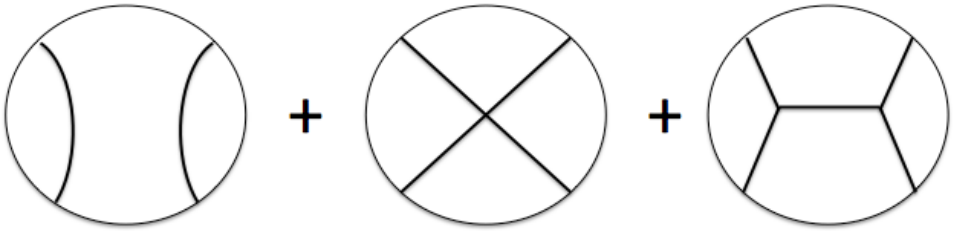

Figure 1.2: The 4 point function of a CFT is calculated by a sum over Bulk Feynman diagrams. The diagrams that appear in the bulk depend on the interactions of the gravity theory.

The AdS/CFT conjecture was originally introduced in a very stringy context starting from a stack of N D3-branes in flat space. It was generalized to many other brane constructions such as for example a stack of D-branes at the tip of the conifold in [22] or to the AdS_4/CFT_3 version of the duality relating ABJM theory and M2-branes [23]. It is however widely believed to be based on deeper principles and to extend in more general settings. For example, a version of the holographic duality exists for higher spin theories of gravity, known as Vasiliev theories [24], both in AdS_3/CFT_2 [25, 26] and in AdS_4/CFT_3 [27, 28, 29, 30].

AdS/CFT has played an important role in understanding quantum gravity but has an incredibly wide range of applications, going from QCD and heavy ion collisions (see for instance [31]) to condensed matter [32, 33], passing through quantum information [34] and many more. The focus of the next section will be to explore the importance of quantum entanglement in the AdS/CFT correspondence, which also has ties to a wide range of fields, including naturally quantum information but perhaps more surprisingly condensed matter physics [35, 36, 37] and quantum gravity [38, 39, 40, 41, 42].

1.3 Holographic Entanglement Entropy and the Ryu and Takayanagi Formula

1.3.1 Entanglement Entropy in quantum mechanics and quantum field theory

Entanglement is an astonishing property of quantum mechanical systems that is completely absent classically. It teaches us the extent to which a state (or density) cannot be written as a direct product of states (or densities) living in sub-Hilbert spaces. Consider the Hilbert space of a quantum mechanical system $\mathcal{H}$ and consider a state $|\psi\rangle$ living in that Hilbert space. We consider an arbitrary splitting of the Hilbert space as

$$\mathcal{H} = \mathcal{H}_A \otimes \mathcal{H}_B \tag{1.11}$$

and entangling describes the failure of the state of being a direct product, such that if the state $|\psi\rangle$ is entangled

$$|\psi\rangle \neq |\psi_A\rangle \otimes |\psi_B\rangle \qquad\qquad |\psi_A\rangle \in \mathcal{H}_A, \quad |\psi_B\rangle \in \mathcal{H}_B \,. \tag{1.12}$$

One can consider different measures of entanglement and a standard example is the entanglement entropy. One first computes the reduced density matrix from the density matrix ρ describing our state, by tracing over the Hilbert space $\mathcal{H}_B$

$$\rho_A = \mathrm{tr}_{\mathcal{H}_B} \rho \,. \tag{1.13}$$

The entanglement entropy is then given by the Von Neumann entropy of the reduced density matrix

$$S_A = -\mathrm{tr} \rho_A \log \rho_A \,. \tag{1.14}$$

For a pure state $S_A = S_B$. A standard example is the system of two qubits in an EPR pair

$$|\psi\rangle = \frac{1}{\sqrt{2}} \left(|\uparrow_A\rangle \otimes |\uparrow_B\rangle + |\downarrow_A\rangle \otimes |\downarrow_B\rangle \right) . \tag{1.15}$$

The reduced density matrix is the maximally mixed state $\rho_A = \text{diag}\left(\frac{1}{2}, \frac{1}{2}\right)$ which gives

$$S_A = \log 2\,, \tag{1.16}$$

namely there is one bit of information in the entanglement between the A and B spins. Note that there is some clear correlation between the outcome of measures on A and B: if A is measured being $|\uparrow\rangle$, then so is B. However, correlation is not enough to determine wether the state is entangled or not, some correlations are just classical and are not related to quantum entanglement. This can occur for example in mixed states. Entanglement entropy may also not be a good measure of entanglement for mixed states as is clearly illustrated in the following example: consider the state

$$\rho = \text{diag}(1/2, 1/2)_A \otimes \text{diag}(1, 0)_B\,, \tag{1.17}$$

which is clearly a direct product state. The entanglement entropy S_A gives again $\log 2$, which is the same answer as the one obtained for the EPR pair. For a general density matrix, there is no clear way to quantify entanglement, although measures such as distillable entanglement - a measure of the number of EPR pairs that can be extracted from a state - try to quantify this more precisely. Nevertheless, we will be mostly interested in entanglement of pure states in which case entanglement entropy is a good measure of separability.

Of course, we have so far only considered entanglement entropy in quantum mechanics with finite dimensional Hilbert spaces. We are really interested in understanding entanglement entropy in quantum field theory (or CFTs) which is a much more complicated task, as they have an infinite number of freedom per unit volume. Some early attempts, also relating this work to black hole entropy and the information loss paradox, go back to the 1990s by Wilczek et. al [43, 44] and Kabat and Strassler [45]. In principle, there is no issue in computing the reduced density matrix and entanglement entropy in a quantum field theory using the path integral formalism. We will consider the vacuum state to simplify the following steps but excited states can be considered by a different contour of integration in the path integral. One might worry that the vacuum state is too simple and doesn't contain much information. Indeed, this is true in *momentum* space where for free theories, the Fock

vacuum is a direct product state and is not entangled. However, there is a lot of information contained in *position* space entanglement, even in low energy states such as the vacuum.

The entanglement entropy we consider is then spatial entanglement entropy, quantifying entanglement between the Hilbert spaces associated with two spatial regions. This is done by fixing a time slice (for example $t = 0$) and separating the spatial slices into two regions A and B. We can consider for example splitting space in half as showed in Fig. 1.3.

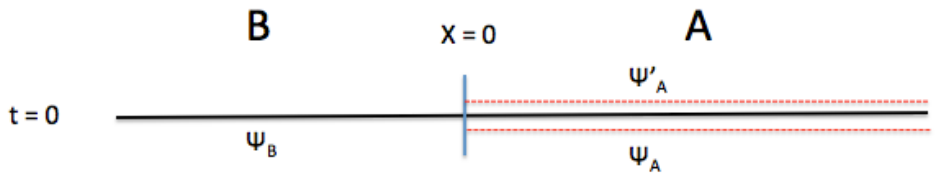

Figure 1.3: Space is separated into two regions A ($x > 0$) and B ($x < 0$). The boundary conditions in the path integral fix ψ_A and ψ'_A which compute a particular matrix element of the reduced density matrix. ψ_B however is not fixed and is integrated over.

A natural basis to chose for the degrees of freedom in region A are $\psi_A(x)$, the field configurations in region A. One can then write a matrix element of the reduced density matrix by path integrating over the fields with boundary conditions in region A and appropriate fall off of the fields at $t \to \pm\infty$:

$$\langle \psi_A | \rho | \psi'_A \rangle = \frac{1}{Z} \int_{\substack{\psi(t=0_-, x>0)=\psi_A \\ \psi(t=0_+, x>0)=\psi'_A}} \mathcal{D}\psi \; e^{-S_E} \, . \tag{1.18}$$

One then computes entanglement entropy with equation (1.14). Although one can write down formal expressions, actual computations are extremely difficult for several reasons. First of all, the entanglement entropy in a QFT has a UV divergence coming from high entanglement of modes close to the entangling surface separating A and B. One must introduce a UV cutoff to regularize the entanglement entropy, or consider special combinations of entanglement entropy (such as for example mutual information or other quantum information measures)

that are built in a UV-finite way. For the rest of this thesis, we will not worry about the UV divergence and take it to be regularized by a UV cutoff. However, even when regularized actually computing entanglement entropy is a difficult task and can rarely be done analytically. Simple examples such as free field theories enable more explicit calculations but in general, a direct computation is almost impossible.

The trick often used to compute entanglement entropies is called the replica trick. It involves calculating the Rényi entropies defined as

$$S_n = \frac{1}{1-n} \log \mathrm{tr} \rho_A^n \tag{1.19}$$

for integer n. It is important to note that the Rényi entropies are the eigenvalue moments of the reduced density matrix and thus form the most complete basis independent description of the reduced density matrix. They encode far more information than that obtained just from the entanglement entropy and are of great interest outside of their use in the replica trick. The replica trick consists in calculating the Rényi entropies for integer n, which reduces to a calculation of the partition function of the original theory on a multisheeted cover of the initial geometry, see Fig 1.4. This can also be viewed as inserting twist operators at the entangling surface to "jump" to the next sheet. Then, by assuming analyticity of the Rényi entropies in n, one continues n to real values and takes the limit

$$S_A = \lim_{n \to 1} S_n \,, \tag{1.20}$$

and recovers the entanglement entropy [47, 48, 46]. Although quite difficult as well, this is in general easier than a direct computation of the entanglement entropy.

One important point that will be of crucial importance for this thesis is the analyticity assumption used in the replica trick. Carlson's theorem states that there is a unique continuation to real values provided the function satisfies some exponential boundedness for large $n \in \mathbb{R}$ and grows slowly enough as $n \to 1 \pm i\infty$. For finite dimensional systems, the Rényi entropies are analytic but they are ill-defined without a UV cutoff ϵ in quantum field theories. Wether the limits $\epsilon \to 0$ and $n \to 1$ commute is still the object of some debate and this question will be investigated in more details in Chapter 2.

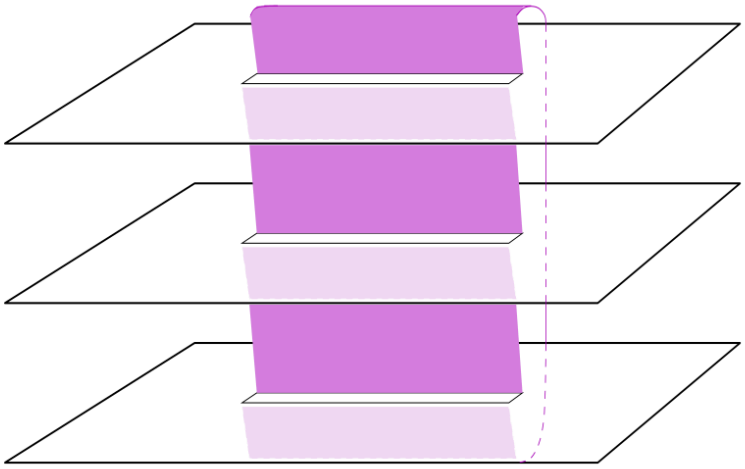

Figure 1.4: A plot of the appropriate manifold for computing S_3 in a 2d field theory [46]. The region connected by the purple stripes is region A. The twist operators are inserted at the entangling surface, where a conical singularity lives. Everytime we go around the entangling surface, we move up a sheet.

Although the replica trick and potential direct calculations of entanglement entropy exist, they are quite complicated as argued above. A remarkable breakthrough in the field came in 2006 when Ryu and Takayanagi proposed a simple way to calculate entanglement entropy holographically by the means of a geometrical object: a minimal surface [49]. This directly connects quantum information on the boundary to geometry in the bulk. We now turn to the Ryu and Takayanagi formula and explain its importance in AdS/CFT.

1.3.2 Holographic Entanglement Entropy and the RT formula

In 2006, Ryu and Takayanagi proposed a simple formula to calculate entanglement entropy in AdS/CFT. The entanglement entropy of a subregion of the boundary CFT A is given by a minimal surface extending in the bulk

$$S_A = \min_{\gamma \sim A} \frac{A_\gamma}{4G_N} \,. \tag{1.21}$$

The minimalization procedure is over all bulk surfaces that are homologous to A and end on ∂A. This is represented in Fig. 1.5.

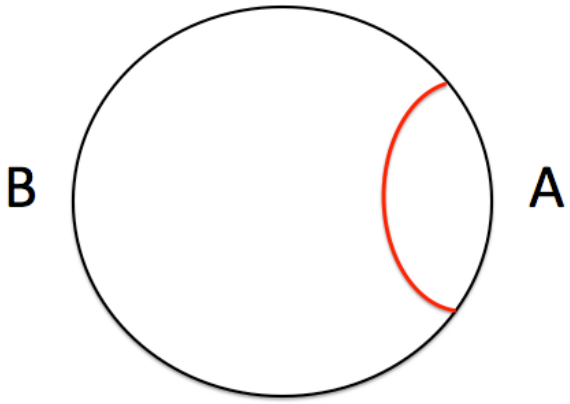

Figure 1.5: A fixed time slice of the AdS_3 geometry. The boundary spatial circle is separated into two regions A and B. The red line is the Ryu and Takayanagi minimal surface (in this case a geodesic) extending into the bulk. Its length measures the entanglement in the CFT between regions A and B.

This exciting proposal reproduced the well known universal result of a 2D CFT [44, 47, 46]

$$S_A = \frac{c}{3} \log \left(\frac{L}{\pi \epsilon} \sin \left(\frac{\pi l}{L} \right) \right) , \tag{1.22}$$

where c is the central charge, L the total size of the boundary circle and l the size of region A. Perhaps just as amazingly, this formula resembled the Bekenstein Hawking formula for black hole entropy. One can view the minimal surface as a type of horizon, a holographic screen for an observer that only has access to region A on the boundary. Entanglement entropy also plays an important role in quantum corrections to the semi-classical area law for black hole entropy [45, 50, 51] and some proposals even try to completely characterize black hole entropy as entanglement entropy [52, 53]. If one considers the thermofield double state - a maximally entangled state between two non-interacting CFTs - dual to the eternal AdS black hole [54], the entanglement entropy between the two conformal field theories is again given by the RT formula, which matches with the black hole entropy which is quite remarkable.

The RT formula can also be used to compute entanglement entropy of subsystems of thermal states in which case the homology constraint becomes important[2]. There must be a smooth manifold that interpolates between the RT surface and the boundary region A such that the entanglement entropies S_A and S_B are not equal in the case of a black hole as can be seen in Fig. 1.6. Indeed, a black hole is dual to a thermal state so they need not agree.

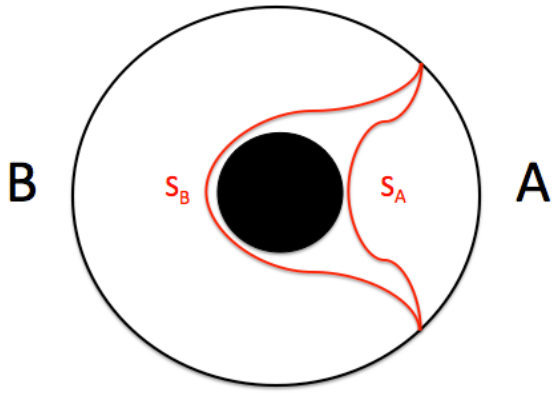

Figure 1.6: A fixed time slice of the BTZ black hole geometry. The boundary spatial circle is separated into two regions A and B. The red lines show the Ryu and Takayanagi minimal surfaces homologous to A and B. In this case they are different.

Many generalizations of the RT formula have been proposed since. The area of the RT surface gives the leading large N contribution to entanglement entropy and quantum $1/N$ corrections were proposed to be given by bulk entanglement entropy through the RT surface [56] (see also [57]). Stringy α' corrections corresponding to higher derivative corrections were also considered in [58]. But the RT proposal has also fuelled a much broader program of relating the emergence of spacetime to entanglement. It has played a central role in understanding how a classical geometry emerges from the dual boundary theory and fine tuning our understanding of the UV/IR relation of AdS/CFT [38, 39, 59, 42, 60, 61, 62, 63]. Perhaps the most interesting discovery in this context is the fact that the linearized Einstein equations in the bulk can be determined through properties of the entanglement entropy in

[2]Recent developments on the homology constraint have been made in [55].

the boundary theory [64, 65]. While it is not a complete proof, it is a solid first step in understanding the emergence of spacetime from quantum entanglement.

Although the Ryu and Takayanagi formula is not proven in full generality, it has been proven when the replica trick is valid in [66] and for spherical entangling surfaces in [67]. In fact, the framework proposed by Casini, Huerta and Myers extends past the Ryu and Takayanagi formula and plays an essential role in this thesis so the goal of the following section is to summarize the results of [67].

1.4 Holographic Entanglement Entropy for Spherical Regions

We will be interested in computing the entanglement entropy of the vacuum state of a CFT_d. We will separate the $t = 0$ spatial slice into two regions, the inside and outside of a S^{d-2} of radius L as shown in Fig 1.7.

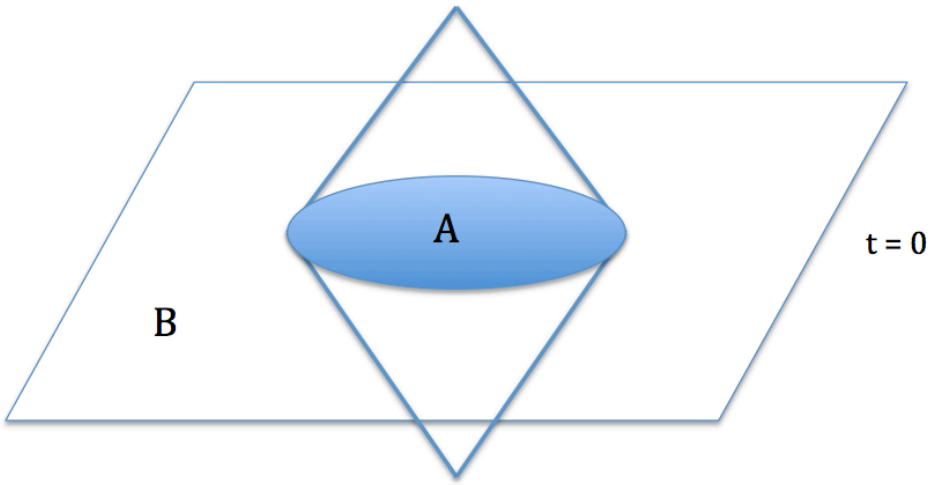

Figure 1.7: The $t = 0$ slice of the boundary region is separated into the inside of a sphere of radius L (region A) and the outside (region B). The cone represents the causal development of region A, the set of all points in causal contact only with region A at $t = 0$.

Let us call region A the inside of the sphere and consider the causal development of that region, namely the set of spacetime points that are only causally connected to region A at $t = 0$. Casini, Huerta and Myers showed that one can perform a conformal transformation to map this region to $\mathbb{H}_{d-1} \times \mathbb{R}_t$. Let us start with the metric on $\mathbb{R}^{d-1,1}$

$$ds^2 = -dt^2 + dr^2 + r^2 d\Omega_{d-2}^2 \,, \tag{1.23}$$

We do the following coordinate transformation

$$t = L\frac{\sinh(\tau/L)}{\cosh u + \cosh(\tau/L)}, \qquad r = L\frac{\sinh u}{\cosh u + \cosh(\tau/L)} \,. \tag{1.24}$$

The metric becomes

$$ds^2 = \Omega^2[-d\tau^2 + L^2(du^2 + \sinh^2 u d\Omega_{d-2}^2)] \tag{1.25}$$

with $\Omega = (\cosh u + \cosh(\tau/L))^{-1}$ One can then remove the factor of Ω^2 by a conformal transformation and we are left with the metric on hyperbolic space times time. Casini, Huerta and Myers showed that one obtains a thermal state on hyperbolic space with temperature $T = 1/2\pi L$, which can be seen by the fact that the τ coordinate is periodic in imaginary time in (1.25). The reduced density matrix ρ_A is positive semi-definite and hermitian so it can always be written as

$$\rho_A = e^{-2\pi L H_E} \tag{1.26}$$

where H_E is called the entanglement or modular hamiltonian. For generic states and/or entangling surfaces, H_E is in principle a complicated and non-local operator but Casini, Huerta and Myers showed that for the case of the vacuum state and spherical entangling surfaces, the symmetries at hand make H_E a local operator with a geometric interpretation: it is the generator of time translations (the standard hamiltonian) on hyperbolic space. As we perform the conformal transformation, the reduced density matrix does get conjugated by a unitary operator implementing the conformal transformation but these cancel out upon taking the trace for calculating entanglement entropy. The conformal transformation has thus mapped the problem of calculating entanglement entropy to that of calculating thermal entropy on hyperbolic space.

So far, these considerations only concern the boundary/CFT side of the story but assuming that the CFT is holographic and has a classical gravity dual, one can go further and prove the Ryu and Takayanagi formula. The thermal state on hyperbolic space should be dual to a black hole in the bulk and one can indeed find a black hole with the right temperature and boundary metric: the massless hyperbolic black hole with metric

$$ds^2 = -f(r)d\tau^2 + \frac{dr^2}{f(r)} + r^2 dH^2_{d-1}\,, \tag{1.27}$$

where

$$f(r) = \frac{r^2}{L^2} - 1\,. \tag{1.28}$$

Note that this "black hole" is in fact simply AdS in Rindler coordinates and that L here is the AdS radius. The thermal entropy on the boundary is calculated by the area of the black hole which was shown to agree with the Ryu and Takayanagi proposal: the minimal surface is mapped to the Rindler horizon of AdS. Notice that the area of the hyperbolic black hole is IR divergent coming from the infinite volume of hyperbolic space, which translates into the UV divergence of entanglement entropy [67].

This exciting result can in fact be pushed even further to include calculations of all Rényi entropies as was done in [68]. The observation is basically that Rényi entropies involve calculating $\mathrm{tr}\rho_A^n$. But $\rho_A^n = e^{-2\pi L n H_E}$ looks in fact like the density matrix of a CFT on hyperbolic space at temperature $1/2\pi Ln$. By using simple thermodynamical properties one can rewrite the Rényi entropies as

$$S_n = \frac{n}{n-1}\frac{1}{T_0}\int_{T_0/n}^{T_0} S_{\mathrm{therm}}(T)dT\,. \tag{1.29}$$

Note that here n can in fact be any real number, this is due to the fact that the high symmetries of the entangling surface promote the usual $\mathbb{Z}_n$ symmetry of the replica space to a U(1) symmetry. Hung et. al showed that one can also calculate these entropies in the bulk by areas of hyperbolic black holes. One needs to find bulk solutions that have hyperbolic horizon but temperature $1/2\pi Ln$, generalizing the metric (1.27) to any temperature. These solutions exist and are called massive hyperbolic black holes with metric (1.27) and blackening factor

replaced by

$$f(r) = \frac{r^2}{L^2} - 1 - \frac{m}{r^{d-2}} \,. \tag{1.30}$$

One can then calculate all Rényi entropies and get a deeper understanding of the spectrum of the reduced density matrix [68] as well as properties of the generalized twist operators located at the entangling surface [69]. The general framework described in this section will be the starting point of this thesis, where we will inquire about analytic properties of S_n and also generalize it to understand the dependence of entanglement on charge distribution, as explained in the following section.

Analyticity properties of Rényi entropies

The analytic properties of S_n as a function of the Rényi parameter n are still an obscure subject in the context of CFTs and holography and it would be of great interest to find a framework where we can test the analyticity explicitly. In some cases, Rényi entropies were shown to have interesting phase structures including possible phase transitions [70, 71]. Finding a similar example in a holographic context would be of great interest and would address potential issues in the use of the replica trick and the validity of Carlson's theorem. The subject of Chap. 2 will be to explore the phase structure of Rényi entropies in a holographic setting and we will indeed find that they can be non analytic in n. This will occur if the CFT has a sufficiently low dimensional operator, which is the case for $\mathcal{N} = 4$ SYM or other canonical examples of AdS/CFT. The mechanism behind this phase transition is the instability of hyperbolic black holes at low temperature in the presence of a light scalar field. The phase transition as a function of temperature relates to a non-analyticity of S_n as a function of n. We explore the phase structure of Rényi entropies in this context and its importance in holography.

Chapter 2

Holograhpic Phases of Rényi Entropies

Alexandre Belin, Alexander Maloney and Shunji Matsuura

Departments of Physics and Mathematics, McGill University, Montréal, Québec, Canada

Abstract

We consider Rényi entropies $S_n = \frac{1}{1-n} \log \mathrm{Tr}\, \rho^n$ of conformal field theories in flat space, with the entangling surface being a sphere. The AdS/CFT correspondence relates this Rényi entropy to that of a black hole with hyperbolic horizon; as the Rényi parameter n increases the temperature of the black hole decreases. If the CFT possesses a sufficiently low dimension scalar operator the black hole will be unstable to the development of hair. Thus, as n is varied, the Rényi entropies will exhibit a phase transition at a critical value of n. The location of the phase transition, along with the spectrum of the reduced density matrix ρ, depends on the dimension of the lowest dimension non-trivial scalar operator in the theory.

Published in Journal of High Energy Physics **1312**, 050 (2013)

2.1 Introduction

Entanglement entropies characterize the degree of entanglement present in a given quantum state, and in doing so probe interesting features of strongly coupled quantum systems. In conformal field theories, certain entanglement entropies are related to conformal anomaly coefficients (see [47, 46] for a review) and play an important role in conjectured holographic duals of conformal field theories [49, 72, 73]. In the condensed matter literature they have, for example, been used to characterize topological order [37, 35] and fractional quantum Hall edge states [36]. The goal of the present paper is to understand the extent to which entanglement entropies encode other interesting features of conformal field theories.

To define an entanglement entropy one starts by considering a quantum system which can be divided into two subsystems, A and B, with associated Hilbert spaces $\mathcal{H}_A$ and $\mathcal{H}_B$. The state of the system is given by a density operator ρ_{AB} acting on the tensor product Hilbert space $\mathcal{H}_A \otimes \mathcal{H}_B$. The degree of entanglement between A and B is characterized by the reduced density matrix $\rho = \mathrm{Tr}_{\mathcal{H}_B}\, \rho_{AB}$. We are interested in basis independent quantities, so will consider the moments of the eigenvalue distribution of ρ:

$$S_n = \frac{1}{1-n} \log \mathrm{Tr}[\rho^n]. \tag{2.1}$$

These are the Rényi entropies, and n is the Rényi parameter. In the limit $n \to 1$, S_n becomes the entanglement (von Neumann) entropy $S_{EE} = -\,\mathrm{Tr}\, \rho \log \rho$. These Rényi entropies have been considered in a variety of contexts [74, 75, 76, 77, 71, 78, 79, 80, 66, 81].

The computation of the reduced density matrix ρ, and of the entanglement entropy S_{EE}, for an interacting quantum system is in general difficult. We will consider the case of a d-dimensional CFT in flat space, with A and B separated by a sphere. In this case conformal invariance relates the Rényi entropy S_n of the ground state to the thermodynamic entropy of the CFT on hyperbolic space $\mathbb{H}_{d-1}$ at temperature $T = T_0/n$ (as described in [67, 68, 82]). Here T_0 is a temperature related to the length scale of the hyperbolic space. The computation of this thermodynamic entropy is still in general quite difficult. We will therefore focus on CFTs with gravity duals, where the AdS/CFT correspondence relates this

thermodynamic entropy to the entropy of a black hole in $d+1$ dimensional AdS space with hyperbolic horizon. This allows us to compute Rényi entropies explicitly.

Solutions of Einstein gravity in AdS describing black holes with hyperbolic horizon are easy to construct; they are hyperbolic versions of the Schwarzchild solution with a cosmological constant. However, black holes of this type are sometimes unstable [83]. As the Hawking temperature $T \to 0$ (i.e. Rényi parameter $n \to \infty$) they typically become more unstable. Such an instability would lead to a non-analyticity in the Rényi entropies, regarded as a function of n. We find that this instability will occur for CFTs with a sufficiently low dimension scalar operator. The reason is that a low dimension operator corresponds to a light scalar field in AdS. If the field is too light, then at a finite, critical value of n the scalar field will condense in the vicinity of the horizon. The dominant solution is now a "hairy" black hole, with non-trivial scalar profile.[1]

One advantage of this result is that it provides a clear dictionary relating properties of the Rényi entropies (i.e. the eigenvalue distribution of the reduced density matrix) and natural CFT quantities. For example, we will see that for a four dimensional CFT with a single scalar operator of dimension $\Delta < 3$ the second derivative of S_n with respect to n will be discontinuous at a value of n which depends on Δ. We expect similar results for large N CFTs with more complicated spectra of light operators. It is interesting to note that a similar result was found in the $O(N)$ model using a direct field theory analysis [70] (see also [71]). In this case the Rényi entropy was found to be non-analytic at $n = 7/4$. Presumably our results are the bulk gravity version of this phase transition.[2]

Many approaches to entanglement entropy in quantum field theory – such as the replica method – implicitly assume that the Rényi entropies are analytic in n. We find that, for large N field theories with a small gap, this assumption is not necessarily valid. Thus the

[1] Similar phase transitions occur in applications of AdS/CFT to condensed matter physics, most famously in the holographic superconductor [84, 85, 86].

[2] One subtlety is that the $O(N)$ model is apparently dual not to general relativity with a light scalar, but to a higher spin theory of gravity [27]. We expect that the transition at $n = 7/4$ is related to an instability of a hyperbolic black hole in Vasiliev theory, but without a better understanding of the Vasiliev equations of motion it is difficult to make a precise statement .

replica trick must be applied with care. We note, however, that our phase transitions always occur at values of n which are strictly larger than 1. Thus the Rényi entropy is analytic in a neighbourhood of $n = 1$, at which point it equals the entanglement entropy. We do not see any indication of non-analyticity near $n = 1$, except in rather exotic circumstances which we will comment on in section 4.

Our paper is organized as follows. In section 2.2, we review Rényi quantities and their computations in quantum field theory. In section 2.3, we review the holographic computation of the Rényi entropy [68]. We analyze the near horizon limit of the extremal black hole, which allows us to determine which black holes should be unstable in the $T \to 0$ limit. This allows us to determine which conformal field theories will have Rényi phase transitions.

In the last two sections we will present numerical results which verify the existence of this phase transition. In section 2.4 we begin with a simplified model (following closely work of [83]) in which the scalar mode which is constant on the hyperboloid condenses. This is a particularly tractable case, as it preserves the hyperbolic symmetries. This allows us to explicitly find the hairy black hole solution, which is used to compute Rényi entropies and the spectrum of ρ. However, the constant mode presented in this section is non-normalizable. We therefore continue in section 2.5 to discuss normalizable modes. Again, we demonstrate that the hyperbolic black holes of Einstein gravity are unstable, so that the Rényi entropies will exhibit a phase transition. The numerics are somewhat more difficult, as the modes no longer preserve the hyperbolic symmetry. We therefore present a linearized analysis – which is sufficient to demonstrate that a phase transition will occur – but leave the investigation of the hairy black hole for future work.

2.2 Rényi entropy in Conformal Field Theory

In the following, we review the computation of Rényi entropies for a relativistic (Lorentz invariant) quantum field theory. Consider a field ψ in d dimensional flat space. The Euclidean signature metric is

$$ds^2 = dt^2 + dx^2 + d\vec{y}_\perp^2 \tag{2.2}$$

with $\vec{y} = (y_{1,\perp}, \cdots, y_{d-2,\perp})$. Before considering the slightly more complicated problem of A and B being separated by a sphere, we will warm up by computing the entanglement entropy between the region $x > 0$ (subsystem A) and the region $x < 0$ (subsystem B). The entangling surface is the plane $x = 0$. We will take the system to be in its ground state.

A convenient basis for $\mathcal{H}_A$ are the states $|\psi_A\rangle$, where $\psi_A = \psi_A(x)$ is a function on A. The matrix elements of the reduced density matrix ρ_A are given by the Euclidean signature functional integral:

$$\langle\psi_A|\rho|\psi'_A\rangle = \frac{1}{Z}\int_{\substack{\psi(t=0_-,x>0)=\psi_A \\ \psi(t=0_+,x>0)=\psi'_A}} \mathcal{D}\psi\ e^{-S_E} \tag{2.3}$$

where Z is a normalization factor. The boundary conditions set ψ to equal ψ_A (ψ'_A) on either side of the cut at $t = 0, x > 0$. ψ is required to fall off as $t \to \pm\infty$; this puts the system in its ground state.

We can also study the system in polar coordinates

$$ds^2 = z^2 d\theta^2 + dz^2 + d\vec{y}_\perp^2, \tag{2.4}$$

where θ has periodicity 2π. The boundary conditions in the path integral (2.3) are enforced on either side of the ray $\theta = 0$. Thus we can interpret ρ_A as an operator which rotates by an angle 2π in the θ direction [45]

$$\rho = \frac{1}{Z}e^{-2\pi H_E} \tag{2.5}$$

where $H_E = i\frac{\partial}{\partial\theta}$ is the Euclidean rotation operator. If H_E is regarded as a physical Hamiltonian (an "entanglement Hamiltonian") this is precisely a thermal density matrix at temperature $T = 1/2\pi$; the normalization factor Z is the usual finite temperature partition function $\mathrm{Tr}\, e^{-2\pi H_E}$. In Lorentzian signature H_E becomes the Rindler Hamiltonian which generates Lorentz boosts in the (x, t) plane, and the origin $z = 0$ is the Rindler horizon associated to an accelerating observer.

Let us now specialize to conformal field theories. This implies that, under a conformal rescaling of the metric, ρ_A will change by conjugation a unitary operator; this is a trivial change of basis which we will suppress. We can conformally rescale the metric (2.4) by a

factor of z^2/L^2 to obtain

$$ds^2_{scaled} = d\tilde{\theta}^2 + L^2 \frac{dz^2 + d\vec{y}_\perp^2}{z^2} \tag{2.6}$$

where $\tilde{\theta} = L\theta$ is periodic with period $2\pi L$. This metric is a product of a circle times hyperbolic space $\mathbb{H}_{d-1}$; the size of the circle, and the size of the hyperbolic space, are set by the parameter L. The reduced density matrix is

$$\rho_A = \frac{e^{-\tilde{H}_E/T_0}}{Z(T_0)} \tag{2.7}$$

where $T_0 = \frac{1}{2\pi L}$ and $\tilde{H}_E = i\frac{\partial}{\partial\tilde{\theta}}$ generates translations in the $\tilde{\theta}$ direction. We note that $\tilde{H}_E$ is the Hamiltonian describing time evolution for a CFT on $\mathbb{H}_{d-1} \times \mathbb{R}_t$. $Z(T_0) = \mathrm{Tr}[e^{-\tilde{H}_E/T_0}]$ is the finite temperature partition of the theory in hyperbolic space. Note that the conformal transformation has mapped the entangling surface to the boundary of hyperbolic space.

Once we consider a conformal field theory many other mappings are possible. For example, the reduced density matrix for a CFT on a sphere, with entangling surface at the equator, can also be put in the form (2.7). So can the CFT on a flat space with entangling surface equal to a sphere. These are all related by conformal transformations (as described in e.g. [67]). More generally, any time the entangling surface is the locus of fixed points of some conformal transformation, one can interpret the entanglement Hamiltonian as the generator of that conformal transformation (in the same way that the point $z = 0$ above is the fixed point of the rotation $\frac{\partial}{\partial\theta}$). A conformal rescaling then turns this into the Hamiltonian on hyperbolic space.

In the following sections, we will consider the entangling surface to be a sphere of radius L, following [67, 68]. We take the flat space-time metric to be

$$ds^2 = -dt^2 + dr^2 + r^2 d\Omega^2_{d-2}\,, \tag{2.8}$$

with region A being the inside of the sphere $r = L$. We now map the causal development of A to hyperbolic space times time by the following coordinate transformation:

$$t = L\frac{\sinh(\tau/L)}{\cosh u + \cosh(\tau/L)}, \qquad r = L\frac{\sinh u}{\cosh u + \cosh(\tau/L)}\,. \tag{2.9}$$

The metric becomes

$$ds^2 = \Omega^2[-d\tau^2 + L^2(du^2 + \sinh^2 u d\Omega_{d-2}^2)] \tag{2.10}$$

with $\Omega = (\cosh u + \cosh(\tau/L))^{-1}$. This is conformally equivalent to hyperbolic space times time, i.e. to the metric (2.6). The temperature as well as the curvature of hyperbolic space are fixed by the radius of the sphere L. Conformal transformations act as unitary operators on the Hilbert space of the theory. Thus the reduced density matrix is simply given by (2.7), except conjugated by some Unitary operator U:

$$\rho_A = U\frac{e^{-\tilde{H_E}/T_0}}{Z(T_0)}U^{-1}. \tag{2.11}$$

We can now use the equivalence between the reduced density matrix and the thermal density matrix on the hyperbolic space to relate the entanglement entropy and Rényi entropy to the thermal entropy in hyperbolic space. The entanglement entropy S_{EE} and the Rényi entropy S_n are defined as

$$S_{EE} = -\mathrm{Tr}_A \rho \log \rho, \tag{2.12}$$

and

$$S_n = \frac{1}{1-n}\log \mathrm{Tr}[\rho^n]. \tag{2.13}$$

We call n the Rényi parameter. If S_n is analytic near $n = 1$, then $S_{EE} = \lim_{n\to 1} S_n$. The trace of the n-th power of ρ is then given by thermal partition function on a hyperbolic space with radius L at temperature $T = 1/2\pi Ln$:

$$\mathrm{Tr}[\rho^n] = \frac{\mathrm{Tr}[e^{-nH_E/T_0}]}{Z(T_0)^n} = \frac{Z(T_0/n)}{Z(T_0)^n}. \tag{2.14}$$

Thus the Rényi entropy is

$$S_n = \frac{n}{1-n}\frac{1}{T_0}[F(T_0) - F(T_0/n)]. \tag{2.15}$$

where $F(T) = -T\log Z(T)$ is the free energy of a CFT on $\mathbb{H}_{d-1}$. This can be written as

$$S_n = \frac{n}{n-1}\frac{1}{T_0}\int_{T_0/n}^{T_0} S_{\mathrm{therm}}(T)dT. \tag{2.16}$$

where

$$S_{\mathrm{therm}}(T) = -\partial F(T)/\partial T \tag{2.17}$$

is the usual thermal entropy on $\mathbb{H}_{d-1}$.

We are interested in computing the entanglement spectrum (i.e. the eigenvalue spectrum of the reduced density matrix). In general this will have both a discrete and continuous part. In the basis that diagonalizes the reduced density matrix, the Rényi entropy is

$$S_n = \frac{1}{1-n} \log \left[\sum_i \bar{d}_i \lambda_i^n + \int_0^1 d\lambda d(\lambda) \lambda^n \right] \tag{2.18}$$

where λ_i are the eigenvalues of ρ_A with $\lambda_1 > \lambda_2 > \cdots$, and $\bar{d}_i$ ($d(\lambda)$) are the discrete (continuous) degeneracies of the eigenvalues λ_i and λ. Note that the eigenvalues of the entanglement hamiltonian H_E, which we denote $h_i = -\log \lambda_i$, satisfy $h_1 < h_2 < \cdots$. Since λ_i and λ are equal or smaller than 1, the Rényi entropy is a monotonically decreasing function of n. Thus, if we expand S_n in powers of n, it will contain only constant terms or negative powers of n. In the large n limit, only the constant term survives; it gives the largest eigenvalue λ_1:

$$S_\infty = -\log \lambda_1. \tag{2.19}$$

We note that the entanglement entropy in a continuum theory is UV divergent unless one employs a cutoff near the entangling surface. Likewise, the thermal entropy on hyperbolic space diverges because of the infinite volume unless one employs an IR cutoff.[3] One can show that these two divergences are essentially the same thing; they are mapped to one another by the conformal transformation [67].

2.3 Holographic Rényi entropies

We now consider the computation of Rényi entropies in CFTs with bulk gravity duals, where they are related to entropies of hyperbolic black holes. We will describe the instabilities of these black holes in section 2.3.2, using a simple near-horizon analysis of the extremal black hole.

[3] In general, the theory may also have standard UV divergences which have nothing to do with the entangling surface. We assume that these are regularized in ordinary ways, e.g. via zeta function regularization or background subtraction.

2.3.1 Hyperbolic Black Hole

In a CFT, the Rényi entropies S_n are related to the thermal entropies $S(T)$ of the theory on hyperbolic space $\mathbb{H}_{d-1}$ times time. In particular, from equation (2.16), S_n is an integral of $S(T)$ from $T = T_0 = 1/2\pi L$ to $T = T_0/n$. Thus we must compute $S(T)$ for T between 0 and T_0.

We will consider CFTs with gravity duals. In this case the thermal entropy $S(T)$ is equal to the entropy of a black hole in AdS_{d+1} with hyperbolic horizon and Hawking temperature T [67, 68]:

$$S_{therm} = \frac{r_H^{d-1}\text{vol}(\mathbb{H}_{d-1})}{4G_N} \tag{2.20}$$

Here r_H is the value of the radial coordinate at the event horizon. It is straightforward to construct such solutions in Einstein gravity with a negative cosmological constant. The metric is

$$ds^2 = -f(r)d\theta^2 + \frac{dr^2}{f(r)} + r^2 dH_{d-1}^2. \tag{2.21}$$

where

$$f(r) = \frac{r^2}{L^2} - 1 - \frac{m}{r^{d-2}}, \tag{2.22}$$

and m is the black hole mass. The AdS metric (in Rindler-like coordinates) is recovered by setting $m = 0$. The horizon location r_H is determined by

$$f(r_H) = 0. \tag{2.23}$$

The black hole temperature is

$$T = \frac{f'(r_H)}{4\pi} = \frac{1}{2\pi L}\left(\frac{r_H}{L} + \frac{d-2}{2}\frac{mL}{r_H^{d-2}}\right) \tag{2.24}$$

Asymptotically, the black hole metric becomes

$$ds^2 \sim \left(\frac{r^2}{L^2}\right)\left(-d\theta^2 + L^2 dH_{d-1}^2\right) \qquad \text{as } r \to \infty \tag{2.25}$$

Thus the black hole is dual to the CFT on $\mathcal{R} \times \mathbb{H}_{d-1}$ at temperature T given by (2.24). The black hole entropy therefore computes the thermal entropy of the CFT, which is in turn

related to the Rényi entropy via (2.16). Note that the AdS radius L has been related to the radius of the entangling surface.

The relation between the Rényi parameter n and the mass m is

$$n = \left(\frac{r_H}{L} + \frac{d-2}{2} \frac{mL}{r_H^{d-2}} \right)^{-1} \tag{2.26}$$

For the Rényi parameter $n > 1$, the black hole mass m needs to take a negative value. The extremal case is

$$r_H^{\text{ext}} = \sqrt{\frac{d-2}{d}} L < L \tag{2.27}$$

at which the black hole temperature becomes zero. The black hole exists only for

$$r_H \geq r_H^{\text{ext}}. \tag{2.28}$$

In the extremal limit, the near horizon geometry becomes $AdS_2 \times \mathbb{H}_{d-1}$ with AdS_2 radius $L/\sqrt{d}$, and the temperature $T \to 0$.

2.3.2 Phase transitions: Analytic Estimates

So far we have considered only vacuum solutions of Einstein gravity. Let us consider the case where the CFT contains a scalar operator of dimension Δ, which in the bulk corresponds to a scalar field of mass $\mu^2 L^2 = \Delta(\Delta - d)$. If Δ is sufficiently small, then it is possible for asymptotically AdS black holes to be unstable at low temperature [83, 84, 85, 86]. This would lead to a phase transition where the scalar field condenses.

In the case of the hyperbolic black holes described above, a similar instability was considered in [83]. The authors of [83] considered only modes which are constant on the hyperboloid, which are normalizable only if the hyperboloid is quotiented to form a compact space. In the present case the hyperboloid is not quotiented. We will therefore consider here a more general class of instabilities, where a normalizable mode on the hyperboloid condenses.

The physics of the problem is easy to understand. Consider a minimally coupled scalar field Φ with mass μ, which behaves asymptotically as

$$\Phi \sim \frac{a_1}{r^{\Delta_+}} + \frac{a_2}{r^{\Delta_-}} + \cdots, \qquad \Delta_\pm = \frac{d}{2} \pm \sqrt{\frac{d^2}{4} + \mu^2 L^2}. \tag{2.29}$$

We will consider cases where the mass μ is between the Breitenlohner-Freedman (BF) bound of AdS_{d+1} and AdS_2,

$$-\frac{d^2}{4L^2} \leq \mu^2 < -\frac{d}{4L^2}. \tag{2.30}$$

Let us first consider the case of a mode which is constant on the hyperboloid. In this case, for sufficiently high temperature black holes – in particular when $T > T_0$ – the scalar field will always be stable in the black hole background.[4] Thus the dominant saddle point will be the one with $a_1 = a_2 = 0$. However, as $T \to 0$ the near horizon geometry becomes AdS_2 and the scalar field is unstable. Thus there is a critical temperature $T_c < T_0$ at which Φ becomes unstable. Below T_c, either a_1 or a_2 (depending on which boundary conditions we choose for the scalar field) will become non-zero. The dominant solution is a hairy black hole, which must be obtained numerically.

This instability was discussed in [83], who obtained the phase diagram as a function of the temperature and the scalar's mass. As expected, for μ at the AdS_2 BF bound, the extremal ($T \to 0$) black hole is unstable. As μ^2 is decreased the critical temperature T_c increases until we reach the AdS_{d+1} BF bound, which corresponds to the threshold of instability for the massless black hole (which has $T = T_0$). We note that, as long as the field obeys the AdS_{d+1} BF bound, the locally AdS solution with $T = T_0$ will be stable. We will reproduce these results in the next section, where they will be summarized in Fig. 2.5. This condensation will generate a phase transition in the thermal entropy and from (2.16), a phase transition in the Rényi entropy.[5]

[4]This is easiest to see by noting that the $T = T_0$ black hole is just AdS_{d+1}, which is stable, and that black holes only become more stable as the temperature is increased.

[5]These results are for standard (Dirichlet) boundary conditions for the scalar field ($a_2 = 0$). However, it is also possible to consider non-standard (Neumann, $a_1 = 0$) boundary conditions. In this case the critical temperature continues to increase as Δ_- decreases. In fact, the critical temperature is *higher* than that of the massless black hole. The massless black hole is the one which computes the entanglement entropy. Thus the entanglement entropy would no longer given by the area of the hairless black hole! Note, however, that this result is true only if we include the (non-normalizable) constant mode. When we restrict to normalizable modes below, the massless black hole will remain hairless. This emphasizes the important qualitative differences between the constant and normalizable modes. Related considerations will

The above analysis, however, is incomplete because it considers a mode which is non-normalizable on the hyperboloid. Such modes are easy to study, as they preserve the symmetries of the hyperboloid. Only normalizable modes, however, will lead to true instabilities of the black hole. On a hyperboloid $\mathbb{H}_{d-1}$, normalizable modes can be expanded in eigenfunctions of the hyperbolic laplacian, $\nabla^2_{\mathbb{H}_{d-1}}\phi = -\lambda\phi$ with $\lambda > (d-2)^2/4$. The extremal black hole has a near horizon region $AdS_2 \times \mathbb{H}_{d-1}$ with radii

$$L_{AdS_2} = \frac{L_{AdS_{d+1}}}{\sqrt{d}} \qquad L_{\mathbb{H}_{d-1}} = \sqrt{\frac{d-2}{d}} L_{AdS_{d+1}} \tag{2.31}$$

The full Laplacian is the sum of the AdS_2 and $\mathbb{H}_{d-1}$ Laplacians. Thus, for a mode which is an eigenfunction of $\nabla^2_{\mathbb{H}_{d-1}}$, the effective mass of the field in AdS_2 is shifted. We therefore expect an instability when

$$\mu^2 + \frac{\lambda}{L^2_{\mathbb{H}_{d-1}}} \leq -\frac{1}{4L^2_{AdS_2}} \tag{2.32}$$

where λ is the lowest eigenvalue of the laplacian on $\mathbb{H}_{d-1}$. This occurs when the scalar masses are in the following range:

$$-\frac{d^2}{4} \leq \mu^2 L^2_{AdS_{d+1}} \leq -\frac{d(d-1)}{4} \tag{2.33}$$

There will be masses in this range for any dimension d. For example in AdS_5 we will find an instability when

$$-4 \leq \mu^2 L^2_{AdS_5} \leq -3 \tag{2.34}$$

We will now turn to a numerical analysis of this instability.

2.4 The Constant Mode and a Hairy Black Hole

We will now study numerically the instability of the hyperbolic black hole to the development of scalar hair. We will begin with a discussion of the constant mode on the hyperboloid. This mode is particularly simple, as it preserves all of the hyperbolic symmetries. Thus the hairy black hole can be constructed relatively easily using a full non-linear numerical

be discussed in [87].

method. However, this mode is non-normalizable so will not fluctuate in the gravity theory. The results of this section can therefore be viewed as a simplified model (one where the hairy black hole can be constructed explicitly) of the more complicated case considered in the next section.

We note that, although the constant mode considered in this section is non-normalizable on the hyperboloid $\mathbb{H}_{d-1}$, it is normalizable on compact quotients of $\mathbb{H}_{d-1}$. Moreover, one may wish to consider entanglement entropies with insertions of operators at the entangling surface (the boundary of the hyperboloid) which source the scalar field. If these operators turn on the constant mode of the scalar, then the results of this section would be precisely correct, rather than just a simplified model.

To present numerical results we focus on the specific case of a scalar field theory coupled to Einstein gravity in 5 dimensions.[6] Our numerical approach follows [83] closely. The action is

$$S = \frac{1}{16\pi G_N}\int d^5x\sqrt{-g}\left[R + \frac{12}{L^2} - (\nabla\Phi)^2 - \mu^2\Phi^2\right] \tag{2.35}$$

where μ is a mass of the scalar field. We use the following metric and scalar field ansatz

$$ds^2 = -f(r)e^{2\chi(r)}dt^2 + \frac{dr^2}{f(r)} + r^2 dH_3^2, \qquad \Phi = \Phi(r). \tag{2.36}$$

We are considering only constant modes on the hyperboloid; such modes will not fall off at the boundary of $\mathbb{H}_{d-1}$, i.e. the entangling surface.

The equations of motion are

$$\Phi''(r) + \frac{1}{rf(r)}\left[\left(-\frac{\mu^2}{3}r^2\Phi(r)^2 + f(r) + \frac{4r^2}{L^2} - 2\right)\Phi'(r) - \mu^2 r\Phi(r)\right] = 0, \tag{2.37}$$

$$f'(r) + \left(\frac{2}{r} + \frac{r}{3}\Phi'(r)^2\right)f(r) + \frac{\mu^2}{3}r\Phi(r)^2 + \frac{2}{r} - \frac{4r}{L^2} = 0, \tag{2.38}$$

$$\chi'(r) - \frac{r}{3}\Phi'(r)^2 = 0. \tag{2.39}$$

For an asymptotically AdS_5 space-time, the scalar field behaves as (2.29). For $a_1 = 0$, a_2 gives the expectation value of conformal dimension Δ_- operator, and for $a_2 = 0$, a_1 gives the expectation value of conformal dimension Δ_+ operator. In this section, we set $a_2 = 0$;

[6] We will consider charged black holes in [88].

this is the "standard" (i.e. Dirichlet) boundary condition, where the mode which falls of more slowly at $r \to \infty$ is set to zero. At the AdS_5 BF bound, i.e., $\mu^2 L^2 = -4$ ($\Delta = 2$), $\Delta_\pm$ degenerate and the asymptotic behaviour of the scalar field becomes

$$\Phi(r) \sim \frac{a_1}{r^2} + \frac{a_2 \log(r)}{r^2} + \cdots \tag{2.40}$$

In this case, we set $a_2 = 0$.

The metric functions behave as

$$f(r \to \infty) = \frac{r^2}{L^2} - 1 + \frac{r_0^2}{r^2}, \quad \chi(r \to \infty) = \mathcal{O}(r^{-2\Delta_+}), \tag{2.41}$$

and the thermodynamical quantities are

$$T = \frac{f'(r_H)e^{\chi(r_H)}}{4\pi}, \quad S_{\text{therm}} = \frac{r_H^3 \text{vol}(\mathbb{H}_3)}{4G_N}, \quad E = \frac{(-3r_0^2 + \delta_\Delta^2 2(a_1^2/L^2))\text{vol}(\mathbb{H}_3)}{16\pi} \tag{2.42}$$

We have numerically investigated hairy black hole solutions. For each value of $\mu^2 L^2 < -1$ we find hairy black holes below a critical temperature T_c. When they exist, the hairy black holes have lower free energy than the Einstein black hole. Thus the scalar condensate phase ($a_1 \neq 0$) is thermodynamically favoured. When the scalar mass is equal or greater than the AdS_2 BF bound ($\mu^2 L^2 \geq -1$, $\Delta \geq 2 + \sqrt{3}$), the Einstein black hole is stable and the expectation value of the scalar field (a_1) is always zero.

Our results are presented in Fig 2.1, which shows the thermal entropy as a function of the temperature.[7] The Einstein black hole is the top curve (red) in Fig. 2.1. We have also plotted in Fig. 2.1 the entropy of the hairy black hole for a variety of masses below the AdS_2 BF bound. The critical temperature T_c at which the scalar condenses is where these curves meet the Einstein black hole curve. This temperature gets larger as we decreases the scalar mass. At the AdS_5 BF bound ($\mu^2 L^2 = -4$, $\Delta = 2$), the critical temperature becomes the Rindler temperature $T_c = T_0 = \frac{1}{2\pi L}$. This is the blue line in Fig. 2.1. Note that the hairy black hole has smaller thermal entropy, but lower free energy, than the Einstein black hole. Fig. 2.5 shows the critical temperatures as a function of Δ, the dimension of the lowest dimension scalar operator.

[7] In this graph we set $L = \text{vol}(\mathbb{H}_3) = 1$ (i.e. we plot the entropy density).

From these thermal entropies we can compute the Rényi entropy, via (2.16)

$$S_n = \frac{n}{n-1}\frac{1}{T_0}\left(\int_{T_0/n}^{T_{crit}} S^{ES}_{\rm therm}(T)dT + \int_{T_{crit}}^{T_0} S^{E}_{\rm therm}(T)dT\right), \tag{2.43}$$

where $S^{ES}_{\rm therm}(T)$ is the entropy of the hairy black hole (the broken phase) and $S^{E}_{\rm therm}(T)$ is the entropy of the Einstein black hole (the unbroken phase). The Rényi entropy as a function of n is plotted in Fig. 2.2. As the derivative of the thermal entropy with respect to the temperature is discontinuous, the second derivative with respect to n of the Rényi entropy is discontinuous (we have integrated once)[8]. The upper (red) curve is the Einstein black hole. The other curves describe cases where a scalar field condenses at some value of n. Note that the Rényi entropy S_n will always approach the Einstein black hole result as $n \to 1$, because the massless black hole is stable for any scalar obeying the BF bound. As one decreases the mass, the critical temperature gets higher and the asymptotic value of the Rényi entropy at large n gets farther from the Einstein result.

The spectral function $\bar{d}_i$ and $d(\lambda)$ in (2.18) can be obtained from the inverse Laplace transformation

$$\exp\left((1-n)S_n\right) = \sum_i \bar{d}_i \lambda_i^n + \int_0^{\lambda_1} d\lambda d(\lambda)\lambda^n. \tag{2.44}$$

We can now use our numerical results to plot the spectral density $d(\lambda)$ (including the discrete part $\bar{d}_i$ in $d(\lambda)$ by allowing a delta function). We will focus on the two simplest cases: $\mu^2 L^2 = -1$ and $\mu^2 L^2 = -4$, for which the critical temperatures are $T_c = 0$ and $T_c = T_0 = 1/2\pi L$.

We first note that, since Renyi entropies are UV divergent, the eigenvalues are exponentially suppressed with the cutoff. For example, as explained in [68], the eigenvalue λ_1 scales as

$$\lambda_1 \sim e^{-\text{const.}\times C_T \times \mathcal{A}/\epsilon^{d-2}} \tag{2.45}$$

where $\mathcal{A}$ and ϵ are respectively the area of the entangling surface and the UV cutoff. Here C_T is related to the 2-point function of the stress tensor and counts the degrees of freedom

[8] Just as in the holographic superconductor, the condensation of the scalar field is a second order phase transition [84, 85, 86]. This translates into the discontinuity of the second derivative of S_n with respect to n.

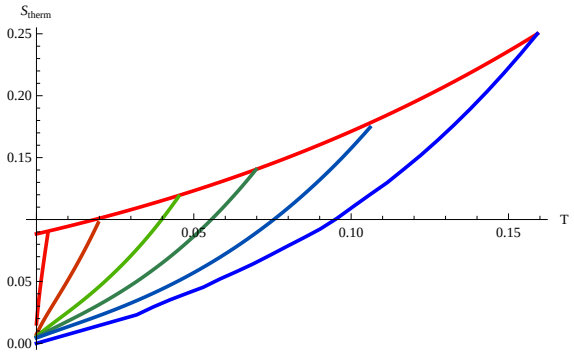

Figure 2.1: Thermal entropy S_{therm} as a function of the temperature T. The upper (red) curve is for the unbroken phase (Einstein black hole). The lower (light red, orange, light green, green, blue-green and blue) curves are for hairy black holes with $\mu^2 L^2 = -2.2, -3, -3.5, -3.75, -3.9375, -4$ ($\Delta = 3.34, 3, 2+1/\sqrt{2}, 2.5, 2.25, 2$). The critical temperatures are $T_c = 0.0037,\ 0.020,\ 0.045,\ 0.070, 0.106, 1/2\pi$. Note the lower right (blue) curve is for the scalar at the AdS_5 BF bound, for which the critical temperature is that of the massless black hole.

of the theory, which is typically taken to be large for gravity to be classical in the bulk. For even dimensional CFTs, it is related to the A-type trace anomaly. In the bulk gravity calculation, C_T is set by the AdS radius in Planck units ($C_T \sim (L/\ell_p)^{d-1}$) and the UV divergence becomes the volume divergence of the hyperboloid. We may therefore introduce a UV regulator by taking the volume of the hyperboloid to be finite.

We can now go ahead and compute the spectral densities (2.44) explicitly. To exhibit a simple numerical answer, we will set $V_{\mathbb{H}_{d-1}} = L = G_N = 1$. Performing an inverse Laplace transform numerically is a bit tricky, so we expand the left hand side of (2.44) in the large n limit as

$$\exp\left((1-n)S_n\right) = \exp((s_0 - s_1) - s_0 n)\left(1 + \frac{g_1}{n} + \frac{g_2}{n^2} + \frac{g_3}{n^3} + \cdots\right). \tag{2.46}$$

where $S_n = \sum_{i=0}^{\infty} s_i n^{-i}$ and the g_i are functions of the s_i. The inverse Laplace transformation of the first term gives a delta function and the rest of the terms include the Heaviside step function and continuous functions. The constant s_0 determines both the location of the delta

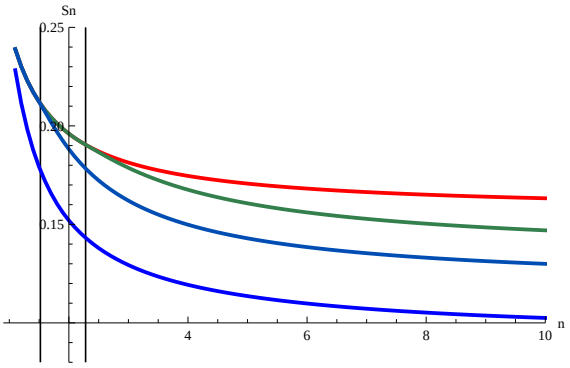

Figure 2.2: Rényi entropy as a function of n for $\mu^2 L^2 = -1, -4, -3.75$ and -3.9375. The phase transition is at $n_{crit} \simeq 2.28$ for $\mu^2 L^2 = -3.75$ and 1.52 for $\mu^2 L^2 = -3.9375$.

function and the Heaviside step function. The result is

$$d(\lambda) = \frac{\exp(s_0 - s_1)}{\lambda}(l_0 \delta(\lambda - \lambda_1) + \Theta(\lambda - \lambda_1) \sum_{n=0} l_{n+1}(-\log \lambda)^n) \tag{2.47}$$

where l_i is a function of s_i. Note that $-\log \lambda$ is the eigenvalue of the entanglement hamiltonian H_E (2.7). The numerical result for the spectral density is plotted in Fig.2.3. Of course, the Rényi entropies are UV-divergent but we are calculating the constant in front of the divergent piece. Similar arguments can be found in section 5 of [68].

It is worth noting that these results for the spectral density are consistent with those found by Calabrese and Lefevre [77]. In two dimensional conformal theory, the n dependence of the Rényi entropy is

$$S_n \propto \left(1 + \frac{1}{n}\right). \tag{2.48}$$

This is determined by the conformal dimension of the twist operators. By taking the inverse Laplace transformation, Calabrese and Lefevre obtained a universal scaling behaviour for the entanglement spectrum. The structure of the spectrum, the delta function at the largest eigenvalue and the Heaviside step function, depends only on the asymptotic behaviour of the Rényi entropy at large n. We have found a very similar structure for our 4d CFTs.

For a general mass, it is technically difficult to perform the inverse Laplace transformation. However, from the asymptotic behaviour of the Rényi entropy, we can see that the

spectral function has only one delta function which sits between λ_1^E and λ_1^{ES}. Fig. 2.4 shows the relation between the maximum eigenvalue of H_E and Δ. Note that as we increase the dimension of the conformal operator Δ, the maximum eigenvalue λ_1 of the entanglement spectrum monotonically decreases, i.e.

$$\frac{dS_\infty}{d\Delta} \geq 0 \tag{2.49}$$

This suggests that the ground state of a CFT with smaller lowest dimension operator is closer to a pure state. In other words, the ground state of a theory with a large gap is more mixed than one with a small gap. This result is obtained using black hole thermodynamics, so is likely to be generic for large N theories. It would be interesting to investigate the generality of this inequality, and the analytic relation between S_∞ and Δ.

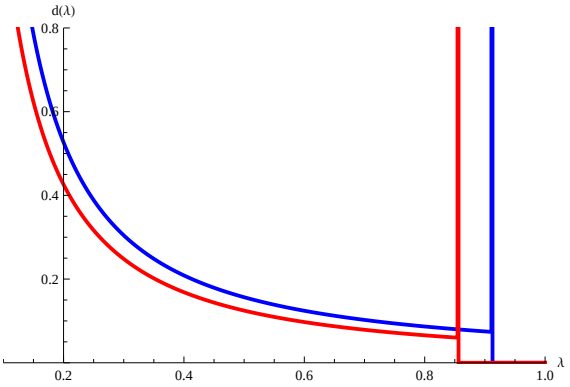

Figure 2.3: The spectral function $d(\lambda)$ for the cases $\mu^2 L^2 = -1$, where the black hole is always Einstein, and $\mu^2 L^2 = -4$, where the black hole always has scalar hair. There are delta functions at the lowest eigenvalues, $\lambda_1^E = 0.855$ for the Einstein (red line) and $\lambda_1^{ES} = 0.911$ for the Einstein-scalar (blue line). For the pure Einstein case and with $V_H = G_N = L = 1$, we obtain the same result as [68].

2.5 Instability for the Normalizable Mode

We now turn our attention to the more physical case of the mode which is normalizable on the hyperboloid. In this case the condensation of the mode will break the hyperbolic symmetries,

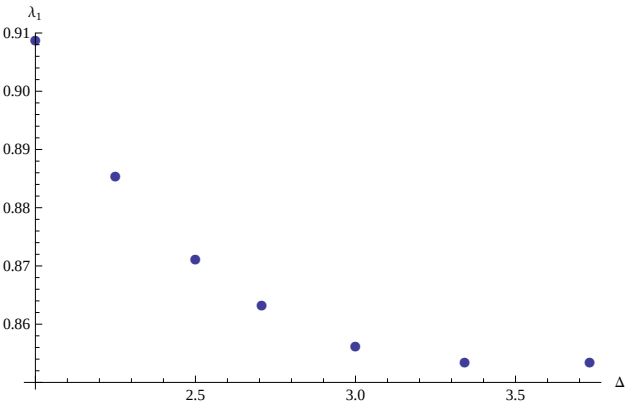

Figure 2.4: Lowest eigenvalue of ρ as a function of conformal dimension.

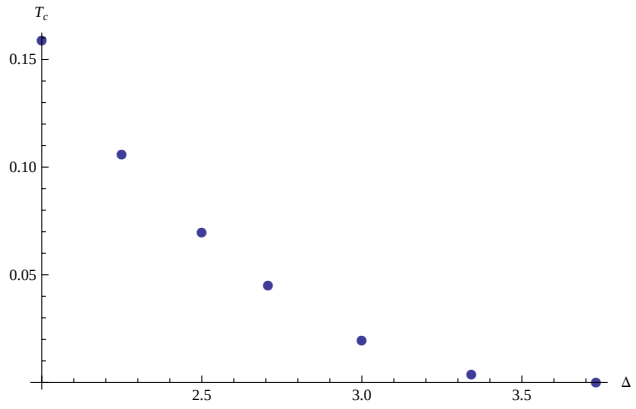

Figure 2.5: Critical temperature as a function of conformal dimension.

so the construction of hairy black holes at the non-linear level is considerably more difficult. We will simply perform the linearized analysis, which is sufficient to demonstrate that an instability exists and that the Rényi entropies will undergo a phase transition. We leave the construction of hairy black hole solutions to future work.

In $d = 4$, the wave equation for a scalar of mass μ is[9]

$$\left(-\frac{\omega^2}{f(r)} - \frac{\lambda}{r^2} - \mu^2\right)\phi(r) + \left(f'(r) + 3\frac{f(r)}{r}\right)\phi'(r) + f(r)\phi''(r) = 0 \tag{2.50}$$

where we considered the following ansatz for the field:

$$\Phi(t, r, \sigma_i) = e^{\omega t}\phi(r)Y(\sigma_i), \quad \nabla^2_{\mathbb{H}_3}Y(\sigma_i) = -\lambda Y(\sigma_i). \tag{2.51}$$

The black hole will be unstable if (2.50) has a solution with ω real and positive with the field satisfying specified boundary conditions at infinity and the horizon. We can put the wave equation in Schrodinger form by letting $\psi(r) = r^{(d-1)/2}\phi(r)$, so

$$\left(-\left(f(r)\frac{d}{dr}\right)^2 + V(r)\right)\psi(r) = -\omega^2\psi(r) \tag{2.52}$$

with

$$V(r) = \frac{f(r)}{r^2}\left(\lambda + f'(r)\frac{d-1}{2}r + f(r)\frac{(d-1)(d-3)}{4} + \mu^2 r^2\right) \tag{2.53}$$

[9]Similar equations hold in other dimensions; we focus on $d = 4$ for simplicity.

In tortoise coordinates ($dr_* = dr/f(r)$), this is the problem of determining whether the potential $V(r_*)$ has a negative energy bound state. We impose the following boundary conditions [10]

$$\psi(r_+) = 0 \qquad \psi'(r_+) = 1 \qquad \psi(r)|_{r\to\infty} \to \frac{1}{r^{\Delta-(d-1)/2}} \ . \tag{2.54}$$

Note that we consider here both Dirichlet and Neumann boundary conditions.

We can solve (2.52) numerically using a standard shooting method from the horizon. We find that, for every mass in the range

$$-\frac{d^2}{4} \leq \mu^2 L^2_{AdS_{d+1}} \leq -\frac{d(d-1)}{4} \tag{2.55}$$

there is a temperature $T > 0$ for which the Einstein black hole is unstable to the development of scalar hair.[11] We have checked this in four and five dimensions. We plot the curve of marginal stability in Figs. 2.6 and 2.7 for four and five dimensions. Every configuration in the zone above the curves is unstable. We conclude that Rényi entropies will undergo a phase transition at values of the Rényi parameters n_c which depend on the dimension of the lowest nontrivial operator.

These results have one important feature which distinguishes them from the instabilities considered in the previous section. They take place at *much* lower temperatures (i.e. larger values of n). It turns out that, for scalars which are non-constant on the hyperboloid, the $AdS_2 \times \mathbb{H}_{d-1}$ instability becomes relevant only very close to extremality. A similar phenomenon was noted in [83] for a different class of black holes. This suggests that it is primarily the lowest eigenvalues of the entanglement spectrum which are effected by the scalar field instability.

[10] The field should vanish at the horizon as unstable modes behave as $\phi(r) \sim (r - r_+)^\omega$ as $r \to r_+$.

[11] We have also checked this result using the method of trial wave functions, for which we thank G. Salton for useful discussions.

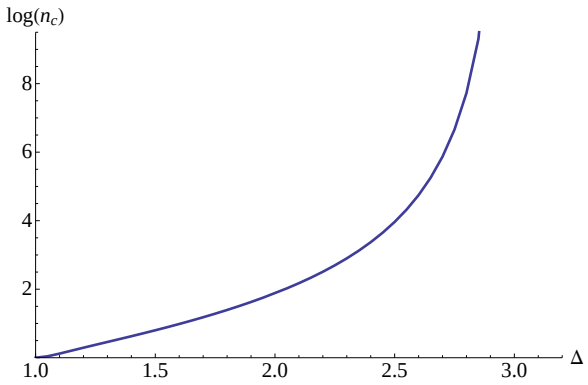

Figure 2.6: Log of the critical Rényi parameter for instability as a function of conformal dimension in AdS_5/CFT_4. As Δ approaches 3 the instability disappears.

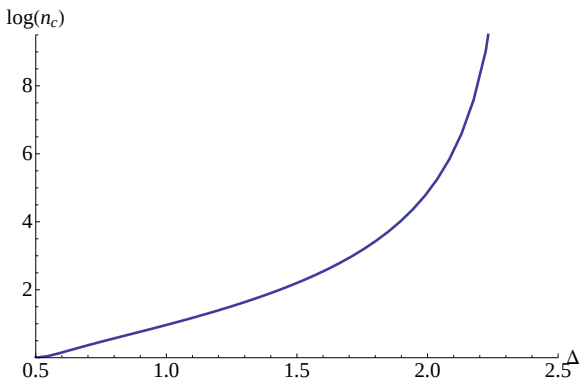

Figure 2.7: Log of the critical Rényi parameter for instability as a function of conformal dimension in AdS_4/CFT_3. The instability disappears as $\Delta \to \frac{3+\sqrt{3}}{2} \approx 2.37$.

2.6 Acknowledgements

We thank Jaume Gomis, Nabil Iqbal, Kristan Jensen, Max Metlits, Rob Myers, Harvey Reall, Subir Sachdev, Jorge Santos, Stephen Shenker, and Tadashi Takayanagi for helpful discussions. This research was supported by the National Science and Engineering Research Council of Canada. SM thanks University of British Columbia, University of Victoria, Kavli Institute for the Physics and Mathematics of the Universe (Kavli IPMU), Kyoto University and the Perimeter Institute for theoretical physics for hospitality.

Charged Rényi entropies

It is also interesting to understand the dependence of entanglement on various parameters that define it such as for example the dependence on the shape of the entangling surface [89]. Another such interesting example is the dependence on charge distribution of the Rényi entropies. One can imagine separating charge in the boundary theory and putting charge Q in region A and charge $-Q$ in region B as in Fig 2.8.

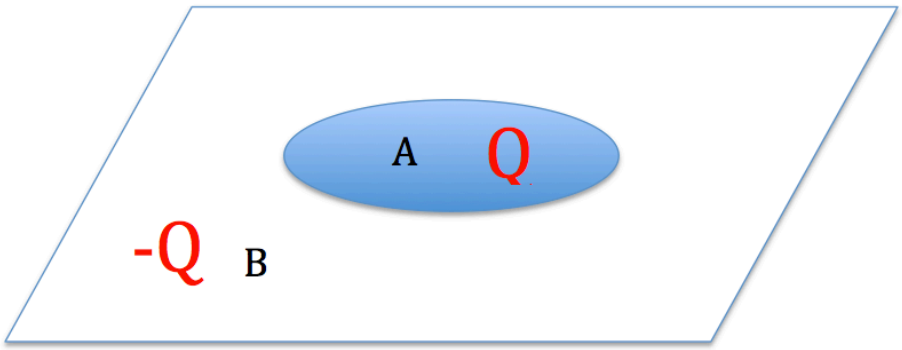

Figure 2.8: The $t = 0$ slice of the boundary region is separated into the inside of a sphere (region A) and the outside (region B). Charge is separated and there is a net charge Q in region A and an opposite charge in region B such that the total charge still vanishes.

Although this is hard to calculate in full generality, we discuss how to calculate it explicitly in Chap. 3 for the ground state of CFTs with a global U(1) symmetry and for spherical entangling surfaces. This is done in the path integral by adding a non trivial Wilson line around the entangling surface. We define such quantities as charged Rényi entropies and discuss how to calculate them both for free theories and holographically, by the means of charged hyperbolic black holes. We also derive properties of the generalized twist operators located at the entangling surface that encode both the replica n and the Wilson line characterized by an entangling chemical potential μ.

Chapter 3

Holographic Charged Rényi Entropies

Alexandre Belin[a,b], Ling-Yan Hung[b], Alexander Maloney[a,b], Shunji Matsuura[a], Robert C. Myers[c] and Todd Sierens[c,d]

[a] *Departments of Physics and Mathematics, McGill University, Montréal, Québec, Canada*

[b] *Department of Physics, Harvard University, Cambridge, MA 02138 USA*

[c] *Perimeter Institute for Theoretical Physics, Waterloo, Ontario N2L 2Y5, Canada*

[d] *Department of Physics & Astronomy and Guelph-Waterloo Physics Institute, University of Waterloo, Waterloo, Ontario N2L 3G1, Canada*

Abstract

We construct a new class of entanglement measures by extending the usual definition of Rényi entropy to include a chemical potential. These charged Rényi entropies measure the degree of entanglement in different charge sectors of the theory and are given by Euclidean path integrals with the insertion of a Wilson line encircling the entangling surface. We compute these entropies for a spherical entangling surface in CFT's with holographic duals, where they are related to entropies of charged black holes with hyperbolic horizons. We also compute charged Rényi entropies in free field theories.

Published in Journal of High Energy Physics **1312**, 059 (2013)

3.1 Introduction

Entanglement and Rényi entropies have emerged as diagnostic probes of considerable practical and formal interest in areas ranging from condensed matter physics, *e.g.,* [37, 47, 48] to quantum gravity, *e.g.,* [49, 72, 73, 38, 39, 40, 41, 42]. In this paper we will consider a generalization of these entropies for systems with a conserved global charge.

Consider a quantum system consisting of two components, A and B, in a state described by the density matrix ρ. We will consider quantum field theories, where A and B are spatial regions separated by an entangling surface Σ. We then trace over the degrees of freedom in region B to construct the reduced density matrix $\rho_{\rm A} = {\rm Tr}_{\rm B}\,\rho$. The latter contains information about the entanglement between A and B. The Rényi entropies [74, 90, 91, 75]

$$S_n = \frac{1}{1-n}\,\log\,{\rm Tr}\,\rho_{\rm A}^n\,, \tag{3.1}$$

are the moments of this reduced density matrix. The limit $n \to 1$ gives the entanglement entropy, $S_{\rm EE} = \lim_{n\to 1} S_n = -\,{\rm Tr}[\rho_{\rm A}\log\rho_{\rm A}]$.

In this paper, we will consider quantum field theories with a conserved (global) charge. In this case we can ask whether the entanglement between A and B depends on how charge is distributed between the two subsystems. This is characterized by the following 'grand canonical' generalization of the Rényi entropy:

$$S_n(\mu) = \frac{1}{1-n}\log{\rm Tr}\left[\rho_{\rm A}\,\frac{e^{\mu\,Q_{\rm A}}}{n_{\rm A}(\mu)}\right]^n\,. \tag{3.2}$$

Here μ is a chemical potential conjugate to $Q_{\rm A}$, the charge contained in subsystem A. We have also introduced $n_{\rm A}(\mu) \equiv {\rm Tr}\left[\,\rho_{\rm A}\,e^{\mu\,Q_{\rm A}}\right]$ to ensure that the new density matrix (enclosed by the square brackets above) is properly normalized with unit trace. The μ-dependence of these 'charged' Rényi entropies $S_n(\mu)$ encodes the dependence of the entanglement on the charge.

We will also be interested in the entropies constructed with an imaginary chemical potential

$$\tilde{S}_n(\mu_{\rm E}) = \frac{1}{1-n}\log{\rm Tr}\left[\rho_{\rm A}\,\frac{e^{i\mu_{\rm E}\,Q_{\rm A}}}{\tilde{n}_{\rm A}(\mu_{\rm E})}\right]^n\,, \tag{3.3}$$

where $\mu_{\rm E}$ is real and $\tilde{n}_{\rm A}(\mu) \equiv {\rm Tr}\left[\,\rho_{\rm A}\, e^{i\mu_{\rm E} Q_{\rm A}}\right]$. As we will see below, the analytic continuation between (3.2) and (3.3) is typically straightforward in the vicinity of the origin $\mu = 0$, but one typically encounters an interesting structure of singularities along the imaginary μ-axis.

In quantum field theory, Rényi entropies can be evaluated using the replica trick [47, 48], which relates them to a Euclidean path integral on an n-sheeted geometry. These path integral calculations of S_n are easily extended to compute our new charged Rényi entropies. As we will describe below, the key new ingredient is a Wilson line encircling the entangling surface. This generalizes the twist operator σ_n appearing in the replica trick to include a 'magnetic flux' proportional to μ.

In conformal field theories, these entropies can be studied rather explicitly. A useful approach was introduced in [67] to evaluate the entanglement entropy across a spherical entangling surface for an arbitrary d-dimensional CFT in flat space. The latter entropy is related by a conformal mapping to the thermal entropy of the CFT on a hyperbolic cylinder $R \times H^{d-1}$, where the temperature and curvature are fixed by the radius of the original entangling surface. If the temperature is allowed to vary, the thermal entropy calculates Rényi entropies [68, 78]. In theories with holographic gravity duals, the thermal entropy is the horizon entropy of a black hole with H^{d-1} horizon. Our charged entropies $S_n(\mu)$ can also be computed for spherical entangling surfaces with a simple extension of this procedure. The same conformal mapping leads to a grand canonical ensemble with chemical potential μ for the CFT on the hyperbolic cylinder. In the holographic context, the presence of a global symmetry in the boundary CFT leads to a gauge field in the dual gravity theory. $S_n(\mu)$ is then related to the entropy of a hyperbolic black hole which is charged under this gauge field.

This paper is organized as follows: In section 3.2, we will discuss general features of the charged Rényi entropy and outline its computation in CFT. We also describe the various properties of the corresponding twist operators. In section 3.3, we compute $S_n(\mu)$ in holographic CFT's (in spacetime dimensions $d \geq 3$) by considering the charged hyperbolic black holes of the dual Einstein-Maxwell theory. We conclude with a discussion and general comments on the properties of the charge Rényi entropy in section 3.4. Three appendices are also

included. Appendix 3.5 describes computations of $\tilde{S}_n(\mu_{\rm E})$ in simple free field theories and appendix 3.6 gives the holographic computation in AdS_3/CFT_2. The latter case is notable in that the dependence of the charged Rényi entropy on n agrees with the free field theory result. Finally appendix 3.7 contains various details of the holographic calculations, which are used in section 3.3.

Charged Rényi entropies arose in several recent papers which appeared while this paper was in preparation. First, they were briefly considered in [66, 92]. Charged Rényi entropies appear in [93], which investigates the dynamical evolution of entanglement entropy in two-dimensional CFT's. The supersymmetric Rényi entropies three-dimensional $\mathcal{N} \geq 2$ superconformal theores calculated in [94] can be cast in the form (3.3) with an imaginary chemical potential for a circular entangling surface, using the conformal mappings presented in [67, 68]. In this case, $Q_{\rm A}$ corresponds to the R-charge of the underlying theory.

3.2 Charged Rényi entropies for CFT's

In this section, we begin with some general comments about the charged Rényi entropies (3.2). We then focus on their computation in conformal field theories, extending the approach of [67, 68], to relate charged Rényi entropies for spherical entangling surfaces in flat space to the thermal entropy of the CFT on $R \times H^{d-1}$ in grand canonical ensemble. We also describe the calculation of the conformal weight and magnetic response of the corresponding twist operator. Finally, we describe the computation of these entropies for two-dimensional CFT using twist operators.

3.2.1 Replica Trick

To begin, let us recall the replica trick [47, 48, 49, 72, 73]. For simplicity, we focus on entanglements in the ground state of a QFT in d-dimensional flat space. One begins by introducing an entangling surface Σ which divides the spatial slice at time $t_{\rm E} = 0$ into two

regions, A and B.[1] Integer powers of the reduced density matrix $\rho_{\rm A}$ are represented by a Euclidean path integral

$$\text{Tr}\ \rho_{\rm A}^n = Z_n/(Z_1)^n\,. \tag{3.4}$$

Here Z_n is the partition function on an n-fold cover of (Euclidean) flat space with cuts introduced on region A at $t_{\rm E} = 0$. At the cut, copy n is connected to copy n+1 when approaching from $t_{\rm E} \to 0^-$ and to copy n–1 when approaching from $t_{\rm E} \to 0^+$. In this construction, the entangling surface Σ becomes the branch-point of the branch-cut which separates different copies in the n-fold covering geometry. It is convenient to think of these boundary conditions as produced by the insertion of a (d–2)-dimensional surface operator at Σ, *i.e.,* a twist operator σ_n [47, 48].[2] The factors of Z_1 appear above to ensure that the density matrix is properly normalized with $Tr\,[\rho_{\rm A}] = 1$. With the usual definition (3.1), the Rényi entropies become

$$S_n = \frac{1}{n-1}\,\left(n\,\log Z_1 - \log Z_n\right)\,. \tag{3.5}$$

Of course, one would like to consider an analytic continuation to real values of n to determine the entanglement entropy with $S_{\rm EE} = \lim_{n\to 1} S_n$. Similarly, two other interesting limits are given by $n \to 0$ and ∞, which yield expressions which are known as the Hartley entropy and the min-entropy, respectively [79]. In particular, one finds $S_0 = \log(\mathbf{d})$ where $\mathbf{d}$ is the number of nonvanishing eigenvalues of $\rho_{\rm A}$ and $S_\infty = -\log(\lambda_1)$ where λ_1 is the largest eigenvalue of $\rho_{\rm A}$.

We wish to extend these path integral calculations of S_n to compute charged Rényi entropies. Let us first recall how a chemical potential μ is included in the standard Euclidean path integral representation of a (grand canonical) thermal ensemble. In this framework, the chemical potential is represented by a fixed background gauge potential[3] B_μ which couples to the relevant conserved current. Of course, in the 'thermal' path integral, the Euclidean time

[1] Implicitly, an initial step in these calculations is to Wick rotate the time coordinate: $t_{\rm E} = it$.

[2] For further discussion of twist operators beyond $d = 2$, see also [68, 95, 96, 69].

[3] We use B_μ to distinguish this nondynamical gauge field from the bulk gauge potential A_μ appearing in our holographic calculations. This background gauge field is imaginary in the Euclidean path integral, corresponding to a real chemical potential.

direction is compactified with period $\Delta t_{\rm E} = 1/T$ and then the chemical potential appears as a nontrivial Wilson line on this thermal circle, *i.e.,* $\oint B = -i\mu/T$.

To evaluate the charged Rényi entropies (3.2), we must compute a grand canonical version of eq. (3.4), *i.e.,*

$$\mathrm{Tr}\left[\rho_{\rm A}\,\frac{e^{\mu\,Q_{\rm A}}}{n_{\rm A}(\mu)}\right]^n = \frac{Z_n(\mu)}{(Z_1(\mu))^n}\,. \tag{3.6}$$

with $n_{\rm A}(\mu) \equiv \mathrm{Tr}\left[\,\rho_{\rm A}\,e^{\mu\,Q_{\rm A}}\right]$. Here $Z_n(\mu)$ is computed as above, except with the insertion of a Wilson line encircling the entangling surface Σ. That is, we introduce a fixed background gauge field coupling to the conserved current. This background field is such that loops encircling the entangling surface carry a nontrivial Wilson line, $\oint_{\mathcal{C}} B = -in\mu$.[4] Here the factor n is analogous to the $1/T$ factor appearing for the thermal ensemble above and arises here because the loop $\mathcal{C}$ circles n times around Σ, passing through all n sheets of the covering geometry. The Wilson line should be the same on all such curves and so the background gauge field is flat, *i.e.,* $dB = 0$, away from the entangling surface. By Stokes' theorem these loops enclose a fixed flux, *i.e.,* $\int_M dB = \oint_{\mathcal{C}=\partial M} B = -in\mu$ for any two-dimensional surface pierced by Σ. Thus the entangling surface carries a 'magnetic flux' $-in\mu$ of the background gauge field. An alternative perspective is that eq. (3.6) defines a generalized class of twist operators $\tilde{\sigma}_n(\mu)$, which are constructed by binding to the original twist operators σ_n, a (d–2)-dimensional 'Dirac sheet' carrying the magnetic flux $-in\mu$. Another noteworthy comment is that with the above definitions, the chemical potential in our charged Rényi entropy (3.6) is dimensionless, in contrast to the standard chemical potential in a thermal context, which carries the units of energy.[5] In any event, given the path integral construction describing eq. (3.6), the charged Rényi entropies (3.2) become

$$S_n(\mu) = \frac{1}{n-1}\,\left(n\,\log Z_1(\mu) - \log Z_n(\mu)\right)\,. \tag{3.7}$$

Above, we considered a real chemical potential μ, as would appear in standard thermodyanmics. We will also consider analytic continuations of the chemical potential to imag-

[4]The orientation of the contour will become evident in our examples below.

[5]In the thermal context, these units have a natural meaning by comparing the chemical potential to the temperature. In the entanglement context, there is no such natural reference scale with which to compare μ.

inary values, as in eq. (3.3). As motivation, we note that working with an imaginary chemical potential has proven to be a useful way to probe the confinement phase transition in QCD [97] and to avoid the sign problem in the lattice fermion algorithms [98]. Computations of the Witten index can also be interpreted in a similar fashion [99]. Replacing $\mu = i\mu_{\rm E}$ in our analysis above, the Wilson loop of the background gauge field now becomes real with $\oint_{\mathcal{C}} B = n\mu_{\rm E}$. Further the corresponding magnetic flux carried by the generalized twist operators is also real. Hence the effect of the imaginary chemical potential is to introduce a simple phase as a charged operator circles around the entangling surface. Note that the analytic continuation between real and imaginary values requires care because, as we will see below, the partition function has an interesting singularity structure in the complex μ-plane. We will consider both real and imaginary chemical potentials in the following. These two cases will always be distinguished by the notation μ and $\mu_{\rm E}$, respectively.

3.2.2 Spherical entangling surfaces

For the remainder of this section we will focus on computations of charged Rényi entropy in d-dimensional conformal field theories. We will consider a CFT in flat space in its vacuum state, and choose the entangling surface to be a sphere of radius R (in a constant time slice). In this case, the argument of [67] implies that the usual entanglement entropy equals the thermal entropy of the CFT on a hyperbolic cylinder $R \times H^{d-1}$, where the temperature and curvature are fixed by the radius of the original entangling surface. A simple extension of this approach also allows one to calculate Rényi entropies [68]. We will compute charged Rényi entropies by further extending the procedure to include a background gauge field. For simplicity of notation we will use an imaginary chemical potential, but of course the same construction applies for a real chemical potential.

We begin with a brief review of [67, 68]. First, we write the metric on flat Euclidean space in terms of a complex coordinate $\omega = r + it_{\rm E}$:

$$ds^2_{R^d} = d\omega d\bar{\omega} + \left(\frac{\omega + \bar{\omega}}{2}\right)^2 d\Omega^2_{d-2}\,, \tag{3.8}$$

where $t_{\rm E}$ is the Euclidean time coordinate, r is the radial coordinate on the constant time

slices and $d\Omega_{d-2}$ is a standard round metric on a unit $(d-2)$-sphere. The entangling surface is the sphere at $(t_{\rm E}, r) = (0, R)$.

We will perform a conformal transformation of the above R^d geometry to $H^{d-1} \times S^1$ as follows. Introducing a second complex coordinate $\sigma = u + i\frac{\tau_{\rm E}}{R}$, we perform the coordinate transformation, which, in terms of the complex coordinate σ defined by

$$e^{-\sigma} = \frac{R-\omega}{R+\omega}\,. \tag{3.9}$$

the metric (3.8) then takes the form

$$ds^2_{R^d} = \Omega^{-2}\, R^2 \left[d\sigma d\bar{\sigma} + \sinh^2\left(\frac{\sigma+\bar{\sigma}}{2}\right) d\Omega^2_{d-2} \right], \tag{3.10}$$

where

$$\Omega = \frac{2R^2}{|R^2-\omega^2|} = |1+\cosh\sigma|\,. \tag{3.11}$$

The Ω^{-2} prefactor can now be removed by a simple Weyl rescaling. Letting $\sigma = u + i\frac{\tau_{\rm E}}{R}$, the resulting conformally transformed metric is

$$ds^2_{H^{d-1}\times S^1} = \Omega^2\, ds^2_{R^d} = d\tau^2_{\rm E} + R^2\left(du^2 + \sinh^2 u\, d\Omega^2_{d-2}\right). \tag{3.12}$$

This is $S^1 \times H^{d-1}$; u is the (dimensionless) radial coordinate on the hyperboloid H^{d-1} and $\tau_{\rm E}$ is the Euclidean time coordinate on S^1. The curvature radius of H^{d-1} is R, the radius of the original spherical entangling surface. The periodicity of the $\tau_{\rm E}$ circle is $2\pi R$. Note that the original entangling surface has been pushed out to the asymptotic boundary, *i.e.,* $u \to \infty$, in the conformally transformed geometry (3.12).

The key point is that, under this conformal mapping, the density matrix describing the CFT vacuum state on the interior of the entangling surface is transformed to a thermal density matrix with temperature

$$T_0 = \frac{1}{2\pi R} \tag{3.13}$$

on the new hyperbolic geometry. That is, the reduced density matrix related to the thermal density matrix as

$$\rho_{\rm A} = U^{-1}\, \frac{e^{-H/T_0}}{Z(T_0)}\, U\,, \tag{3.14}$$

where U is the unitary transformation implementing the conformal transformation. Since the entropy is insensitive to unitary transformations, the desired entanglement entropy just equals the thermal entropy in the transformed space. This same conformal mapping can also be used to evaluate the Rényi entropy. The only difference is that it would be applied to the n-fold cover of flat space used to evaluate eq. (3.4). In this case the period of $\tau_{\rm E}$ is $2\pi Rn$, so the corresponding thermal ensemble has a temperature $T = T_0/n$.

We can compute charged Rényi entropies (3.3) by generalizing this approach. First after having identified the appropriate charge Q, we introduce a (dimensionless) chemical potential μ and the previous density matrix (3.14) becomes

$$\rho_{\rm therm} = \frac{e^{-H/T_0+\mu Q}}{Z(T_0,\mu)}\,. \tag{3.15}$$

Now, in fact, our discussion is slightly simplified if we consider instead an imaginary chemical potential $\mu_{\rm E} = -i\mu$ with which the above expression turns into

$$\rho_{\rm therm} = \frac{e^{-H/T_0+i\mu_{\rm E} Q}}{Z(T_0,\mu_{\rm E})}\,. \tag{3.16}$$

As discussed above, this chemical potential is incorporated into the thermal path integral via a background gauge field with a nontrivial Wilson line on the Euclidean time circle:

$$\mu_{\rm E} = \oint B = \int_0^{2\pi R} B_{\tau_{\rm E}} d\tau_{\rm E}\,. \tag{3.17}$$

In this case the potential is just constant: $B_{\tau_{\rm E}} = \mu_{\rm E}/(2\pi R)$. The background gauge field is invariant under the conformal transformation mapping between the hyperbolic geometry and flat space. Therefore in the flat space coordinates, we may express this gauge field as

$$\begin{aligned} B &= \frac{iR}{2\pi}\mu_{\rm E}\left[\frac{d\omega}{R^2-\omega^2} - \frac{d\bar\omega}{R^2-\bar\omega^2}\right] \\ &= -\frac{R}{\pi}\mu_{\rm E}\,\frac{2t_{\rm E} r\,dr + (R^2-r^2+t_{\rm E}^2)\,dt_{\rm E}}{(R^2-r^2+t_{\rm E}^2)^2+4t_{\rm E}^2 r^2}\,. \end{aligned} \tag{3.18}$$

Now one can readily verify that this background gauge field yields $\oint B = \mu_{\rm E}$ for any contour encircling the entangling surface at $(t_{\rm E}, r) = (0, R)$ in the flat space geometry.[6] Of course,

[6] An interesting exercise to gain better intuition for this background gauge field (3.18) is to expand the coordinates near the spherical entangling surface: $t_{\rm E} = \rho\sin\theta$ and $r = R + \rho\cos\theta$ with $\rho \ll R$. To leading order in ρ/R, one then finds that the potential reduces to $B \simeq \frac{\mu_{\rm E}}{2\pi} d\theta$.

we also have $dB = 0$ and so this is precisely the background required to evaluate the charged Rényi entropy (3.3) in this particular case.

Hence we must simply supplement the conformal mapping approach of [67, 68] with the background gauge field (3.18) to evaluate the charged Rényi entropy across a spherical entangling surface for the CFT vacuum in flat space. The effective reduced density matrix in eq. (3.3) is again simply related to the thermal density matrix (3.16) on the hyperbolic space:

$$\rho_{\mathrm{A}}\,\frac{e^{i\mu_{\mathrm{E}}\,Q_{\mathrm{A}}}}{\tilde{n}_{\mathrm{A}}(\mu_{\mathrm{E}})} \;=\; U^{-1}\,\rho_{\mathrm{therm}}\,U \;=\; U^{-1}\,\frac{e^{-H/T_0+i\mu_{\mathrm{E}}Q}}{Z(T_0,\mu_{\mathrm{E}})}\,U\,, \tag{3.19}$$

where as in eq. (3.14), U is the unitary transformation implementing the conformal transformation between the two geometries. Given this expression, the charged Rényi entropy (3.3) can be evaluated in terms of the corresponding thermal partition function for the CFT on the hyperbolic geometry as

$$\tilde{S}_n(\mu_{\mathrm{E}}) = \frac{1}{1-n}\log\frac{Z(T_0/n,\mu_{\mathrm{E}})}{Z(T_0,\mu_{\mathrm{E}})^n}\,. \tag{3.20}$$

Recall that in evaluating $Z(T_0/n,\mu_{\mathrm{E}})$, the period of τ_{E} is extended to $2\pi Rn$, however, the gauge potential remains fixed as $B_{\tau_{\mathrm{E}}} = \mu_{\mathrm{E}}/(2\pi R)$. Hence the total Wilson line around the thermal circle increases by a factor of n as desired, *i.e.,* $\oint B = n\mu_{\mathrm{E}}$. Now using the standard thermodynamic identity for the grand canonical ensemble

$$S_{\mathrm{therm}}(T,\mu_{\mathrm{E}}) = -\left.\frac{\partial F(T,\mu_{\mathrm{E}})}{\partial T}\right|_{\mu_{\mathrm{E}}} = \frac{\partial}{\partial T}(T\log Z(T,\mu_{\mathrm{E}}))\big|_{\mu_{\mathrm{E}}}\,, \tag{3.21}$$

one easily derives the following relation between the charged Rényi entropy and the thermal entropy [68]:

$$\tilde{S}_n(\mu_{\mathrm{E}}) = \frac{n}{n-1}\frac{1}{T_0}\int_{T_0/n}^{T_0} S_{\mathrm{therm}}(T,\mu_{\mathrm{E}})\,dT\,. \tag{3.22}$$

At this point, we may remind the reader that the above discussion makes no reference to the AdS/CFT correspondence. In the special case of a holographic CFT, this analysis may be further extended by evaluating the thermal entropy on the hyperbolic background in terms of the horizon entropy of a topological black hole in the bulk with a hyperbolic horizon [67, 68] — see also [100, 101]. In the context of the charged Rényi entropy (3.2), the boundary CFT

also contains a conserved current corresponding to the charge probed by these entropies and hence the bulk theory will also include a dual gauge field. The holographic representation of the grand canonical ensemble considered above will then be a topological black hole which is charged under this gauge field. We will turn to such holographic calculations in section 3.3. First, however, we continue below with some further remarks which apply to general CFT's.

3.2.3 Properties of generalized twist operators

As discussed at the beginning of this section, the calculation of (either ordinary or charged) Rényi entropies can be viewed as involving the insertion of a twist operator at the entangling surface. A generalized notion of conformal dimension can be defined for these surface operators by considering the leading singularity in the correlator $\langle T_{\mu\nu}\, \sigma_n \rangle$. This leading singularity is fixed by symmetry, as well as the tracelessness and conservation of the stress tensor. To be precise, consider inserting the stress tensor $T_{\mu\nu}$ at a perpendicular distance y from the twist operator σ_n, such that y is much smaller than any scales defining the geometry of the entangling surface Σ. Then the leading singularity takes the following form[7]

$$\begin{aligned} \langle T_{ab}\, \sigma_n \rangle &= -\frac{h_n}{2\pi} \frac{\delta_{ab}}{y^d}\,, \qquad \langle T_{ai}\, \sigma_n \rangle = 0\,, \\ \langle T_{ij}\, \sigma_n \rangle &= \frac{h_n}{2\pi} \frac{(d-1)\delta_{ij} - d n_i n_j}{y^d}\,, \end{aligned} \tag{3.23}$$

where a, b (i, j) denote tangential (normal) directions to the twist operator and n_i is the unit vector directed orthogonally from the twist operator to the $T_{\mu\nu}$ insertion. Thus the singularity is completely fixed up to the constant h_n, which is referred to as the conformal dimension of σ_n. The approach reviewed in the previous section can be applied to determine the value of h_n in terms of the thermal energy density $\mathcal{E}(T, \mu)$ on the hyperbolic cylinder [68],[8]

$$h_n(\mu) = \frac{2\pi n}{d-1}\, R^d \left(\mathcal{E}(T_0, \mu = 0) - \mathcal{E}(T_0/n, \mu) \right). \tag{3.24}$$

[7]These correlators (3.23) should be normalized by dividing by $\langle \sigma_n \rangle$. However, we leave this implicit to avoid further clutter.

[8]Note that in the Euclidean background, $\mathcal{E}(T, \mu) = -\langle T_{\tau_{\rm E}\tau_{\rm E}} \rangle$. Also observe that we phrase the discussion in this subsection in terms of a real chemical potential μ.

The first term above arises because of the anomalous behaviour of the stress tensor under conformal transformations. Of course, as is implicit above, these remarks apply equally well for the original twist operators σ_n and for the generalized twist operators $\tilde{\sigma}_n(\mu)$ appearing in the calculation of the charged Rényi entropy. In particular, the arguments of [68] yielding eq. (3.24) apply without any change in the presence of the background gauge potential.

In the context of the charged Rényi entropies, another operator in the underlying CFT is the current J_μ, associated with the global charge appearing in eq. (3.2), *i.e.,*

$$Q_{\rm A} = \int_A d^{d-1}x \; J_t \,. \tag{3.25}$$

Again, symmetries and conservation of the current dictate the form of the leading singularity in the correlator $\langle J_\mu \, \tilde{\sigma}_n(\mu)\rangle$. In this case, the singularity takes the form[9]

$$\langle J_i \, \tilde{\sigma}_n(\mu)\rangle = \frac{i\, k_n(\mu)}{2\pi} \, \frac{\epsilon_{ij}\, n^j}{y^{d-1}} \,, \qquad \langle J_a \, \sigma_n\rangle = 0 \,, \tag{3.26}$$

where ϵ_{ij} is the volume form in the two-dimensional space transverse to Σ. This parity-odd tensor appears in the correlator because of the magnetic flux carried by the generalized twist operator. We refer to k_n as the 'magnetic response,' since this parameter characterizes the response of the current to the magnetic flux.

Following [68], we can determine the value of k_n using the conformal mapping in the above discussion of spherical entangling surfaces. In this case, one begins with the charge density that appears in the grand canonical ensemble on the hyperbolic cylinder: $\langle J_{\tau_{\rm E}}\rangle = -i\rho(n,\mu)$. Now conformally mapping to the n-fold cover of R^d, this expectation value becomes

$$\langle J_\mu \, \tilde{\sigma}_n(\mu)\rangle_{flat} = \Omega^{d-2} \, \frac{\partial X^\alpha}{\partial Y^\mu} \, \langle J_\alpha\rangle_{hyperbolic} \,. \tag{3.27}$$

The form of the transformation is fixed because the current has conformal dimension d–1.[10] Now as indicated on the left-hand side of eq. (3.27), this mapping yields the correlator of

[9] Note that the correlators here and in eq. (3.23) are implicitly evaluated in the Euclidean path integral.

[10] One can also verify that this transformation (3.27) ensures that the charge operator (3.25) defined on the interior of the sphere, *i.e.,* $Q_{\rm A} = i\int_{t_{\rm E}=0, r<R} d^{d-1}x \, J_{t_{\rm E}}$, is just the conformal transformation of the charge defined by integrating $J_{\tau_{\rm E}}$ over the entire hyperbolic plane H^{d-1} — as is implicit in our discussions above.

the current with the spherical twist operator. Further, taking the limit where the current insertion approaches the twist operator, one recovers the leading singularity in eq. (3.26). Hence using eqs. (3.9) and (3.11), the magnetic response can be evaluated as

$$k_n(\mu) = 2\pi n\, R^{d-1}\, \rho(n,\mu)\,. \tag{3.28}$$

Here, the additional factor of n appears because the correlators in eq. (3.26) are understood to involve the the total current for the entire n-fold replicated CFT whereas eq. (3.27) corresponds to the insertion of J_μ on a single sheet of the n-fold cover. Hence we must multiply by an extra factor of n to compare the two expressions.

An interesting universal property of h_n was obtained for higher dimensional twist operators in [68, 69] (see also [102]):

$$\partial_n h_n|_{n=1} = 2\pi^{\frac{d}{2}+1}\, \frac{\Gamma\left(d/2\right)}{\Gamma(d+2)}\; C_T\,. \tag{3.29}$$

Here C_T is the central charge defined by the two-point function of the stress tensor[11]

$$\langle T_{\mu\nu}(x) T_{\rho\sigma}(0)\rangle = \frac{C_T}{x^{2d}}\, \mathcal{I}_{\mu\nu,\rho\sigma} \tag{3.30}$$

where

$$\mathcal{I}_{\mu\nu,\rho\sigma} = \frac{1}{2}(I_{\mu\rho}I_{\nu\sigma} + I_{\mu\sigma}I_{\nu\rho}) - \frac{1}{d}\delta_{\mu\nu}\delta_{\rho\sigma} \quad \text{with} \;\; I_{\mu\nu}(x) = \quad \delta_{\mu\nu} - 2\frac{x^\mu x^\nu}{|x|^2}\,. \tag{3.31}$$

In fact, similar universal properties is also found for higher derivatives of h_n in the vicinity of $n = 1$.

The above universal behaviour does not immediately extend to the conformal weight of the generalized twist operators $\tilde{\sigma}(\mu)$. Instead, the natural extension involves an expansion about both $n = 1$ and $\mu = 0$, as follows:

$$h_n(\mu) = \sum_{a,b} \frac{1}{a!\, b!}\; h_{ab}\; (n-1)^a\, \mu^b \tag{3.32}$$

[11]Note that our normalization for C_T here is a standard one but it is not the same as in [68]. Hence the numerical factors in eq. (3.29) are slightly different than in that reference.

where we defined the coefficients

$$h_{ab} \equiv (\partial_n)^a (\partial_\mu)^b \, h_n(\mu)\big|_{n=1,\mu=0} \,. \tag{3.33}$$

Note that the twist operator becomes trivial when $n = 1$ and $\mu = 0$ and hence the first term in this expansion vanishes, *i.e.,* $h_{00} = 0$. Further $h_{10} = \partial_n h_n(\mu)\big|_{n=1,\mu=0}$ is precisely the term appearing in eq. (3.29). Now recall the expression (3.24) for the weight, which we rewrite as

$$h_n(\mu) = \frac{2\pi n}{d-1} \, R^d \left(\langle T_{\tau_{\rm E}\tau_{\rm E}} \rangle\big|_{T_0/n,\mu} - \langle T_{\tau_{\rm E}\tau_{\rm E}} \rangle\big|_{T_0,\mu=0} \right). \tag{3.34}$$

in terms of the Euclidean stress tensor. Here both expectation values are in the grand canonical ensemble on the hyperbolic space. That is, in terms of the thermal density matrix given in eq. (3.15), the density matrix determining the second expectation value is $\rho_{\rm therm}(\mu = 0)$ while that in the first is $[\rho_{\rm therm}]^n$. Now we can produce the same double expansion as in eq. (3.32) by re-expressing the latter with

$$\left[e^{-H/T_0+\mu Q}\right]^n = e^{-H/T_0} \, \left[e^{-(n-1)H/T_0+n\mu Q}\right] \tag{3.35}$$

and expanding the last factor in terms of $n-1$ and μ [69, 102]. Here, we note that the manipulation in eq. (3.35) is valid since Q is a conserved charge and hence $[H, Q] = 0$. Now it is straightforward to show that the expansion coefficients h_{ab} in eq. (3.33) are given by

$$h_{ab} = \frac{2\pi}{d-1} R^d (\partial_n)^a (\partial_\mu)^b \left(n \, \frac{Z(T_0, \mu = 0)}{Z(T_0/n, \mu)} \langle T_{\tau_{\rm E}\tau_{\rm E}} e^{-(n-1)H/T_0+n\mu Q} \rangle - n \, \langle T_{\tau_{\rm E}\tau_{\rm E}} \rangle \right) \Big|_{n=1,\mu=0} \tag{3.36}$$

Note that both of the expectation values above are evaluated in the thermal ensemble with $T = T_0$ and $\mu = 0$. Hence these coefficients can be determined in terms of correlators of the stress tensor and the conserved current in the thermal bath on the hyperbolic geometry at temperature T_0. However, by applying the conformal transformation, these correlators may also be evaluated for the CFT vacuum in flat space.

Let us focus here on the corrections to the conformal dimension of the twist operator coming from a small chemical potential μ at $n = 1$, *i.e.,*

$$h_{0b} = \frac{2\pi \, R^d}{d-1} \, i^b \langle \, T_{\tau_{\rm E}\tau_{\rm E}} \, \prod_{i=1}^{b} \int_{H^{d-1}} d^{d-1}\sigma_i \, J_{\tau_{\rm E}}(\sigma_i) \, \rangle_c \tag{3.37}$$

where the subscript c denotes the connected correlator. Again, this correlator is evaluated in the thermal ensemble on the hyperbolic space with $T = T_0$ and $\mu = 0$. However, as noted above, it is convenient to transform back to flat space where the correlators will be evaluated in the CFT vacuum. First, however, we observe that if we evaluate the correlator in eq. (3.37) with a Euclidean path integral on $S^1 \times H^{d-1}$, then the stress tensor maybe inserted at any position in this background. Hence we choose to place $T_{\tau_{\rm E}\tau_{\rm E}}$ at $(\tau_{\rm E}, \sigma) = (\pi R, 0)$ which the conformal transformation then maps to $(t_{\rm E}, r) = (\infty, 0)$ in the corresponding flat space background. To be precise, with this choice, the conformal transformation yields the following simple expression:

$$T_{\tau_{\rm E}\tau_{\rm E}} = \lim_{t_{\rm E}\to\infty} \left(\frac{t_{\rm E}^2}{2R^2}\right)^d T_{t_{\rm E}t_{\rm E}}\,. \tag{3.38}$$

and so eq. (3.37) becomes

$$h_{0b} = \frac{2\pi\, R^d}{d-1}\, i^b \lim_{t_{\rm E}\to\infty} \left(\frac{t_{\rm E}^2}{2R^2}\right)^d \langle\, T_{t_{\rm E}t_{\rm E}} \prod_{i=1}^{b} \int_{r<R} d^{d-1}x_i\, J_{t_{\rm E}}(x_i)\,\rangle_c \tag{3.39}$$

One immediate observation is that in the CFT vacuum in flat space, the two-point correlator $\langle TJ\rangle$ will vanish and hence we must have $h_{01} = 0$. That is, the linear correction in μ to the conformal weight of the twist operator vanishes at $n = 1$.

Hence the leading contribution should appear at order μ^2 and is determined by the three-point correlator $\langle TJJ\rangle$. The latter correlation function has a universal form dictated by conformal symmetry, up to a few constants which are determined by the underlying CFT [103]. Therefore h_{02} can be determined entirely in terms of these few parameters. More explicitly, the $\langle TJJ\rangle$ correlator takes the following form in a d-dimensional CFT [103]

$$\langle\, T_{\mu\nu}(x_1)\, J_\gamma(x_2)\, J_\delta(x_3)\,\rangle = \frac{t_{\mu\nu\alpha\beta}(\mathbf{X_{23}})\, I_\gamma{}^\alpha(x_{21})\, I_\delta{}^\beta(x_{31})}{|x_{12}|^d |x_{13}|^d |x_{23}|^{d-2}}\,, \tag{3.40}$$

where

$$\mathbf{x_{12}} = \mathbf{x_1} - \mathbf{x_2}, \qquad \mathbf{X_{23}} = \frac{\mathbf{x_{21}}}{|x_{21}|^2} - \frac{\mathbf{x_{31}}}{|x_{31}|^2}, \qquad \hat{\mathbf{X}} = \frac{\mathbf{X}}{|\mathbf{X}|}, \tag{3.41}$$

where $|\mathbf{x}|$ is the norm of the vector. Recall that $I_{\mu\nu}(x)$ was defined in eq. (3.31) and further

we have

$$\begin{aligned} t_{\mu\nu\rho\sigma}(\mathbf{X}) &= \hat{a}\, h^1_{\mu\nu}(\hat{\mathbf{X}})\, \delta_{\rho\sigma} + \hat{b}\, h^1_{\mu\nu}(\hat{\mathbf{X}})\, h^1_{\rho\sigma}(\hat{\mathbf{X}}) + \hat{c}\, h^2_{\mu\nu\rho\sigma}(\hat{\mathbf{X}}) + \hat{e}\, h^3_{\mu\nu\rho\sigma}(\hat{\mathbf{X}})\,, \\ h^1_{\mu\nu}(\hat{\mathbf{X}}) &= \hat{X}^\mu \hat{X}^\nu - \frac{1}{d}\delta_{\mu\nu}\,, \\ h^2_{\mu\nu\rho\sigma}(\hat{\mathbf{X}}) &= \hat{X}^\mu \hat{X}^\rho\, \delta_{\nu\sigma} + \{\mu \leftrightarrow \nu, \rho \leftrightarrow \sigma\} \\ &\qquad -\frac{4}{d}\hat{X}^\mu \hat{X}^\nu \delta_{\rho\sigma} - \frac{4}{d}\hat{X}^\rho \hat{X}^\sigma \delta_{\mu\nu} + \frac{4}{d^2}\delta_{\mu\nu}\delta_{\rho\sigma}\,, \\ h^3_{\mu\nu\rho\sigma}(\hat{\mathbf{X}}) &= \delta_{\mu\rho}\delta_{\nu\sigma} + \delta_{\mu\sigma}\delta_{\nu\rho} - \frac{2}{d}\delta_{\mu\nu}\delta_{\rho\sigma}\,. \end{aligned} \tag{3.42}$$

The coefficients $\hat{a}, \hat{b}, \hat{c}, \hat{e}$ are the parameters characterizing the underlying CFT. However, only two of these constants are independent as they satisfy the following constraints [103]:

$$d\,\hat{a} - 2\,\hat{b} + 2(d-2)\,\hat{c} = 0\,, \qquad \hat{b} - d(d-2)\,\hat{e} = 0\,. \tag{3.43}$$

Notice that in the special case $d = 2$, both $\hat{a}$ and $\hat{b}$ vanish.

Now we only need to consider the correlator $\langle T_{t_{\rm E}t_{\rm E}}(x_1) J_{t_{\rm E}}(x_2) J_{t_{\rm E}}(x_3)\rangle$ in the limit that $x_1^0 \equiv \chi \to \infty$, $x_1^i = 0$, while $x_2^0 = x_3^0 = 0$ and $|x_2|, |x_3| < R$. To leading order in χ, we find

$$I_{00} \quad = -1 + \cdots\,, \qquad I_{ij} = \delta_{ij} + \cdots\,, \qquad I_{i0} = \mathcal{O}(1/\chi) \tag{3.44}$$

$$\tag{3.45}$$

This immediately implies that for $\mu = \nu = \gamma = \delta = 0$ in eq. (3.40), we need only consider t_{0000} to leading order and further we have

$$t_{0000} \to \frac{1}{d^2}(-d\,\hat{a} + \hat{b} + 4\,\hat{c} + 2d(d-1)\,\hat{e}) = \frac{2}{d}\hat{c} + \hat{e}\,. \tag{3.46}$$

Then for h_{02} in eq. (3.39), we are left with

$$\begin{aligned} &\langle T_{00}(x_1^0 \to \infty) \int_{|x_2|<R} d^{d-1}x_2 J_0(x_2) \int_{|x_3|<R} d^{d-1}x_3 J_0(x_3)\rangle \\ &\quad = \int_{|x_2|<R} d^{d-1}x_2 \int_{|x_3|<R} d^{d-1}x_3\, \frac{\frac{2}{d}\hat{c} + \hat{e}}{x_1^{2d}|x_{23}|^{d-2}}\,. \end{aligned} \tag{3.47}$$

The integral can be evaluated exactly. Using equation (3.39), we finally arrive at

$$h_{02} = -\frac{4\pi^{d-1}}{\Gamma(d+1)}\left(\frac{2}{d}\,\hat{c} + \hat{e}\right)\,. \tag{3.48}$$

Now an analogous double expansion about $n = 1$ and $\mu = 0$ can also be applied to the magnetic response:

$$k_n(\mu) = \sum_{a,b} \frac{1}{a!\, b!}\; k_{ab}\; (n-1)^a\, \mu^b \tag{3.49}$$

where we defined the coefficients

$$k_{ab} \equiv (\partial_n)^a (\partial_\mu)^b k_n(\mu)\big|_{n=1,\mu=0}\,. \tag{3.50}$$

Next we recall the expression (3.28), which we rewrite in terms of the Euclidean current as

$$k_n(\mu) = 2\pi i n\, R^{d-1}\, \langle J_{\tau_{\rm E}} \rangle\big|_{T_0/n,\mu}\,. \tag{3.51}$$

Again this expectation value is in the grand canonical ensemble on the hyperbolic space. Now following the same manipulations of the corresponding density matrix as in eq. (3.35), we arrive at the following expressions for k_{ab}

$$k_{ab} = 2\pi i\, R^{d-1}\, (\partial_n)^a (\partial_\mu)^b \left(n\, \frac{Z(T_0,\mu=0)}{Z(T_0/n,\mu)} \langle J_{\tau_{\rm E}} e^{-(n-1)H/T_0 + n\mu Q} \rangle \right) \Big|_{n=1,\mu=0} \tag{3.52}$$

where the remaining expectation value above is evaluated in the thermal ensemble with $T = T_0$ and $\mu = 0$. Hence these coefficients can again be determined in terms of correlators of the stress tensor and the conserved current in the thermal bath on the hyperbolic geometry at temperature T_0. However, by conformally mapping to flat space, the correlators may alternatively be evaluated in the CFT vacuum.

Let us evaluate a few coefficients for the low order contributions in the expansion (3.49). First, let us note that the coefficient k_{10} will determined in terms of the two-point correlator $\langle JT \rangle$ and so upon mapping this correlator back to flat space, we will find a vanishing result, *i.e.,* $k_{10} = 0$. Considering the next two coefficients, eq. (3.52) yields

$$\begin{aligned} k_{01} &= 2\pi i\, R^{d-1}\, \langle J_{\tau_{\rm E}}\, Q \rangle_c\,, & (3.53)\\ k_{11} &= -2\pi i\, R^{d-1} \left(\frac{1}{T_0} \langle J_{\tau_{\rm E}}\, Q\, H \rangle_c - 2 \langle J_{\tau_{\rm E}}\, Q \rangle_c \right)\,, & (3.54) \end{aligned}$$

where subscript c again denotes the connected correlators. These correlators can be evaluated following the approach described above in evaluating h_{02}. In particular, we conformally map

these expressions back to flat space after making a judicious choice for the position of the current insertion. The resulting three-point function in eq. (3.54) can be evaluated using the $\langle TJJ\rangle$ correlator given in eq. (3.40). Similarly, the two-point function appearing in both expressions can be evaluated using the current-current correlator

$$\langle J_\mu(x) J_\nu(0)\rangle = \frac{C_V}{x^{2(d-1)}}\, I_{\mu\nu}(x)\,, \tag{3.55}$$

where $I_{\mu\nu}(x)$ was defined in eq. (3.31). Note that a Ward identity relates the constant C_V to the parameters appearing in the three-point correlator (3.40) with [103]

$$C_V = \frac{2\pi^{d/2}}{\Gamma\left(\frac{d+2}{2}\right)}\,(\hat{c}+\hat{e})\ . \tag{3.56}$$

Without discussing the calculations in more detail, let us present the following results

$$\begin{aligned}
\langle J_{\tau_{\rm E}}\, Q\rangle_c &= -i\frac{\pi^{(d-1)/2}}{2^{d-2}(d-1)\Gamma((d-1)/2)}\,\frac{C_V}{R^{d-1}}\,,\\
\langle J_{\tau_{\rm E}}\, Q\, H\rangle_c &= -i\frac{2\pi^{d-2}}{d\Gamma(d-1)}\,\frac{1}{R^d}\left(\frac{2}{d}\hat{c}+\hat{e}\right)\,.
\end{aligned} \tag{3.57}$$

Substituting these results (3.57), as well as eq. (3.56), into eqs. (3.53) and (3.54) then yields

$$k_{01} = \frac{8\pi^d}{\Gamma(d+1)}(\hat{c}+\hat{e})\,, \tag{3.58}$$

$$k_{11} = \frac{8\pi^d}{d\Gamma(d+1)}(2\hat{c}-d(d-3)\hat{e})\,. \tag{3.59}$$

We might re-express the result for k_{01} in a form similar to that appearing in eq. (3.29) for the conformal weight, namely,

$$\partial_\mu k_n(\mu)|_{n=1,\mu=0} = 4\pi^{d/2}\frac{\Gamma\left(\frac{d+2}{2}\right)}{\Gamma(d+1)}\,C_V\,, \tag{3.60}$$

where C_V is the central charge appearing in the current-current correlator (3.55).

3.2.4 Generalized twist operators in d=2

In this subsection, we compute charged Rényi entropies using twist operators in a simple two-dimensional CFT.[12] In particular, we consider a free massless Dirac fermion ψ on an infinite

[12]The analysis in this section was first done by T. Takayanagi [104]. We thank him for sharing these results with us.

line and we are interested in the Rényi entropy of a subsystem $x \in [u, v]$. In accord with the review at the beginning of this section, the Rényi entropy can determined by evaluating the partition function of ψ on an n-sheeted cover of R^2, which is equivalent to the correlation function of twist operators inserted at the entangling surface, *i.e.,* the two points $x = u$, v [47, 48]. Let us first review the computation of the free fermion without the Wilson loop, as in [105, 106, 107]. On a n-fold cover, there is a branch cut connecting $x = u$ and v and each time we cross the branch cut, we change from one sheet to the next. Let us label the fermion on k-th sheet as ψ_k, where k runs from 1 to n. Then the fields on the different sheets are identified as follows:

$$\psi_k(e^{2\pi i}(w-u)) = \psi_{k+1}(w-u)\,, \qquad \psi_k(e^{2\pi i}(w-v)) = \psi_{k-1}(w-v)\,, \tag{3.61}$$

where we used the complexified coordinate $w = x + it_{\rm E}$. These boundary conditions can be 'diagonalized' by defining n new fields

$$\tilde{\psi}_m = \frac{1}{n}\sum_{k=1}^{n} e^{2\pi i k m/n}\,\psi_k \tag{3.62}$$

for which the boundary conditions (3.61) become

$$\tilde{\psi}_m(e^{2\pi i}(w-u)) = e^{2\pi i m/n}\tilde{\psi}_m(w-u)\,,\ \tilde{\psi}_m(e^{2\pi i}(w-v)) = e^{-2\pi i m/n}\tilde{\psi}_m(w-v) \tag{3.63}$$

where $m = -(n-1)/2, -(n-1)/2+1, \cdots, (n-1)/2$. The phase shifts in eq. (3.63) are generated by standard twist operators $\sigma_{m/n}$, each of which act only on the corresponding $\tilde{\psi}_m$ and which have conformal dimension $\Delta_m = \frac{1}{2}(m/n)^2$. The full twist operator σ_n appearing in evaluating the Rényi entropy can then be written as $\sigma_n = \prod \sigma_{m/n}$ and hence the desired correlator of the twist operators σ_n and σ_{-n} yields:

$$Z_n = \langle \sigma_n(u)\,\sigma_{-n}(v)\rangle = \prod_{m=-\frac{n-1}{2}}^{\frac{n-1}{2}} \langle \sigma_{m/n}(u)\,\sigma_{-m/n}(v)\rangle \sim |u-v|^{-4\Delta_n}\,, \tag{3.64}$$

where total conformal dimension Δ_n appearing above is given by

$$\Delta_n = \sum_{m=-\frac{n-1}{2}}^{\frac{n-1}{2}} \frac{1}{2}\left(\frac{m}{n}\right)^2 = \frac{1}{24}\left(n - \frac{1}{n}\right)\,. \tag{3.65}$$

Then applying eq. (3.5) to evaluate the Rényi entropy, we recover the well-known result

$$S_n = \frac{1}{6}\left(1+\frac{1}{n}\right)\log|u-v|\,. \tag{3.66}$$

We now generalize the above discussion to evaluate the charged Rényi entropy. In particular, the charge, which we consider here, will be that associated with global phase rotations of the fermion, $\psi \to e^{i\theta}\psi$. If we consider an imaginary chemical potential $\mu_{\rm E}$, the effect of the Wilson loop is easily represented by extending the original boundary conditions (3.61) to include a additional phase:

$$\psi_k(e^{2\pi i}(w-u)) = e^{i\mu_{\rm E}}\psi_{k+1}(w-u)\,, \qquad \psi_k(e^{2\pi i}(w-v)) = e^{-i\mu_{\rm E}}\psi_{k-1}(w-v) \tag{3.67}$$

Since this additional phase is added uniformly, the 'diagonal' fields (3.62) now satisfy

$$\begin{aligned}\tilde{\psi}_m(e^{2\pi i}(w-u)) &= e^{2\pi i m/n + i\mu_{\rm E}}\tilde{\psi}_m(w-u)\,,\\ \tilde{\psi}_m(e^{2\pi i}(w-v)) &= e^{-2\pi i m/n - i\mu_{\rm E}}\tilde{\psi}_m(w-v)\,.\end{aligned} \tag{3.68}$$

These phase shifts are accomplished by introducing twist operators, $\sigma_{\alpha(m,\mu_{\rm E})}$ and $\sigma_{-\alpha(m,\mu_{\rm E})}$, where

$$\alpha(m,\mu_{\rm E}) = \frac{m}{n} + \frac{\mu_{\rm E}}{2\pi} + \ell_m\,, \tag{3.69}$$

where m runs from $-\frac{n-1}{2}$ to $\frac{n-1}{2}$ as, before. The conformal dimension of these twist operators is now

$$\Delta_{\alpha(m,\mu_{\rm E})} = \frac{1}{2}\alpha(m,\mu_{\rm E})^2 = \frac{1}{2}\left(\frac{m}{n}+\frac{\mu_{\rm E}}{2\pi}+\ell_m\right)^2\,. \tag{3.70}$$

The constant ℓ_m appearing above is an integer which is chosen to minimize the conformal dimension of the corresponding twist operator. This freedom arises because of the ambiguity in defining the phase factors in eq. (3.68) modulo 2π. For example, shifting ℓ_m from 0 to 1 changes the corresponding phase factor by 2π and so leaves the corresponding boundary condition in eq. (3.68) unchanged. The conformal dimension (3.70) is always minimized by choosing ℓ_m so that the phase factor generated by the twist operator lies between $-\pi$ and π, *i.e.,* such that $-\frac{1}{2} \le \alpha(m,\mu_{\rm E}) \le \frac{1}{2}$.

When $\mu_{\rm E}$ is small enough that all of the phase factors lie between $-\pi$ and π, *i.e.,*

$$\left|\frac{m}{n}+\frac{\mu_{\rm E}}{2\pi}\right|\leq\frac{1}{2}\quad\text{for}\quad m\in\left[-\frac{n-1}{2},\frac{n-1}{2}\right], \tag{3.71}$$

we will have $\ell_m=0$ for all m. If we assume the latter holds, the conformal dimension of the generalized twist operator $\tilde{\sigma}_n=\prod\tilde{\sigma}_{\alpha(m,\mu_{\rm E})}$ becomes

$$\Delta_n=\frac{1}{24}\left(n-\frac{1}{n}\right)+\frac{n}{2}\left(\frac{\mu_{\rm E}}{2\pi}\right)^2, \tag{3.72}$$

and the charged Rényi entropy is given by

$$\tilde{S}_n(\mu_{\rm E})=\frac{1}{6}\left(1+\frac{1}{n}\right)\log|u-v|\,. \tag{3.73}$$

That is, for small $\mu_{\rm E}$, the charged Rényi entropy is exactly the same as the result in eq. (3.66), *i.e.,* the Rényi entropy without the Wilson line. As $\mu_{\rm E}$ increases, we can no longer choose all of the ℓ_m to be zero. The first transition occurs for $m=\frac{n-1}{2}$ when

$$\frac{n-1}{2n}+\frac{\mu_{\rm E}}{2\pi}=\frac{1}{2}\quad\longleftrightarrow\quad\mu_{\rm E}=\frac{\pi}{n} \tag{3.74}$$

beyond which the naive phase factor would be larger than π. Setting $\ell_{\frac{n-1}{2}}=-1$ and using the appropriate conformal dimension, we find that the charged Rényi entropy within the range $\frac{\pi}{n}\leq\mu_{\rm E}<\frac{3\pi}{n}$ becomes

$$\tilde{S}_n(\mu_{\rm E})=\left[\frac{1}{6}\left(1+\frac{1}{n}\right)-\frac{4}{n-1}\left(\frac{\mu_{\rm E}}{2\pi}-\frac{1}{2n}\right)\right]\log|u-v|\,. \tag{3.75}$$

Further phase transitions occur whenever $\mu_{\rm E}=\frac{\pi}{n}(2k+1)$. For example, for $\frac{3\pi}{n}\leq\mu_{\rm E}<\frac{5\pi}{n}$, the charged Rényi entropy becomes

$$\tilde{S}_n(\mu_{\rm E})=\left[\frac{1}{6}\left(1+\frac{1}{n}\right)+\frac{4}{n-1}\left(\frac{\mu_{\rm E}}{2\pi}-\frac{5}{2n}\right)\right]\log|u-v|\,. \tag{3.76}$$

Of course, it is straightforward to extend these results to all values of $\mu_{\rm E}$. As can be anticipated from eq. (3.67), the charged Rényi entropy exhibits a periodicity

$$\tilde{S}_n(\mu_{\rm E})=\tilde{S}_n(\mu_{\rm E}+2\pi)\,. \tag{3.77}$$

Hence within a single period, there will be n separate branches running from $\mu_{\rm E}=\frac{\pi}{n}(2k-1)$ to $\frac{\pi}{n}(2k+1)$ for integer k. The result for $n=3$ is shown in figure 3.1. Of course, these results

show that the charged Rényi entropy is a non-analytic function of $\mu_{\rm E}$ and n. In particular, we might note that the apparent singularities at $n = 1$ in eqs. (3.75) and (3.76) are not physical. As a final comment, we remark that the results derived here using twist operators agree with those coming from the heat kernel computations in Appendix 3.5.

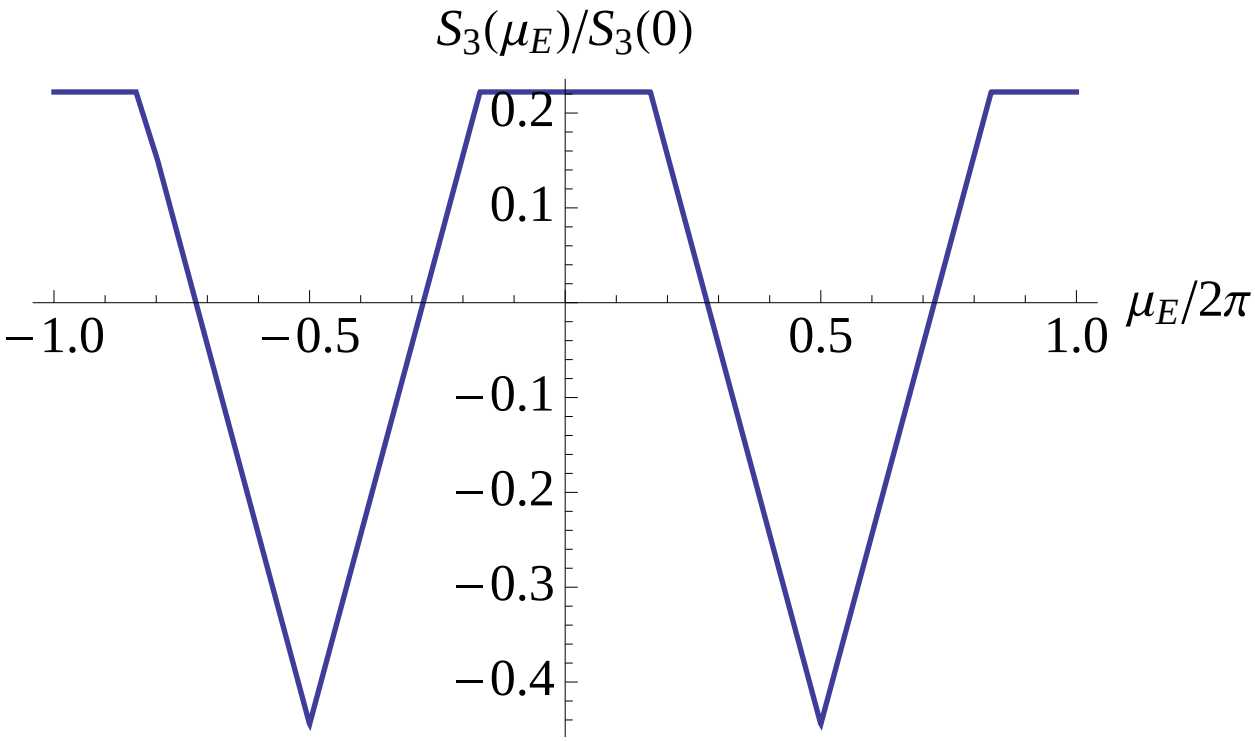

Figure 3.1: Charged Rényi entropy with $n = 3$ for a two-dimensional free fermion as a function of $\mu_{\rm E}$.

3.3 Holographic computations

In this section we calculate holographic Rényi entropies for boundary theories dual to Einstein gravity coupled to a Maxwell gauge field in the bulk. The relevant bulk solutions are charged topological black holes with hyperbolic horizons. These solutions represent the grand canonical ensemble of the boundary CFT on the hyperbolic cylinder. We only present the salient steps in the following calculations and refer the reader to [68] for a detailed

description of how the holographic Rényi entropies are calculated. We consider boundary theories in dimension $d \geq 3$ here and provide holographic calculations for $d = 2$ in appendix 3.6.

3.3.1 Charged black hole solution

In $d+1$ bulk dimensions, we write the Einstein-Maxwell action with negative cosmological constant as[13]

$$I_{E-M} = \frac{1}{2\ell_{\rm P}^{d-1}} \int d^{d+1}x \, \sqrt{-g} \left(\frac{d(d-1)}{L^2} + \mathcal{R} - \frac{\ell_*^2}{4} F_{\mu\nu} F^{\mu\nu} \right) . \tag{3.78}$$

For $d \geq 3$, the metric for the charged topological black hole takes the form

$$ds^2 = -f(r) \frac{L^2}{R^2} \, d\tau^2 + \frac{dr^2}{f(r)} + r^2 \, d\Sigma_{d-1}^2 \, , \tag{3.79}$$

with

$$f(r) = \frac{r^2}{L^2} - 1 - \frac{m}{r^{d-2}} + \frac{q^2}{r^{2d-4}} \tag{3.80}$$

where $d\Sigma_{d-1}^2 = du^2 + \sinh^2 u \, d\Omega_{d-2}^2$ is the metric on H^{d-1} with unit curvature. Note that the time coordinate is normalized here [67] so that the boundary metric naturally becomes $ds_{CFT}^2 = -d\tau^2 + R^2 d\Sigma_{d-1}^2$, *i.e.,* the Minkowski continuation of eq. (3.12). The corresponding bulk gauge field is

$$A = \left(\sqrt{\frac{2(d-1)}{(d-2)}} \frac{L \, q}{R \ell_* \, r^{d-2}} - \frac{\mu}{2\pi R} \right) d\tau \, , \tag{3.81}$$

The chemical potential μ is fixed by requiring that the gauge field vanish at the horizon $r = r_H$, *i.e.,*

$$\mu = 2\pi \sqrt{\frac{2(d-1)}{(d-2)}} \frac{L \, q}{\ell_* r_H^{d-2}} \, . \tag{3.82}$$

The mass parameter m is related to the horizon radius r_H by

$$m = \frac{r_H^{d-2}}{L^2} (r_H^2 - L^2) + \frac{q^2}{r_H^{d-2}} \, . \tag{3.83}$$

[13]The scale ℓ_* appearing in the prefactor of the Maxwell term should be fixed by the details of the boundary theory. With this notation, the $(d+1)$-dimensional gauge coupling becomes $g_5^2 = 2\ell_{\rm P}^{d-1}/\ell_*^2$.

Hence, we may rewrite the function $f(r)$ (3.80) in terms of the horizon radius r_H and the charge q, giving

$$f(r) = \frac{r^2}{L^2} - 1 + \frac{q^2}{r^{2d-4}} - \left(\frac{r_H}{r}\right)^{d-2} \left(\frac{r_H^2}{L^2} - 1 + \frac{q^2}{r_H^{2d-4}}\right) . \tag{3.84}$$

The temperature of this black hole is given by

$$T = \frac{T_0}{2}\, L f'(r_H) = \frac{T_0}{2} \left[d\, \frac{r_H}{L} - (d-2) \frac{L}{r_H} \left(1 + \frac{d-2}{2(d-1)} \left(\frac{\mu\, \ell_*}{2\pi L} \right)^2 \right) \right] \tag{3.85}$$

where T_0 is the temperature given in eq. (3.13) and the 'prime' denotes differentiation with respect to r. The thermal entropy is given by the Bekenstein-Hawking formula

$$S = \frac{2\pi}{\ell_{\rm P}^{d-1}} V_\Sigma\, r_H^{d-1} , \tag{3.86}$$

where V_Σ denotes the regulated (dimensionless) volume of the hyperbolic plane H^{d-1}, as described in [68]. Recall that this volume is a function of R/δ, the ratio of the radius of the entangling sphere to the short-distance cut-off in the boundary theory. Further the leading contribution takes the form

$$V_\Sigma \simeq \frac{\Omega_{d-2}}{d-2}\, \frac{R^{d-2}}{\delta^{d-2}} + \cdots , \tag{3.87}$$

where $\Omega_{d-2} = 2\pi^{(d-1)/2}/\Gamma((d-1)/2)$ is the area of a unit (d–2)-sphere. Hence the corresponding Rényi entropies in the following begin with an area law contribution.

As a final comment, we note that we have presented the Minkowski-signature solution here with a real chemical potential μ. This gives the holographic representation of the grand canonical ensemble on the hyperbolic cylinder $R \times H^{d-1}$. One can easily transform to Euclidean signature by replacing $\tau = -i\tau_{\rm E}$ to produce the dual of the thermal ensemble for the boundary CFT on $S^1 \times H^{d-1}$. In this replacement, the form of the metric function $f(r)$ is unchanged and as usual, the Euclidean time is made periodic with $\Delta\tau_{\rm E} = 1/T$ to ensure that the bulk geometry is smooth at $r = r_H$. The gauge field becomes imaginary for this Euclidean bulk solution. Of course, the latter is in keeping with our discussion of the Euclidean path integral in section 3.2, where an imaginary background gauge field was introduced to describe the grand canonical ensemble. Here, this background field in the boundary theory is simply given by the non-normalizable of the bulk gauge field, *i.e.,* $B_\mu = -\lim_{r\to\infty} A_\mu$.

3.3.2 Charged Rényi entropies

Applying eq. (3.22) with a real chemical potential, we see that the charged Rényi entropy for a spherical entangling surface can be expressed as

$$S_n(\mu) = \frac{n}{n-1}\frac{1}{T_0}\int_{x_n}^{x_1} S(x,\mu)\,\partial_x T(x,\mu)\,dx\,, \tag{3.88}$$

where $x = r_H/L$ and $S(x,\mu)$ is the horizon entropy (3.86). Evaluating eq. (3.85) in terms of x gives

$$T(x,\mu) = \frac{T_0}{2x}\left(dx^2 - (d-2) - \frac{(d-2)^2}{2(d-1)}\left(\frac{\mu\ell_*}{2\pi L}\right)^2\right)\,. \tag{3.89}$$

Then x_n is the largest solution of $T(x_n,\mu) = T_0/n$ and is given by

$$x_n = \frac{1}{dn} + \sqrt{\frac{1}{d^2n^2} + \frac{d-2}{d} + \frac{(d-2)^2}{2d(d-1)}\left(\frac{\mu\ell_*}{2\pi L}\right)^2}\,. \tag{3.90}$$

Combining these expressions then yields

$$S_n(\mu) \;=\; \pi V_\Sigma \left(\frac{L}{\ell_{\rm P}}\right)^{d-1}\frac{n}{n-1}\left[\left(1 + \frac{d-2}{2(d-1)}\left(\frac{\mu\ell_*}{2\pi L}\right)^2\right)(x_1^{d-2} - x_n^{d-2}) + x_1^d - x_n^d\right]\,. \tag{3.91}$$

Note that when $\ell_* = 0$, eqs. (3.90) and (3.91) reduce to the results found in [68].

Expressions for the charged Rényi entropy with specific choices for n are:

$$\begin{aligned}
\lim_{n\to 0} S_n &= \pi V_\Sigma \left(\frac{L}{\ell_{\rm P}}\right)^{d-1}\left(\frac{2}{d}\right)^d \frac{1}{n^{d-1}} \qquad (3.92)\\
S_{\rm EE} = \lim_{n\to 1} S_n &= \pi V_\Sigma \left(\frac{L}{\ell_{\rm P}}\right)^{d-1}\frac{(d-2)x_1^{d-2}}{dx_1 - 1}\left(1 + \frac{d-2}{2(d-1)}\left(\frac{\mu\ell_*}{2\pi L}\right)^2 + \frac{d\,x_1^2}{d-2}\right)\\
S_2 &= 2\pi V_\Sigma \left(\frac{L}{\ell_{\rm P}}\right)^{d-1}\left(\left(1 + \frac{d-2}{2(d-1)}\left(\frac{\mu\ell_*}{2\pi L}\right)^2\right)(x_1^{d-2} - x_2^{d-2}) + x_1^d - x_2^d\right)\\
\lim_{n\to\infty} S_n &= \pi V_\Sigma \left(\frac{L}{\ell_{\rm P}}\right)^{d-1}\left(\left(1 + \frac{d-2}{2(d-1)}\left(\frac{\mu\ell_*}{2\pi L}\right)^2\right)(x_1^{d-2} - x_\infty^{d-2}) + x_1^d - x_\infty^d\right)
\end{aligned}$$

where

$$x_\infty^2 = \frac{d-2}{d}\left(1 + \frac{d-2}{2(d-1)}\left(\frac{\mu\ell_*}{2\pi L}\right)^2\right)\,. \tag{3.93}$$

Another interesting limit to consider is holding n fixed while $\mu \to \infty$, which yields

$$\lim_{\mu\to\infty} S_n(\mu) = 2\pi V_\Sigma \left(\frac{(d-2)^2}{2d(d-1)}\right)^{\frac{d-1}{2}} \left(\frac{\ell_*}{\ell_{\rm P}}\right)^{d-1} \left(\frac{\mu}{2\pi}\right)^{d-1} . \tag{3.94}$$

Hence we have the curious result that, to leading order in μ, the Rényi entropies are independent of n in this limit.

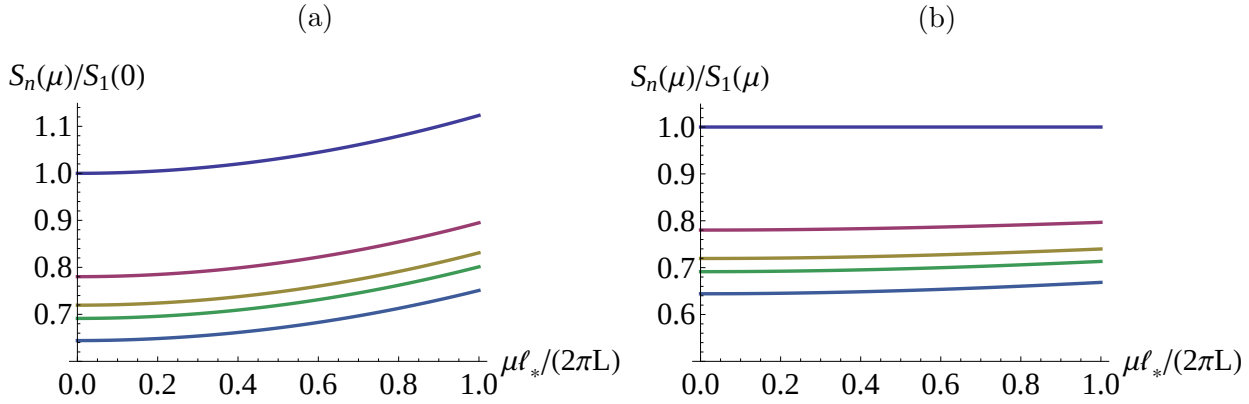

Figure 3.2: The $d = 3$ charged Rényi entropy (normalized by (a) $S_1(0)$ and (b) $S_1(\mu)$) as a function of μ. The curves correspond to (from top to bottom) n=1,2,3,4,10

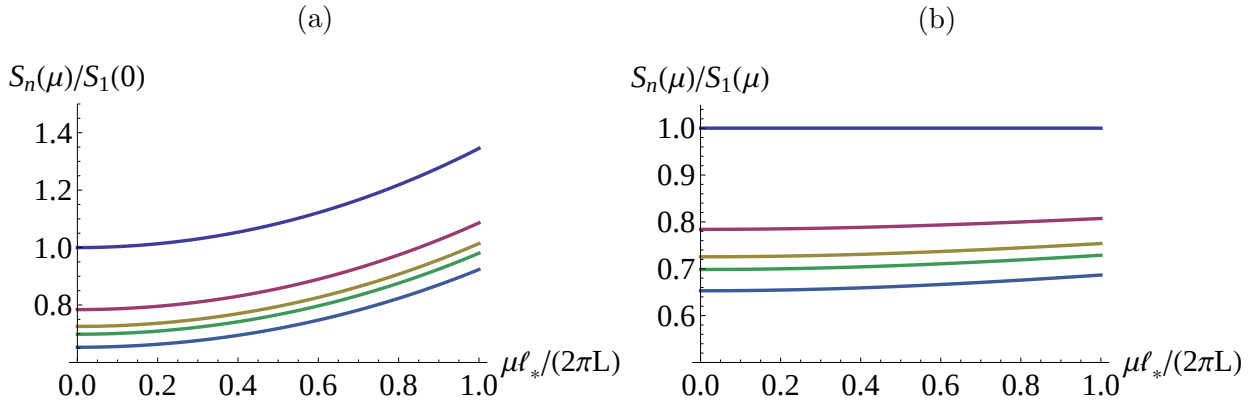

Figure 3.3: The $d = 4$ charged Rényi entropy (normalized by (a) $S_1(0)$ and (b) $S_1(\mu)$) as a function of μ. The curves correspond to (from top to bottom) n=1,2,3,4,10

The results for the charge Rényi entropy (3.91) are illustrated in figures 3.2 and 3.3, which plot $S_n(\mu)$ as a function of μ for various values of n in $d = 3$ and 4. In these figures,

it is evident that for fixed μ, the Rényi entropy decreases as n increases. This behaviour is also shown in figure 3.4a where the charged Rényi entropy in $d = 3$ is shown as a function of n. The figure shows very clearly in this example that $\partial_n S_n(\mu) < 0$. As discussed in [68] (see also [91]), standard Rényi entropies must satisfy various inequalities:

$$\begin{aligned} \frac{\partial S_n}{\partial n} &\leq 0\,, & \frac{\partial}{\partial n}\left(\frac{n-1}{n} S_n\right) &\geq 0\,, \\ \frac{\partial}{\partial n}((n-1)S_n) &\geq 0\,, & \frac{\partial^2}{\partial n^2}((n-1)S_n) &\leq 0\,. \end{aligned} \tag{3.95}$$

By examining plots of the numerical results, *e.g.,* see $\frac{n-1}{n} S_n(\mu)$ in figure 3.4b, we find that these inequalities still appear to hold in the charged case. The analysis in [68] found that this result essentially follows from the connection between the Rényi entropies for a spherical entangling surface and the thermal entropy on the hyperbolic cylinder $R \times H^{d-1}$. In particular, it follows that these inequalities (3.95) will be satisfied for any CFT, as long as the corresponding thermal ensemble is stable. Thus we expect that the inequalities (3.95) will continue to hold for charged Rényi entropies. Of course, the arguments in [68] will not apply where the Rényi entropies exhibit phase transitions [108], as discussed in section 3.3.4.

As we mentioned above, both real and imaginary chemical potentials are of interest. Our holographic results are easily analytically continued to imaginary chemical potential by simply replacing $\mu = i\mu_{\rm E}$ and $q = iq_{\rm E}$. Note that with this replacement, the root x_n in eq. (3.90) fails to exist if $\mu_{\rm E}$ becomes too large. The region of validity of analytically continued solutions is given by

$$\mu_{\rm E}^2 \leq \frac{8\pi^2(d-1)}{d-2}\left(\frac{L}{\ell_*}\right)^2\left(1 + \frac{1}{d(d-2)n^2}\right)\,. \tag{3.96}$$

If $\mu_{\rm E}$ increases beyond this bound (with fixed n), the event horizon disappears and we are left with a naked singularity. Typical results for the charged Rényi entropy with imaginary chemical potential are shown in figure 3.5. In comparing the figures, we see that while the charged Rényi entropy increases slowly with increasing μ in figures 3.2 and 3.3, $\tilde{S}_n(\mu_{\rm E})$ decreases, and in a much more dramatic fashion, as $\mu_{\rm E}$ increases in figure 3.5.

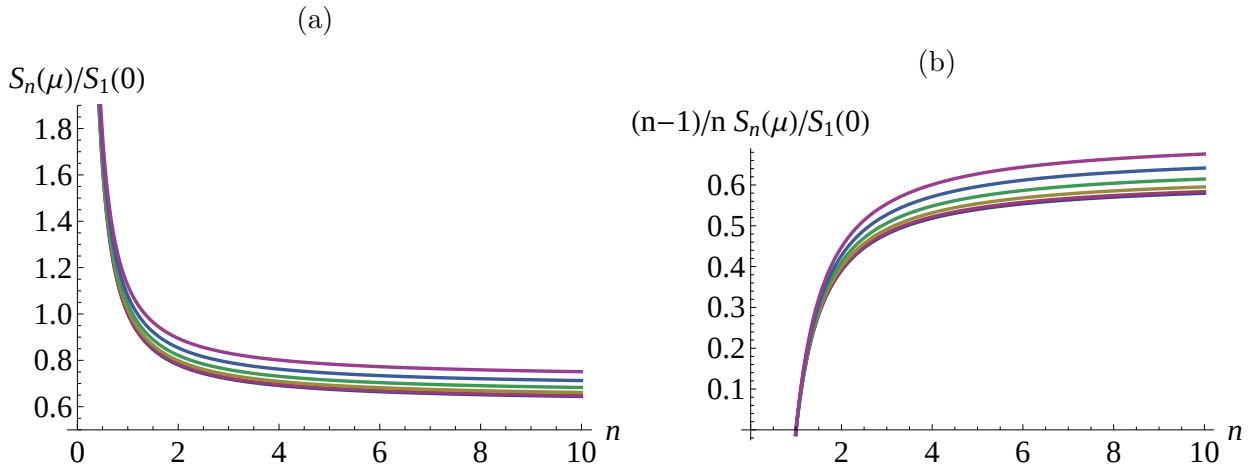

Figure 3.4: The charged Rényi entropy (normalized by $S_1(0)$) in $d = 3$ shown function of n in panel (a). In panel (b), we show $\frac{n-1}{n} S_n(\mu)$ as a function of n. Note that the slope of the curves is negative in panel (a) and positive in panel (b). In both cases, the curves correspond to (from top to bottom) $\frac{\mu \ell_*}{2\pi L} = 1.0, 0.8, 0.6, 0.4, 0.2$ and 0.0.

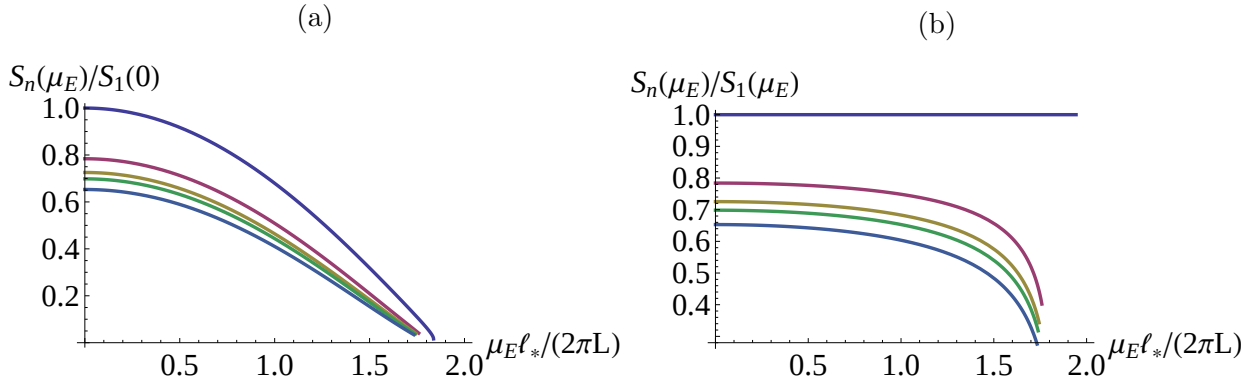

Figure 3.5: The $d = 4$ charged Rényi entropy (normalized by (a) $\tilde{S}_1(0)$ and (b) $\tilde{S}_1(\mu_E)$) as a function of the imaginary chemical potential μ_E. The curves correspond to (from top to bottom) n=1,2,3,4,10

3.3.3 Twist operators

In section 3.2.3, we derived various expressions for the conformal weight and the magnetic response of the twist operators, as well as various expansion coefficients appearing in these. Here we wish to examine these properties of the twist operators in the boundary CFT dual

to the Einstein-Maxwell theory (3.78).

To begin, recall eq. (3.24) for the conformal weight of the twist operator,

$$h_n(\mu) = \frac{2\pi n}{d-1} R^d \left(\mathcal{E}(T_0, \mu = 0) - \mathcal{E}(T_0/n, \mu)\right). \tag{3.97}$$

The details of the holographic calculation of the corresponding energy densities are given in appendix 3.7.1. Then using eq. (3.208), the desired conformal weight can be written as

$$h_n(\mu) \;=\; n\pi \frac{L^{d-1}}{\ell_{\rm P}^{d-1}} \left(x_n^{d-2}(1-x_n^2) - \frac{x_n^{d-2}(d-2)}{2(d-1)} \left(\frac{\mu \ell_*}{2\pi L}\right)^2 \right). \tag{3.98}$$

Here we might note that this result can be expressed entirely in terms of parameters in the boundary theory using eqs. (3.219) and (3.222), which show that $L^{d-1}/\ell_{\rm P}^{d-1} \sim C_T$ and $\ell_*^2 L^{d-3}/\ell_{\rm P}^{d-1} \sim C_V$.

Next we would like to recover eqs. (3.29) and (3.48) for the expansion coefficients of the above conformal weight. Hence given eq. (3.98), we evaluated the following two coefficients:

$$h_{10} = \partial_n h_n(\mu)|_{n=1,\mu=0} \;=\; \frac{2\pi}{d-1} \frac{L^{d-1}}{\ell_{\rm P}^{d-1}}, \tag{3.99}$$

$$h_{02} = \partial_\mu^2 h_n(\mu)|_{n=1,\mu=0} \;=\; -\frac{(d-2)(2d-3)}{4\pi(d-1)^2} \frac{\ell_*^2 L^{d-3}}{\ell_{\rm P}^{d-1}}. \tag{3.100}$$

At this point, using eq. (3.222), we can substitute for C_T in terms of the ratio $L^{d-1}/\ell_{\rm P}^{d-1}$ in eq. (3.29) and we recover precisely eq. (3.99). Similarly, using eqs. (3.220) and (3.221) in eq. (3.48), we reproduce exactly the expression in eq. (3.100). We also note that $h_{01} = \partial_\mu h_n(\mu)|_{n=1,\mu=0} = 0$ from eq. (3.98), which is in agreement with our general expectations in section 3.2.3.

Now we turn our attention to the magnetic response, which was given by eq. (3.28),

$$k_n(\mu) = 2\pi n R^{d-1} \rho(n, \mu). \tag{3.101}$$

Now in the holographic framework, we know that the charge density, *i.e.,* $\langle J_\tau \rangle$ is determined by the normalizable component of the gauge field (3.81), however, we leave its determination, including the precise normalization, to appendix 3.7.2. Substituting the holographic result (3.212) into eq. (3.101), we find the magnetic response in our holographic model is

$$k_n(\mu) = \frac{d-2}{2} \frac{\ell_*^2 L^{d-3}}{\ell_{\rm P}^{d-1}} n x_n^{d-2} \mu. \tag{3.102}$$

Again, this result can be expressed entirely in terms of parameters of the boundary CFT using eq. (3.219). As above, we would like to examine the expansion coefficients of the above magnetic response and hence we calculate

$$k_{01} = \partial_\mu k_n(\mu)|_{n=1,\mu=0} = \frac{d-2}{2}\,\frac{\ell_*^2\,L^{d-3}}{\ell_{\rm P}^{d-1}}\,, \tag{3.103}$$

$$k_{11} = \partial_n\partial_\mu k_n(\mu)|_{n=1,\mu=0} = \frac{d-2}{2(d-1)}\,\frac{\ell_*^2\,L^{d-3}}{\ell_{\rm P}^{d-1}}\,. \tag{3.104}$$

These two coefficients can then be compared with eqs. (3.58) and (3.59) using the results in appendix 3.7.3. As expected, the holographic expression (3.219) of C_V yields a precise agreement of eq. (3.103) above with eqs. (3.58) and (3.60) in section 3.2.3. Similarly, eqs. (3.59) and (3.104) match exactly using eqs. (3.220) and (3.221).

3.3.4 Thermodynamics, stability and phase transitions

It is natural to investigate the thermodynamical properties of the charged hyperbolic black holes. Thermodynamical instability in some regions of phase space could be responsible for interesting features in the Rényi entropies. One could also imagine that at low temperatures, a different geometry would be prefered over the black hole phase, and the system would go through a Hawking-Page phase transition as the temperature is increased. It turns out none of these features occur for charged hyperbolic black hole in the grand canonical ensemble. The Gibbs free energy $G = (M - M_c) - TS - \mu q$ was calculated in [109]:

$$G = -\frac{V_\Sigma\, r_H^{d-2}}{2\,\ell_{\rm P}^{d-1}}\left(1 + \frac{(d-2)}{2(d-1)}\left(\frac{\mu\,\ell_*}{2\pi\,L}\right)^2 + \frac{r_H^2}{L^2} - m_c(\mu)\right) \tag{3.105}$$

where $m_c(\mu)$ is the critical mass at which the temperature vanishes, *i.e.,*

$$m_c = -2(d-1)r_c^{n-1}\left(1 - \frac{(d-1)r_c^2}{(d-2)L^2}\right) \quad \text{with} \quad \frac{r_c^2}{L^2} = \frac{d-2}{d}\left(1 + \frac{(d-2)}{2(d-1)}\left(\frac{\mu\,\ell_*}{2\pi\,L}\right)^2\right) \tag{3.106}$$

One can check that the Gibbs energy is always negative and equals zero when the black hole is extremal, excluding any Hawking-Page phase transition. The specific heat was calculated

in [109] as well:

$$C_\mu = T\left(\frac{\partial S}{\partial T}\right)_\mu = \frac{8\pi^2(d-1)V_\Sigma T r_H^d}{(d-2)\ell_{\rm P}^{d-1}}\left(1+\frac{d}{d-2}\frac{r_H^2}{L^2}+\frac{d-2}{d-1}\left(\frac{\mu\,\ell_*}{2\pi L}\right)^2\right)^{-1} \tag{3.107}$$

which is always positive, meaning the black holes are thermodynamically stable.

Before leaving the subject of instabilities, it is interesting to note that the presence of a light scalar in the bulk would render the black holes unstable at low temperatures. Indeed, the extremal charged black hole has a $AdS_2 \times H^{d-1}$ near horizon geometry, where the relative radii of the two spaces depends on the charge:

$$L^2_{AdS_2} = \frac{2L^2_{AdS_{d+1}}}{f''(r_H)} \qquad L^2_{H^{d-1}} = r_H^2 \tag{3.108}$$

with $f(r)$ is the metric function in eq. (3.80) above. For simplicity, let us consider a neutral scalar. The extremal black hole will develop scalar hair if the mass of the scalar is below the BF bound of the near-horizon AdS_2. We wish to consider normalizable modes and these must depend on the hyperbolic coordinates, as the volume of the hyperboloid is infinite. Normalizable modes can be expanded in eigenvalues of the Laplacian as $\nabla^2_{H^{d-1}}\phi = -\lambda\phi$ with $\lambda > (d-2)^2/4$ and near the horizon, this Laplacian will generate an effective shift of the mass of the scalar. Thus we exepct an instability if the scalar mass M lies in the range

$$-\frac{d^2}{4} < M^2L^2 < -\frac{f''(r_H)}{8} - \frac{(d-2)^2}{4r_H^2}\ . \tag{3.109}$$

It turns out the two terms on the right-hand side of this equation combine in such a way that the answer does not depend on charge:

$$-\frac{d^2}{4} < M^2L^2 < -\frac{d(d-1)}{4} \tag{3.110}$$

found in [108]. It seems that at zero temperature, a neutral scalar will not detect changes in the geometry induced by charge. Turning our attention to charged scalars, it was noted in [85] that the effect of the charge will be to induce a shift in the scalar mass. This only makes things worse and a scalar instability is therefore expected as well. We leave the detailed analysis of these effects for future work but note that the Rényi entropies should exhibit phase transitions as n is varied, if light scalars are present in the bulk spectrum.

3.4 Discussion

We have examined a new class of entanglement measures (3.2) which extend the usual definition of Rényi entropy to include a chemical potential for a conserved global charge. These charged Rényi entropies measure the degree of entanglement in different charge sectors of the theory. As described in section 3.2, the evaluation of these entropies proceeds as usual with a Euclidean path integral, but with the addition of a (fixed) background gauge field which introduces a Wilson line, proportional to the chemical potential, around the entangling surface. The latter can be interpreted as binding a sheet of magnetic flux to the standard twist operators which appear in evaluating the Rényi entropy.

For the special case of a CFT with a spherical entangling surface, we can apply a conformal transformation to map charged Rényi entropies to the thermal entropies of a grand canonical ensemble, albeit on the hyperbolic cylinder $R \times H^{d-1}$. This allows us to study the properties of the generalized twist operators, as discussed in section 3.2.3. In particular, the conformal weight and the magnetic response of these twist operators are related to the energy density and the charge density, respectively, in the thermal ensemble on the hyperbolic cylinder. These two parameters are functions of both n and μ and exhibit certain universal characteristics when expanded in the vicinity of $n = 1$ and $\mu = 0$.

In section 3.3, we considered computations of charged Rényi entropies using holography, where they are related to the thermal entropy of charged black holes with hyperbolic horizons. In addition to determining the charged Rényi entropy, we were able to determine the conformal weight and magnetic response of the corresponding twist operators in this holographic model. In a particular, we were able to recover the universal behaviour exhibited by the expansion coefficients in, *e.g.,* eq. (3.60). In section 3.2.4 and appendix 3.5, we described the computation of charged Rényi entropies for free field theories. We found the results to be in qualitative agreement with our holographic calculations. A particularly interesting point of comparison is $d = 2$, which was considered in section 3.2.4 for free fermions, and in appendix 3.6 for holographic models. For free bosons, we observed that the Rényi entropy is non-analytic at $\mu_{\rm E} = 0$. Thus, while there is a range where free fermions can be analytically

continued to the real chemical potential, free bosons can not be so continued.

We found that the charged Rényi entropy in the holographic model obeyed various inequalities (3.95), which were originally established for the standard Rényi entropy without a chemical potential. Following [68], we argued that the stability of the grand canonical ensemble on the hyperbolic geometry was sufficient to guarantee these inequalities would be satisfied by the charged Rényi entropy. However, if one examines the origin of these inequalities [91], the derivation only relied on the fact that the Rényi entropies are moments of a probability distribution with $p_i > 0$ and $\sum_i p_i = 1$. The same statement applies for the charged Rényi entropies (with real chemical potential) and so we can expect that eq. (3.95) will be satisfied quite broadly for these new entanglement measures. It would be interesting to explicitly study the validity of these inequalities for more general QFT's and choices of entangling surface. At the same time, it would be interesting to investigate whether derivatives of $S_n(\mu)$ with respect to μ also satisfy any general properties. For example, in figures (3.2) and (3.3), it seems that $\mu \frac{\partial S_n(\mu)}{\partial \mu} \geq 0$ for our holographic model. Note that an imaginary chemical potential does not respect the above inequality. In particular, the Rényi entries and the free energies can take negative values. The analytic continuation between the imaginary and the real chemical potentials is non-trivial because of poles and branch cuts. In gravity, the regular black hole space time ceases to exist for large μ_{E}, *i.e.,* eq. (3.96).

There are several natural generalizations of the investigations presented here. For example, the holographic computations could be extended to consider bulk theories with higher derivative interactions (*e.g.,* Gauss-Bonnet or F^4 terms), following [110, 111, 112]. Another interesting direction would be to connect our holographic calculations to the large-N limit of super Rényi entropy for the ABJM model in [94].

It may also be of interest to consider a generalization of the Rényi entropy for fixed charge ensembles (instead of fixing the chemical potential). Here, the holographic computations may produce some interesting new behaviour. Finally, in the case of a spherical entangling surface (where the system is rotationally invariant) it is natural to label the states by their angular momentum and introduce a conjugate chemical potential to produce a 'rotating Rényi entropy' — see also [66]. The corresponding holographic calculations would involve

more general classes of spinning hyperbolic black holes. A study of such rotating Rényi entropies at fixed angular potential, as well as charge, could follow very closely the present discussion. Results along these lines will be presented in [113].

Acknowledgments

We would like to thank Horacio Casini, Steve Shenker and especially Tadashi Takayanagi for helpful discussions. Research at Perimeter Institute is supported by the Government of Canada through Industry Canada and by the Province of Ontario through the Ministry of Research & Innovation. AM and RCM gratefully acknowledge support from NSERC Discovery grants. Research by RCM is further supported by funding from the Canadian Institute for Advanced Research. TS acknowledges support from an NSERC Graduate Fellowship.

3.5 Appendix A: Free QFT computations

Here we consider various calculations of charged Rényi entropies for free fields using the heat kernel methods on hyperbolic spaces, and also by direct summing of appropriate modes on spheres. These QFT computations are most readily done if the chemical potential takes is purely imaginary values, *i.e.,* $\mu = i\mu_{\rm E}$ where $\mu_{\rm E}$ is real. In this case, the chemical potential produces to a non-trivial boundary condition. As in section 3.2, we are interested in conformal theories and hence we consider calculations for a massless conformally coupled and complex scalar and for a free massless Dirac fermion. In both cases, the global charge is simply related with phase rotations of the corresponding field.

3.5.1 Heat kernels on $S^1 \times H^{d-1}$

To begin, we gather a few useful results for heat kernel methods [114, 115, 116, 117, 118]. First, heat kernels on a product manifold factorize, for both fermions and bosons,

$$K_{S^1\times H^{d-1}}(\{x_i\},\{y_i\},t) = K_{S^1}(x_1,y_1,t)K_{H^{d-1}}(x_{2,\cdots,d},y_{2,\cdots,d},t) \tag{3.111}$$

The total free energy in $S^1 \times H^{d-1}$ is

$$F = -\frac{(-)^f}{2} \int d^d x \frac{dt}{t} e^{-m_c(1-f)t} K_{S^1 \times H^{d-1}}(x, x, t) \tag{3.112}$$

where $f = 1$ for spin half Dirac fermions, and $f = 0$ for scalars. The conformal mass m_c in H^{d-1} for the conformally coupled scalar is

$$m_c = -\frac{(d-2)^2}{4R^2}, \tag{3.113}$$

where R is the radius of H^{d-1}. For convenience, we will set $R = 1$ in the following.

We will consider finite temperature and purely imaginary chemical potential $\mu_E = i\mu_{\rm E}$ for a $U(1)$ global symmetry. This can be incorporated into the heat kernel by setting appropriate boundary conditions. For example, with inverse temperature $\beta = 2\pi n$ we have the boundary condition

$$K_{S^1 \times H^{d-1}}(\{x_1 + 2\pi n, \cdots, x_d\}, \{y_1, \cdots, y_d\}, t) = (-)^f e^{in\mu_{\rm E}} K_{S^1 \times H^{d-1}}(\{x\}, \{y\}, t). \tag{3.114}$$

Let us first focus on $K_{S^1}(x_1, y_1, t)$. It is not hard to show that

$$K_{\mathbb{R}^1}(x_1, y_1, t) = \frac{1}{\sqrt{4\pi t}} e^{-\frac{(x_1 - y_1)^2}{4t}}. \tag{3.115}$$

Summing over images we find

$$K_{S^1}(x_1, y_1, t) = \frac{1}{\sqrt{4\pi t}} \sum_{m \in \mathbb{Z}} e^{\frac{-(y_1 - x_1 + 2\pi m)^2}{4t}} e^{(-in\mu_{\rm E} - i\pi f)m}, \tag{3.116}$$

which satisfies the boundary condition (3.115). Note that using this method, $n\mu_{\rm E} < 1$. The final result for $\mu_{\rm E} n > 1$ should be obtained from $\mu_{\rm E} n < 1$ by folding. We therefore expect discontinuities in the free energies when $\mu_{\rm E} n$ takes integer values.

In the case where $\mu_{\rm E} = 0$ we recover the usual heat kernel at finite temperature $\beta = 2\pi n$. The S^1 circle has radius $2\pi n$.

The heat kernel for massless scalars in H^D takes the form

$$K^b_{H^{2x+1}}(\rho, t) = \frac{1}{(4\pi t)^{1/2}} \left(\frac{-1}{2\pi R^2 \sinh \rho} \frac{\partial}{\partial \rho} \right)^n e^{-x^2 t/R^2 - \rho^2 R^2/(4t)}, \tag{3.117}$$

for hyperbolic spaces of odd dimensions, and

$$K^b_{H^{2(x+1)}}(\rho,t)=e^{-(2x+1)^2t/(4R^2)}\left(\frac{-1}{2\pi R^2\sinh\rho}\frac{\partial}{\partial\rho}\right)^n f_{H^2}(\rho,t), \tag{3.118}$$

where x is an integer, and ρ is the geodesic distance between two points x and y. The function $f_{H^2}(\rho,t)$ is defined as

$$f_{H^2}(\rho,t)=\frac{\sqrt{2}}{(4\pi t)^{3/2}}\int_\rho^\infty d\tilde{\rho}\frac{\tilde{\rho}e^{-\tilde{\rho}^2/(4t)}}{\sqrt{\cosh\tilde{\rho}-\cosh\rho}} \tag{3.119}$$

For fermions, we have

$$K^f_{H^{2x+1}}(\rho,t)=U(x,y)\cosh(\rho/2)\left(\frac{-1}{2\pi}\frac{\partial}{\partial\cosh\rho}\right)^n\cosh(\rho/2)^{-1}\frac{e^{-\rho^2/(4t)}}{\sqrt{4\pi t}} \tag{3.120}$$

and

$$K^f_{H^{2x}}(\rho,t)=U(x,y)\cosh(\rho/2)\left(\frac{-1}{2\pi}\frac{\partial}{\partial\cosh\rho}\right)^n\cosh(\rho/2)^{-1}k_{H^2}(\rho,t) \tag{3.121}$$

and

$$K_{H^2}(\rho,t)=\frac{\sqrt{2}\cosh^{-1}(\rho/2)}{(4\pi t)^{3/2}}\int_\rho^\infty d\tilde{\rho}\frac{\tilde{\rho}\cosh\tilde{\rho}/2e^{-\tilde{\rho}^2/(4t)}}{\sqrt{\cosh\tilde{\rho}-\cosh\rho}} \tag{3.122}$$

The matrix $U(x,y)$ has a trace given by $2^{[d/2]}$, where $[\cdots]$ denotes the integer part. It counts the dimension of spinor space in d dimensions.

From eq. (3.7), we can write the charged Rényi entropy as

$$S_n=\frac{F(n,\mu_{\rm E})-nF(1,\mu_{\rm E})}{n-1} \tag{3.123}$$

where $F(n,\mu_{\rm E})\equiv-\log Z_n(\mu_{\rm E})$ is the free energy evaluated at temperature $\beta=2\pi n$ and chemical potential $\mu_{\rm E}$. We are thus ready to compute free energies at different dimensions.

$d=2$

At temperature $\beta_n=2\pi n$ and finite chemical potential $\mu_{\rm E}$, the free energy is

$$F(n,\mu_{\rm E})=\frac{(-)^f}{2}(2\pi n)V_{H^{d-1}}\int\frac{dt}{t}\sum_m\frac{e^{-\pi^2m^2/t}}{\sqrt{4\pi t}}e^{(-in\mu_{\rm E}-i\pi f)m}K_{H^1}(\rho=0,t). \tag{3.124}$$

The heat kernel is

$$K_{H^1}(0,t)=K_{\mathbb{R}}(0,t)=\frac{1}{\sqrt{4\pi t}}. \tag{3.125}$$

The free energy $F(n,\mu_{\rm E})$ is divergent due to the $m=0$ mode in the S^1 heat kernel. For $m=0$ the contribution is linear in n, where n appears as the overall volume factor from S^1. This dependence therefore drops out from S_n. We could therefore rewrite the regulated free energy $\hat{F}(n,\mu_{\rm E})$ as

$$\begin{aligned}\hat{F}(n,\mu_{\rm E}) &= \frac{(-)^f}{2}(2\pi n)V_{H^{d-1}}\int\frac{dt}{t}\sum_{m\in\mathbb{Z}_+}\frac{e^{-\pi^2m^2/t}}{\sqrt{4\pi t}}2\cos((n\mu_{\rm E}+\pi f)m)K_{H^1}(0,t)\\ &= \frac{(-)^f}{2}V_{H^{d-1}}\sum_{m\in\mathbb{Z}_+}\frac{8\cos(n\,m\mu_{\rm E})\cos(m\pi f)}{8\pi^2 n\,m^2}\\ &= \frac{(-)^f}{4\pi^2 n}V_{H^{d-1}}\left(\mathrm{Li}_2(e^{in\mu_{\rm E}+i\pi f})+\mathrm{Li}_2(e^{-in\mu_{\rm E}-i\pi f})\right)\end{aligned} \tag{3.126}$$

For $0\leq\mathrm{Re}(x)<1$ and $\mathrm{Im}(x)\geq 0$, or $\mathrm{Re}(x)\geq 1$ and $\mathrm{Im}(x)<0$

$$\mathrm{Li}_2(e^{2\pi ix})+\mathrm{Li}_2(e^{-2\pi ix})=-\frac{(2\pi i)^2}{2}B_2(x)=-\frac{(2\pi)^2}{\Gamma[2]}\zeta(-1,x), \tag{3.127}$$

where B_2 is the Bernoulli polynomial, and $\zeta(a,b)$ the Hurwitz zeta function. We are left with

$$\hat{F}(n,\mu_{\rm E})=\frac{(-)^f V_{H^1}}{2n}B_2\left(\frac{n\,\mu_{\rm E}}{2\pi}+\frac{f}{2}\right)=\frac{(-)^f V_{H^1}}{2n}\left(\frac{1}{12}(2-6f+3f^2)+\frac{(f-1)n\mu_{\rm E}}{2\pi}+\frac{n^2\mu_{\rm E}^2}{4\pi^2}\right). \tag{3.128}$$

For fermions, the linear term in $\mu_{\rm E}$ vanishes, as expected. However, for bosons there is a linear $\mu_{\rm E}$ term despite the fact that the sum is explicitly even. This term appears from a term $n\mu_{\rm E}\ln(n\mu_{\rm E})-n\mu_{\rm E}\ln(-n\mu_{\rm E})$ in the expansion of the poly-log in $\mu_{\rm E}$. This suggests that we are actually taking the absolute value of the linear term. This can be readily confirmed by computing the sum numerically. As a result, the free energy has a diverging slope at $\mu_{\rm E}=0$, suggesting a phase transition there. There are also phase transitions whenever $\mu_{\rm E}n$ is an integer, as noted above. At precisely $\mu_{\rm E}n=1/2$, the first derivative w.r.t. $\mu_{\rm E}$ jumps from zero to V_{H^1}.

The $\mu_{\rm E}^2$ term cancels out in the Rényi entropy (since it is linear in n) for $\mu_{\rm E}n<1/2$. The result for a Dirac fermion is

$$S_n^f=\frac{c}{6}(1+\frac{1}{n})V_{H^1} \tag{3.129}$$

Note that $c = 1/2$ for a single Majorana fermion, but this should be doubled for a charged fermion. This reproduces the result obtained via the twist operator method in the main text.

For bosons we obtain instead

$$S_n^b = c\left(\frac{1}{6}(1+\frac{1}{n}) - \frac{|\mu_{\rm E}|}{2\pi}\right) V_{H^1}, \tag{3.130}$$

Again, $c = 1$ for a real boson, which must be doubled for a charged boson. One might worry that the result for bosons does not appear to agree with that of fermions given that they are related by bosonization in 1+1 dimensions. We note however that via bosonization of $U(1)$ charged fermions, the corresponding bosons transform by translation, and thus should instead satisfy the following boundary condition :$\phi(\tau + 2\pi) = \phi(\tau) + n\mu_{\rm E}$. Therefore, our computation for charged bosons is not related to charged fermions by bosonization. Another point to note is that with the absolute sign, the bosonic result is not analytic even for arbitrarily small $\mu_{\rm E}$, such that it does not analytically continue to the complex plane, as in the case for fermions.

$d = 4$

Let us work out one more example where there is non-trivial $\mu_{\rm E}$ dependence. At $d = 3 + 1$, the main difference is the heat kernel for both bosons and fermions on H^3. For bosons, the equal-point heat kernel is

$$e^{-m_s t} K^b_{H^3}(0,t) = \frac{1}{(4\pi t)^{3/2}}, \tag{3.131}$$

where we have substituted in the conformal mass of the scalar. For a Dirac fermion, the heat kernel is

$$K^f_{H^3}(0,t) = 4\frac{1}{(4\pi t)^{3/2}}(1+\frac{t}{2}) \tag{3.132}$$

Following the same steps as in $d = 3 + 1$, and again ignoring the $m = 0$ term, the Rényi entropy becomes, for bosons :

$$\begin{aligned} S_n &= \mathrm{tr}(1) V_{H^3} \sum_{m\in\mathbb{Z}_+} \frac{n^4 \cos(m\mu_{\mathrm{E}}) - \cos(mn\mu_{\mathrm{E}})}{8m^4\pi^5(n-1)n^3} \\ &= -\frac{1}{8\pi^5(n-1)n^3}\Bigg(- n^4(\mathrm{Li}_4(e^{-i\mu_{\mathrm{E}}}) + \mathrm{Li}_4(e^{i\mu_{\mathrm{E}}})) + \\ &\quad \mathrm{Li}_4(e^{-in\mu_{\mathrm{E}}}) + \mathrm{Li}_4(e^{in\mu_{\mathrm{E}}})\Bigg) \end{aligned} \tag{3.133}$$

where $\mathrm{tr}(1) = 2$ for a pair of real bosons (which together form a complex $U(1)$ charged boson). The above combinations of poly-logs again admit a representation in terms of the Bernoulli polynomial. Altogether we have

$$S_n^b = \frac{V_{H^3}}{2\pi}\left(\frac{1 + n + n^2 + n^3}{180n^3} - \frac{(n+1)\mu_{\mathrm{E}}^2}{24\pi^2 n} + \frac{\mu_{\mathrm{E}}^3}{24\pi^3}\right) \tag{3.134}$$

Again we are left with a μ_{E}^3 term that is odd in μ_{E}, and we argue that this term should be enclosed inside an absolute sign since our summation is even. As a result, once again we lose analyticity even for arbitrarily small values of μ_{E}.

Now let us also look at the corresponding result for fermions. The Rényi entropy is

$$\begin{aligned} S_n^f &= V_{H^3} \sum_{m\in\mathbb{Z}_+} \frac{(-1)^m(2 + m^2\pi^2n^2)\cos(mn\mu_{\mathrm{E}})}{m^4 4\pi^5 n^3} \\ &= V_{H^3} \frac{(1+n)(7 + n^2(37 - 120\mu_{\mathrm{E}}^2)}{1440\pi n^3}, \end{aligned} \tag{3.135}$$

which interestingly, is again automatically even in μ_{E}, and that for purely imaginary μ_{E}, is positive definite. We note that the above expression is not positive definite in μ_{E}. We find that for sufficiently large value of μ_{E} while within the interval $n\mu_{\mathrm{E}} < 1/2$ that the above expression can turn negative. This is as expected since the trace

$$\mathrm{tr}\rho^n = \mathrm{tr}(e^{-n(H - i\mu_{\mathrm{E}}Q)}) \tag{3.136}$$

is not necessarily positive definite quantity. When μ_{E} is purely imaginary, we return to the usual thermodynamic chemical potential and the trace should be positive definite. Note that the Rényi entropy for the fermions, which admit analytic continuation for small values of μ_{E}, is indeed positive definite when μ_{E} is purely imaginary.

Remark: $d = 2 + 1$**.** Here the complication is the more complicated form of the heat kernel in H^2. Because of that, it doesn't have a neat analytic result, but one can evaluate these results numerically. We find precise agreement with the calculation obtained on a sphere in later sections, and we will not repeat the details here.

3.5.2 Wavefunctions on $S^1 \times H^{d-1}$

We can reproduce the heat kernel results by analyzing the wave functions on the hyperbolic space. This method was used in [78] to study the Rényi entropy of the free theories without the chemical potential. In this subsection, we generalize [78] to include the chemical potential.

Free scalar field

We consider a free boson on a $S^1 \times H^{d-1}$ with H^{d-1} radius R

$$S = \int d^d r \sqrt{g} (|\partial_\mu \phi|^2 + M^2 |\phi|^2) \tag{3.137}$$

where M is the conformal mass. The metric is

$$ds^2 = d\theta^2 + R^2 (d\eta^2 + \sinh^2 \eta d\Omega_{d-2}^2). \tag{3.138}$$

The periodicity of the S^1 time circle (θ) is $2\pi n$. The Wilson loop changes boundary condition around the time circle from $\phi(2\pi n) = \phi(0)$ to

$$\phi(2\pi n) = e^{in\mu_{\mathrm{E}}} \phi(0). \tag{3.139}$$

The mode function satisfying this boundary condition is

$$e^{i\left(\frac{m}{n} + \frac{\mu_{\mathrm{E}}}{2\pi}\right)\theta}, \tag{3.140}$$

where m is an integer. The eigenvalue of the Laplace operator $-\Delta - M^2$ is

$$\lambda + \left(\frac{m}{n} + \frac{\mu_{\mathrm{E}}}{2\pi}\right)^2, \qquad \lambda \geq 0. \tag{3.141}$$

We define the free energy

$$\begin{aligned} F_n &= \mathrm{Tr}\log\left(-\Delta - M^2\right) \\ &= \sum_{m\in\mathbb{Z}}\int_0^\infty d\lambda \mathcal{D}(\lambda)\log\left(\lambda + \left(\frac{m}{n}+\frac{\mu_{\mathrm{E}}}{2\pi}\right)^2\right) \qquad (3.142) \\ &= \int_0^\infty d\lambda\mathcal{D}(\lambda)\left(2\pi n\sqrt{\lambda} + \log\left(1-2\cos(n\mu_{\mathrm{E}})e^{-2\pi n\sqrt{\lambda}}+e^{-4\pi n\sqrt{\lambda}}\right)\right) \qquad (3.143) \end{aligned}$$

where $\mathcal{D}(\lambda)$ is the density of states. In the last equation, we used the following formula for the regularized sum

$$\sum_{k\in\mathbb{Z}}\log\left(\frac{(k+\alpha)^2}{n^2}+a^2\right) = \log[2\cosh(2\pi n|a|)-2\cos(2\pi\alpha)]. \qquad (3.144)$$

In the case of scalar bosons, the density of states $\mathcal{D}(\lambda)$ on H^{d-1} is given by [119, 120]

$$\mathcal{D}(\lambda)d\lambda = \frac{\mathrm{vol}(H^{d-1})}{(4\pi)^{\frac{d-1}{2}}\Gamma\left(\frac{d-1}{2}\right)}\frac{|\Gamma(i\sqrt{\lambda}+\frac{d-2}{2})|^2}{\sqrt{\lambda}|\Gamma(i\sqrt{\lambda})|^2}d\lambda. \qquad (3.145)$$

The explicit forms for low dimensions are

$$\begin{aligned} &d-1=1; \qquad \mathcal{D}(\lambda)d\lambda = \frac{\mathrm{vol}(H^1)}{2\pi\sqrt{\lambda}}d\lambda \\ &d-1=2; \qquad \mathcal{D}(\lambda)d\lambda = \frac{\mathrm{vol}(H^2)}{4\pi}\,\mathrm{th}(\pi\sqrt{\lambda})d\lambda \\ &d-1=3; \qquad \mathcal{D}(\lambda)d\lambda = \frac{\mathrm{vol}(H^3)}{(2\pi)^2}\sqrt{\lambda}d\lambda \qquad (3.146) \end{aligned}$$

$\mathrm{vol}(H)$ is the regularized volume of the hyperbolic space.

The first term in (3.143) is divergent and needs a regularization. However, it will not contribute to the Rényi entropy since it linearly depends on n. One can show that this integration reproduces the heat kernel results.

Free Dirac fermion

We also consider a free Fermion

$$S = \int d^dx\sqrt{g}\bar{\psi}(i\not{D})\psi, \qquad (3.147)$$

The free energy is

$$F_n = -\,\mathrm{Tr}\log(i\not{D}), \qquad (3.148)$$

In the presence of the Wilson loop, the boundary condition of ψ along the time circle changes from $\psi(2\pi n) = -\psi(0)$ to

$$\psi(2\pi n) = -e^{in\mu_{\rm E}}\psi(0) \tag{3.149}$$

So the eigenfunction along θ is $e^{im\theta/n}$ with

$$m \in \mathbb{Z} + \frac{1}{2} + \frac{n\mu_{\rm E}}{2\pi}. \tag{3.150}$$

The eigenvalue spectrum of $(i\not{D})$ is

$$\pm\sqrt{\lambda^2 + \frac{m^2}{n^2}}. \tag{3.151}$$

The free energy is

$$\begin{aligned} F_n &= -\frac{1}{2}\sum_{m\in\mathbb{Z}+\frac{1}{2}}\int_0^\infty d\lambda \mathcal{D}(\lambda)\log\left(\lambda^2+\frac{m^2}{n^2}\right) \\ &= -\frac{1}{2}\int_0^\infty d\lambda\mathcal{D}(\lambda)\log\left(2\cosh(2\pi n\lambda)+2\cos(n\mu_{\rm E})\right) \end{aligned} \tag{3.152}$$

As before, we used (3.144) in the last equation.

The density of states $\mathcal{D}(\lambda)$ in $d-1$ dimensions is [119, 120]

$$\frac{\mathcal{D}(\lambda)}{\mathrm{vol}(H^{d-1})} = \left(\frac{\Gamma\left(\frac{d-1}{2}\right)2^{d-4}}{\pi^{(d-1)/2+1}}2^{\left[\frac{(d-1)}{2}\right]}\right)\frac{2^{4-2(d-1)}}{(\Gamma((d-1)/2))^2}\cosh(\pi\lambda)\left|\Gamma\left(i\lambda+\frac{(d-1)}{2}\right)\right|^2. \tag{3.153}$$

Here, $\mathcal{D}(\lambda)$ is normalized so that the spinor ζ-function per unit volume is given by

$$\mathrm{tr}(-\not{D}^2+m^2)^{-s} = \int_0^\infty(\lambda^2+m^2)^{-s}\frac{\mathcal{D}(\lambda)}{\mathrm{vol}(H^{d-1})}d\lambda. \tag{3.154}$$

For odd $d-1$, it is

$$\frac{\mathcal{D}(\lambda)}{\mathrm{vol}(H^{d-1})} = \frac{\pi}{2^{2(d-3)}(\Gamma((d-1)/2))^2}\prod_{j=\frac{1}{2}}^{(d-3)/2}(\lambda^2+j^2) \tag{3.155}$$

and for even $d-1$

$$\frac{\mathcal{D}(\lambda)}{\mathrm{vol}(H^{d-1})} = \frac{\pi\lambda\coth(\pi\lambda)}{2^{2(d-3)}(\Gamma((d-1)/2))^2}\prod_{j=1}^{(d-3)/2}(\lambda^2+j^2) \tag{3.156}$$

The explicit forms for low dimensions are

$$\begin{aligned} d-1=1; \qquad & \mathcal{D}(\lambda)d\lambda = \frac{\text{vol}(H^1)}{\pi}d\lambda \\ d-1=2; \qquad & \mathcal{D}(\lambda)d\lambda = \frac{\text{vol}(H^2)}{\pi}\lambda\coth(\pi\lambda)d\lambda \\ d-1=3; \qquad & \mathcal{D}(\lambda)d\lambda = \text{vol}(H^3)\left(\lambda^2+\frac{1}{4}\right)d\lambda \end{aligned} \tag{3.157}$$

The first term in (3.152) diverges and needs a regularization, while the second term is finite. We can regularize the divergence using zeta function regularization or flat space subtraction. In any case, it doesn't contribute to the Rényi entropy since it is linear in n. The final result agrees with the twist operator computation (Sec 3.2.4), the heat kernel computation (Appendix 3.5.1) and the wave function computation on a sphere (Appendix 3.5.3)

3.5.3 Wavefunctions on S^d

Another convenient way of computing the Rényi entropy of CFT is to map onto a sphere. Let us consider a scalar field on S^3. The metric is

$$ds^2 = \cos^2\theta d\tau^2 + d\theta^2 + \sin^2\theta d\phi^2 \tag{3.158}$$

with $0 \le \tau < 2\pi n, 0 \le \phi < 2\pi$, and $0 \le \theta < \pi/2$. Because of the periodicity of τ, there is a conical singularity at $\cos\theta = 0$. We can do the heat kernel analysis on the sphere in a similar way to the hyperbolic case. However, we need to set a regularity condition at the conical singularity. An alternative way to compute the free energy is to look at the wave functions and their eigenvalues directly. The analysis below is a generalization of [78] and we cite several results from their paper.

Free scalar field

The free energy of the free scalar field on the sphere is

$$F_n = \text{tr}\log\left(-\Delta + \frac{\mathcal{R}}{8}\right) \tag{3.159}$$

where $\mathcal{R} = 6$ for $3d$ case. We assume that the eigenfunction of the Laplacian takes the form $f(\theta)e^{im_\tau \tau + im_\phi \phi}$. The function $f(\theta)$ obeys the following equation

$$f''(\theta) + 2\cot\theta f'(\theta) - \left(\frac{m_\tau^2}{\cos^2\theta} + \frac{m_\phi^2}{\sin^2\theta}\right) f(\theta) = \lambda f(\theta). \tag{3.160}$$

From the regularity of $f(\theta)$, the eigenvalue λ is fixed to

$$\lambda = -s(s+2), \qquad s = |m_\tau| + |m_\phi| + 2a, \quad a \in \mathbb{N} \tag{3.161}$$

The periodicity of ϕ requires m_ϕ to be quantized in $\mathbb{Z}$. In the presence of the Wilson loop, the boundary condition of ϕ becomes

$$\phi(2\pi n) = e^{in\mu_{\rm E}}\phi(0) \tag{3.162}$$

Therefore, m_τ is quantized in $\frac{\mathbb{Z}}{n} + \frac{\mu_{\rm E}}{2\pi}$.

Let us denote

$$m_\tau = \frac{\alpha}{n} + \frac{\mu_{\rm E}}{2\pi}, \qquad m_\phi = \beta, \qquad (\alpha, \beta \in \mathbb{Z}) \tag{3.163}$$

and

$$\alpha = kn + p, \qquad k \in \mathbb{Z}, \quad p \in [0, n-1]. \tag{3.164}$$

The free energy (3.159) is

$$F_n = \sum_{k=-\infty}^{\infty} \sum_{p=0}^{n-1} \sum_{\beta=-\infty}^{\infty} \sum_{a=0}^{\infty} \log\left(s(s+2) + \frac{3}{4}\right) \tag{3.165}$$

with

$$s = \left|k + \frac{p}{n} + \frac{\mu_{\rm E}}{2\pi}\right| + |\beta| + 2a. \tag{3.166}$$

We want to count the degeneracied for a given value of s. Let us first assume that $\mu_{\rm E}$ satisfies $0 \le \frac{\mu_{\rm E}}{2\pi} < \frac{1}{q}$. Then the degeneracy for

$$s = m + \frac{p}{n} + \frac{\mu_{\rm E}}{2\pi}, \quad m - \frac{p}{n} - \frac{\mu_{\rm E}}{2\pi} + 1 \quad (p \in [0, n-1], \quad m \in \mathbb{N}), \tag{3.167}$$

is

$$\frac{(m+1)(m+2)}{2}. \tag{3.168}$$

Therefore, the free energy is

$$\begin{aligned} F_n &= \sum_{p=0}^{q}\sum_{m=0}^{\infty}\Big[\frac{(m+1)(m+2)}{2}\Big\{\log((m+\frac{p}{q}+\frac{\mu_{\rm E}}{2\pi}+1)^2-\frac{1}{4})+\log((m-\frac{p}{q}-\frac{\mu_{\rm E}}{2\pi}+2)^2-\frac{1}{4})\Big\}\Big] \\ &= \sum_{p=0}^{q}\sum_{a=a_1}^{a_4}\left[-\frac{1}{2}\left(\zeta'(-2,a)+(3-2a)\zeta'(-1,a)+(a^2-3a+2)\zeta'(0,a)\right)\right] \end{aligned} \tag{3.169}$$

where $\zeta'(s,a)=\frac{\partial\zeta(s,a)}{\partial s}$ and

$$a_1=(\frac{p}{n}+\frac{\mu_{\rm E}}{2\pi}+\frac{1}{2}),\ \ a_2=(\frac{p}{n}+\frac{\mu_{\rm E}}{2\pi}+\frac{3}{2}),\ \ a_3=(-\frac{p}{n}-\frac{\mu_{\rm E}}{2\pi}+\frac{3}{2}),\ \ a_4=(-\frac{p}{n}-\frac{\mu_{\rm E}}{2\pi}+\frac{5}{2}). \tag{3.170}$$

The expansions near $\mu_{\rm E}=0$ are

$$\begin{aligned} F_1 &= \frac{\log 2}{4}-\frac{3\zeta(3)}{8\pi^2} \\ &\quad -\frac{\mu_{\rm E}^2}{96\pi^2}\left(2\left(-12\zeta^{(1,1)}\left(-1,\frac{1}{2}\right)-24\zeta^{(1,1)}\left(-1,\frac{3}{2}\right)-12\zeta^{(1,1)}\left(-1,\frac{5}{2}\right)+3\zeta^{(1,2)}\left(-2,\frac{1}{2}\right)\right.\right. \\ &\quad +6\zeta^{(1,2)}\left(-2,\frac{3}{2}\right)+3\zeta^{(1,2)}\left(-2,\frac{5}{2}\right)+6\zeta^{(1,2)}\left(-1,\frac{1}{2}\right)-6\zeta^{(1,2)}\left(-1,\frac{5}{2}\right) \\ &\quad \left.\left.+28-36\log 2+6\log 3\right)+3\pi^2\right)+\mathcal{O}(\mu_{\rm E}^4), \end{aligned} \tag{3.171}$$

$$\begin{aligned} F_2 &= \frac{\log 2}{4}+\frac{\zeta(3)}{8\pi^2} \\ &\quad +\frac{\mu_{\rm E}^2}{4\pi^2}\left(\frac{1}{12}\left(12\zeta^{(1,1)}\left(-1,\frac{1}{2}\right)+24\zeta^{(1,1)}(-1,1)+24\zeta^{(1,1)}\left(-1,\frac{3}{2}\right)+24\zeta^{(1,1)}(-1,2)+\right.\right. \\ &\quad 12\zeta^{(1,1)}\left(-1,\frac{5}{2}\right)-3\zeta^{(1,2)}\left(-2,\frac{1}{2}\right)-6\zeta^{(1,2)}(-2,1)-6\zeta^{(1,2)}\left(-2,\frac{3}{2}\right) \\ &\quad -6\zeta^{(1,2)}(-2,2)-3\zeta^{(1,2)}\left(-2,\frac{5}{2}\right)-6\zeta^{(1,2)}\left(-1,\frac{1}{2}\right)-6\zeta^{(1,2)}(-1,1)+6\zeta^{(1,2)}(-1,2) \\ &\quad \left.\left.+6\zeta^{(1,2)}\left(-1,\frac{5}{2}\right)-40-6\log(3)+12\log(16\pi)\right)-\frac{\pi^2}{8}\right)+\mathcal{O}(\mu_{\rm E}^4). \end{aligned} \tag{3.172}$$

Each of the functions $\zeta^{(1,1)},\zeta^{(1,2)}$ etc has some subtlety in evaluation. We may always go back to the expression (3.169) when we evaluate the free energy explicitly. The leading terms agrees with the results in [78].

The expression (3.169) is not valid for $\frac{\mu_{\rm E}}{2\pi} > \frac{1}{n}$. In this case, there is a number $p_1 \leq n-1$ satisfying

$$-1 + \frac{p_1}{n} + \frac{\mu_{\rm E}}{2\pi} < 0, \qquad -1 + \frac{p_1+1}{n} + \frac{\mu_{\rm E}}{2\pi} < 0. \tag{3.173}$$

By using this number, the eigenvalues and their degeneracies become

$$\begin{aligned}
&\frac{(m+1)(m+2)}{2} \qquad \text{for} \quad s = m + \frac{p}{n} + \frac{\mu_{\rm E}}{2\pi}, \;\; m - \frac{p}{n} - \frac{\mu_{\rm E}}{2\pi} + 2 \;\; (p \in [0, n-1]), \\
&(m+1) \qquad \text{for} \quad s = m - \frac{p}{n} - \frac{\mu_{\rm E}}{2\pi} + 1 \;\; (p \in [0, p_1]), \\
&(m+1) \qquad \text{for} \quad s = m + \frac{p}{n} + \frac{\mu_{\rm E}}{2\pi} - 1 \;\; (p \in [p_1+1, n-1]).
\end{aligned} \tag{3.174}$$

The free energy is

$$\begin{aligned}
F_n &= \sum_{p=0}^{n-1} \sum_{m=0}^{\infty} \frac{(m+1)(m+2)}{2} \Big(\log((m + \frac{p}{n} + \frac{\mu_{\rm E}}{2\pi} + 1)^2 - \frac{1}{4}) + \log((m - \frac{p}{n} - \frac{\mu_{\rm E}}{2\pi} + 3)^2 - \frac{1}{4}) \Big) \\
&\quad + \sum_{p=0}^{p_1} \sum_{m=0}^{\infty} (m+1) \Big(\log((m - \frac{p}{n} - \frac{\mu_{\rm E}}{2\pi} + 2)^2 - \frac{1}{4}) \Big) \\
&\quad + \sum_{p=p_1+1}^{n-1} \sum_{m=0}^{\infty} (m+1) \Big(\log((m + \frac{p}{n} + \frac{\mu_{\rm E}}{2\pi})^2 - \frac{1}{4}) \Big) \\
&= \sum_{p=0}^{n} \sum_{a=b_1}^{b_4} (-\frac{1}{2}(\zeta'(-2,a) + (3-2a)\zeta'(-1,a) + (a^2 - 3a + 2)\zeta'(0,a))) \\
&\quad + \sum_{p=0}^{p_1} \sum_{a=c_1}^{c_2} (-(\zeta(-1,a) + (1-a)\zeta(0,a))) + \sum_{p=p_1+1}^{n-1} \sum_{a=c_3}^{c_4} (-(\zeta(-1,a) + (1-a)\zeta(0,a)))
\end{aligned} \tag{3.175}$$

where

$$b_1 = (\frac{p}{q} + \frac{\mu_{\rm E}}{2\pi} + \frac{1}{2}), \;\; b_2 = (\frac{p}{q} + \frac{\mu_{\rm E}}{2\pi} + \frac{3}{2}), \;\; b_3 = (-\frac{p}{q} - \frac{\mu_{\rm E}}{2\pi} + \frac{5}{2}), \;\; b_4 = (-\frac{p}{q} - \frac{\mu_{\rm E}}{2\pi} + \frac{7}{2}), \tag{3.176}$$

and

$$c_1 = (-\frac{p}{q} - \frac{\mu_{\rm E}}{2\pi} + \frac{3}{2}), \;\; c_2 = (-\frac{p}{q} - \frac{\mu_{\rm E}}{2\pi} + \frac{5}{2}), \;\; c_3 = (\frac{p}{q} + \frac{\mu_{\rm E}}{2\pi} - \frac{1}{2}), \;\; c_4 = (\frac{p}{q} + \frac{\mu_{\rm E}}{2\pi} + \frac{1}{2}). \tag{3.177}$$

We show the numerical result in Fig.3.6. It is remarkable that the function is smooth around $\mu_{\rm E} = \frac{1}{n}$.

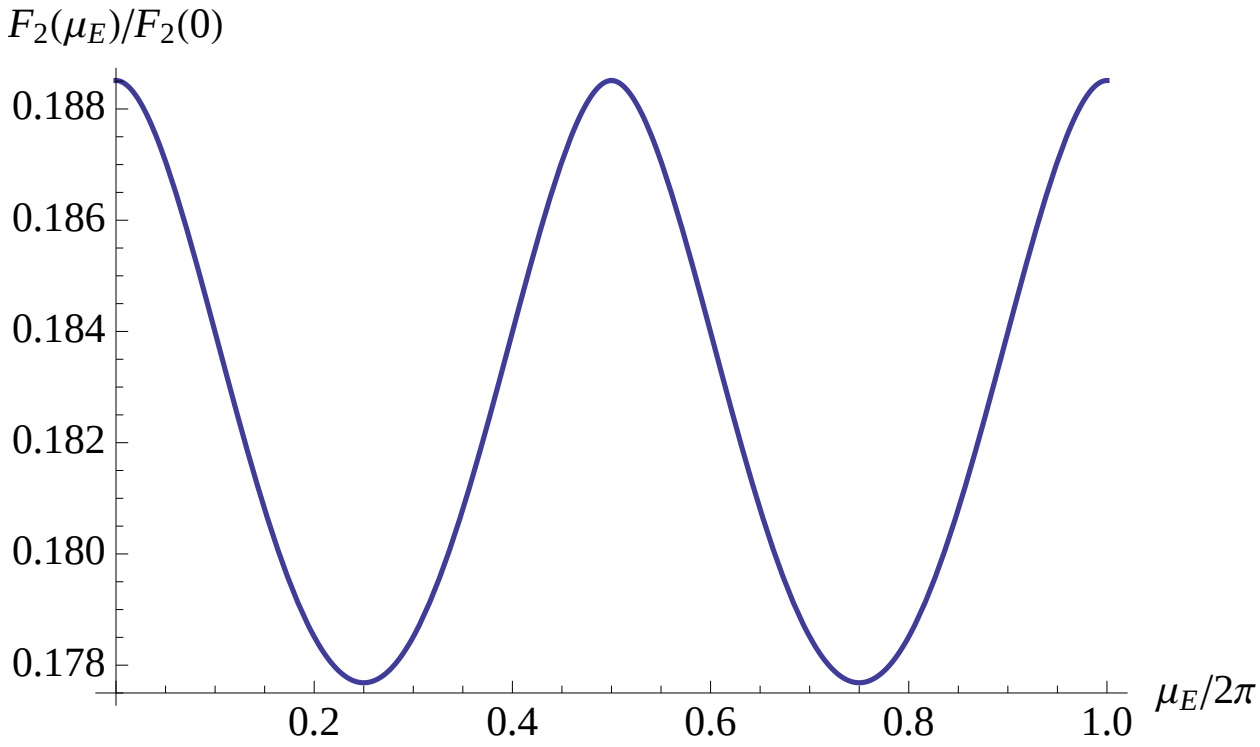

Figure 3.6: Boson free energy $n = 2$

Free Dirac fermion

Next, we consider a spinor ψ on S^3. It satisfies the Dirac equation

$$i\sigma_a^\mu \gamma^a \left(\partial_\mu \psi + \frac{1}{4} \omega_\mu^{ab} \gamma_{ab} \psi \right) = \lambda \psi. \tag{3.178}$$

The periodic part of the spinor ψ in τ and ϕ directions can be written as $e^{im_\tau \tau + im_\phi \phi}$. As shown in [78], the regularity condition at $\theta = 0$ restricts the allowed eigenvalue λ. There are four types of eigenvalues :

Two positive λ

$$\begin{aligned} &\text{Case 1} \quad \lambda = m_\tau + m_\phi + \frac{3}{2} + 2a, \quad m_\tau \geq 0, \quad m_\phi \geq -\frac{1}{2} - a, \quad a \in \mathbb{N}, \\ &\text{Case 2} \quad \lambda = -m_\tau + m_\phi + \frac{1}{2} + 2a, \quad m_\tau < 0, \quad m_\phi \geq \frac{1}{2} - a, \quad a \in \mathbb{N}, \end{aligned} \tag{3.179}$$

and two negative λ

$$\text{Case 3} \quad \lambda = -(m_\tau + m_\phi + \frac{1}{2} + 2a), \quad m_\tau \geq 0, \quad m_\phi \geq \frac{1}{2} - a, \quad a \in \mathbb{N},$$

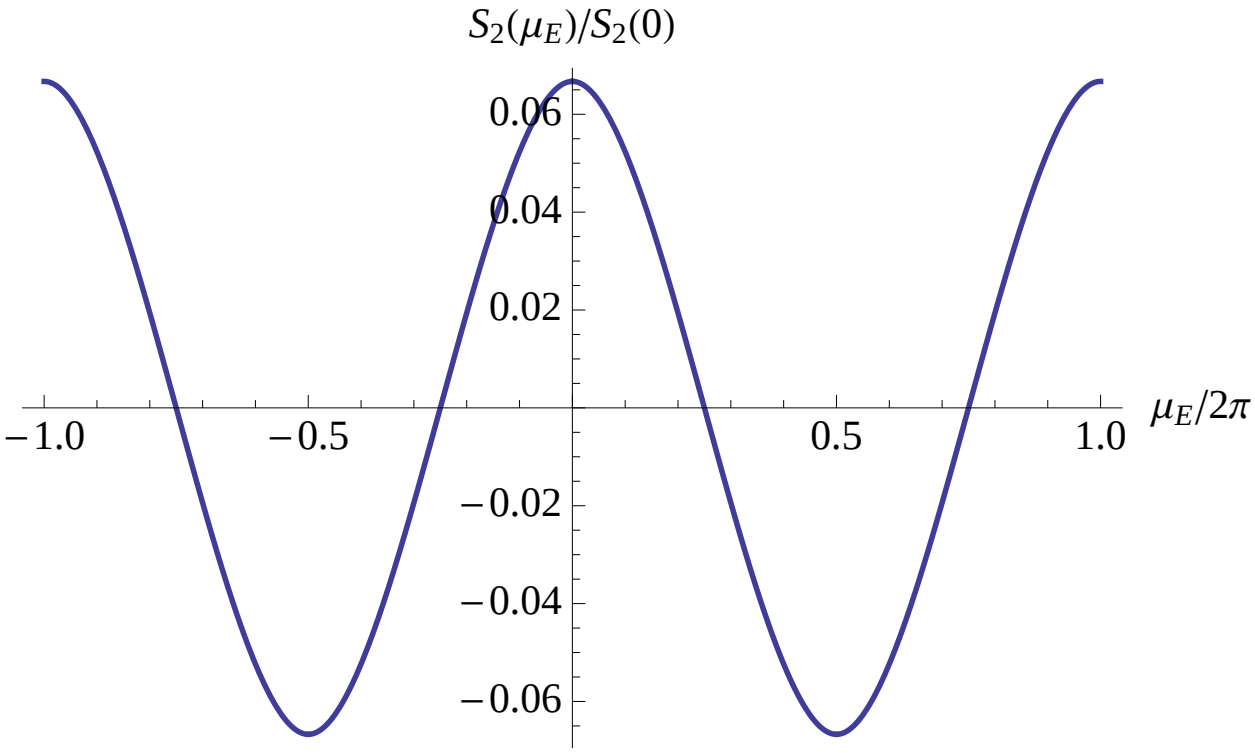

Figure 3.7: Boson Renyi entropy $n = 2$

$$\text{Case 4} \qquad \lambda = -(-m_\tau + m_\phi + \frac{3}{2} + 2a), \quad m_\tau < 0, \quad m_\phi \geq -\frac{1}{2} - a, \quad a \in \mathbb{N}, \tag{3.180}$$

where

$$m_\tau \in \frac{1}{q}(\mathbb{Z} + \frac{1}{2} + \frac{q\mu_{\rm E}}{2\pi}), \qquad m_\phi \in \mathbb{Z} + \frac{1}{2} \tag{3.181}$$

As before, we first consider the case $0 \leq \frac{n\mu_{\rm E}}{2\pi} < \frac{1}{2}$. In this case, the eigenvalues and the degeneracies are

$$\frac{(k+1)(k+2)}{2} \quad \text{for} \quad \lambda = \pm(k + \frac{p}{q} + \frac{1}{2q} + \frac{\mu_{\rm E}}{2\pi} + 1), \ \pm(k + \frac{p}{q} + \frac{1}{2q} - \frac{\mu_{\rm E}}{2\pi} + 1) \tag{3.182}$$

where $k \in \mathbb{N}$.

The free energy is

$$\begin{aligned} F_n &= -2\sum_{p=0}^{q-1}\sum_{k=0}^{\infty}\frac{(k+1)(k+2)}{2}\log(k+1+\frac{p}{n}+\frac{1}{2n}+\frac{\mu_{\rm E}}{2\pi}) \\ &\quad -2\sum_{p=0}^{n-1}\sum_{k=0}^{\infty}\frac{(k+1)(k+2)}{2}\log(k+1+\frac{p}{n}+\frac{1}{2n}-\frac{\mu_{\rm E}}{2\pi}) \end{aligned}$$

$$= \sum_{p=0}^{q-1} \sum_{a=a_1}^{a_2} (\zeta'(-2,a) + (1-2a)\zeta'(-1,a) + a(a-1)\zeta'(0,a)) \tag{3.183}$$

where

$$a_1 = 1 + \frac{p}{n} + \frac{1}{2n} + \frac{\mu_{\rm E}}{2\pi}, \quad a_1 = 1 + \frac{p}{n} + \frac{1}{2n} - \frac{\mu_{\rm E}}{2\pi} \tag{3.184}$$

We show the explicit form of the free energy near $\mu_{\rm E} = 0$.

$$\begin{aligned}
F_1 &= \frac{\log 2}{4} + \frac{3\zeta(3)}{8\pi^2} \\
&+ \left(-\log 8 - 4\zeta^{(1,1)}(-1,\frac{3}{2}) + \zeta^{(1,2)}(-2,\frac{3}{2}) - \frac{1}{4}\zeta^{(1,2)}(0,\frac{3}{2}) \right) \frac{\mu_{\rm E}^2}{4\pi^2} + \mathcal{O}(\mu_{\rm E}^4) \\
F_2 &= \frac{3\zeta(3)}{32\pi^2} + \frac{3\log 2}{16} + \frac{G}{2\pi} \\
&+ \Big(-9\log 2 + 2\log 3 - 4\zeta^{(1,1)}(-1,\frac{5}{4}) - 4\zeta^{(1,1)}(-1,\frac{7}{4}) - \zeta^{(1,1)}(0,\frac{5}{4}) + \zeta^{(1,1)}(0,\frac{7}{4}) \\
&\quad + \zeta^{(1,2)}(-2,\frac{5}{4}) + \zeta^{(1,2)}(-2,\frac{7}{4}) + \frac{1}{2}\zeta^{(1,2)}(-1,\frac{5}{4}) - \frac{1}{2}\zeta^{(1,2)}(-1,\frac{7}{4}) \\
&\quad - \frac{3}{16}\zeta^{(1,2)}(0,\frac{5}{4}) - \frac{3}{16}\zeta^{(1,2)}(0,\frac{7}{4}) \Big) \frac{\mu_{\rm E}^2}{4\pi^2} + \mathcal{O}(\mu_{\rm E}^4)
\end{aligned} \tag{3.185}$$

where G is the Catalan constant. Again, the functions $\zeta^{(1,1)}, \zeta^{(1,2)}$ etc are a formal expression and one may use (3.183) to evaluate the free energy. The leading terms agree with [78]. Notice that only even powers of $\mu_{\rm E}$ appears in the expansion. The expression (3.183) is not valid for $\mu_{\rm E} > \frac{1}{2n}$. In this region there is a number p_1 which satisfies

$$-1 + \frac{p_1}{n} + \frac{1}{2n} + \frac{\mu_{\rm E}}{2\pi} < 0, \quad -1 + \frac{p_1+1}{n} + \frac{1}{2n} + \frac{\mu_{\rm E}}{2\pi} \geq 0. \tag{3.186}$$

Then the eigenvalues, their degeneracies, and the range of p are as follows:

$$\begin{aligned}
&\frac{(k+1)(k+2)}{2} \quad \text{for} \ \ \lambda = \pm(k+1+\frac{p}{n}+\frac{1}{2n}+\frac{\mu_{\rm E}}{2\pi}), \quad p \in [0, n-1] \\
&\frac{(k+1)(k+2)}{2} \quad \text{for} \ \ \lambda = \pm(k+3-\frac{p}{n}-\frac{1}{2n}-\frac{\mu_{\rm E}}{2\pi}), \quad p \in [0, n-1] \\
&(k+1) \quad \text{for} \ \ \lambda = \pm(k+2-\frac{p}{n}-\frac{1}{2n}-\frac{\mu_{\rm E}}{2\pi}), \quad p \in [0, p_1] \\
&(k+1) \quad \text{for} \ \ \lambda = \pm(k+\frac{p}{n}+\frac{1}{2n}+\frac{\mu_{\rm E}}{2\pi}), \quad p \in [p_1+1, n-1]
\end{aligned} \tag{3.187}$$

where $k \in \mathbb{N}$.

The free energy is

$$\begin{aligned} F_n &= \sum_{p=0}^{n-1} \sum_{a=a_1}^{a_2} \left(\zeta'(-2,a) + (3-2a)\zeta'(-1,a) + (a^2-3a+2)\zeta'(0,a)\right) \\ &+ \sum_{p=0}^{p_1} 2(\zeta(-1,c_1) + (1-c_1)\zeta(0,c_1)) + \sum_{p=p_1+1}^{n-1} 2(\zeta(-1,c_2) + (1-c_2)\zeta(0,c_2)) \end{aligned} \quad (3.188)$$

with

$$a_1 = 1+\frac{p}{q}+\frac{1}{2q}+\frac{\mu_{\rm E}}{2\pi},\ \ a_2 = 3-\frac{p}{q}-\frac{1}{2q}-\frac{\mu_{\rm E}}{2\pi},\ \ c_1 = 2-\frac{p}{q}-\frac{1}{2q}-\frac{\mu_{\rm E}}{2\pi},\ \ c_2 = \frac{p}{q}+\frac{1}{2q}+\frac{\mu_{\rm E}}{2\pi}. \quad (3.189)$$

The numerical result is shown in Fig.3.8. There are phase transitions at $\frac{\mu_{\rm E}}{2\pi} = \frac{1}{2n} + \frac{\mathbb{Z}}{n}$ for the free energy and $\frac{\mu_{\rm E}}{2\pi} = \frac{1}{2n} + \frac{\mathbb{Z}}{n}$ and $\frac{1}{2} + \mathbb{Z}$ for the Rényi entropy.

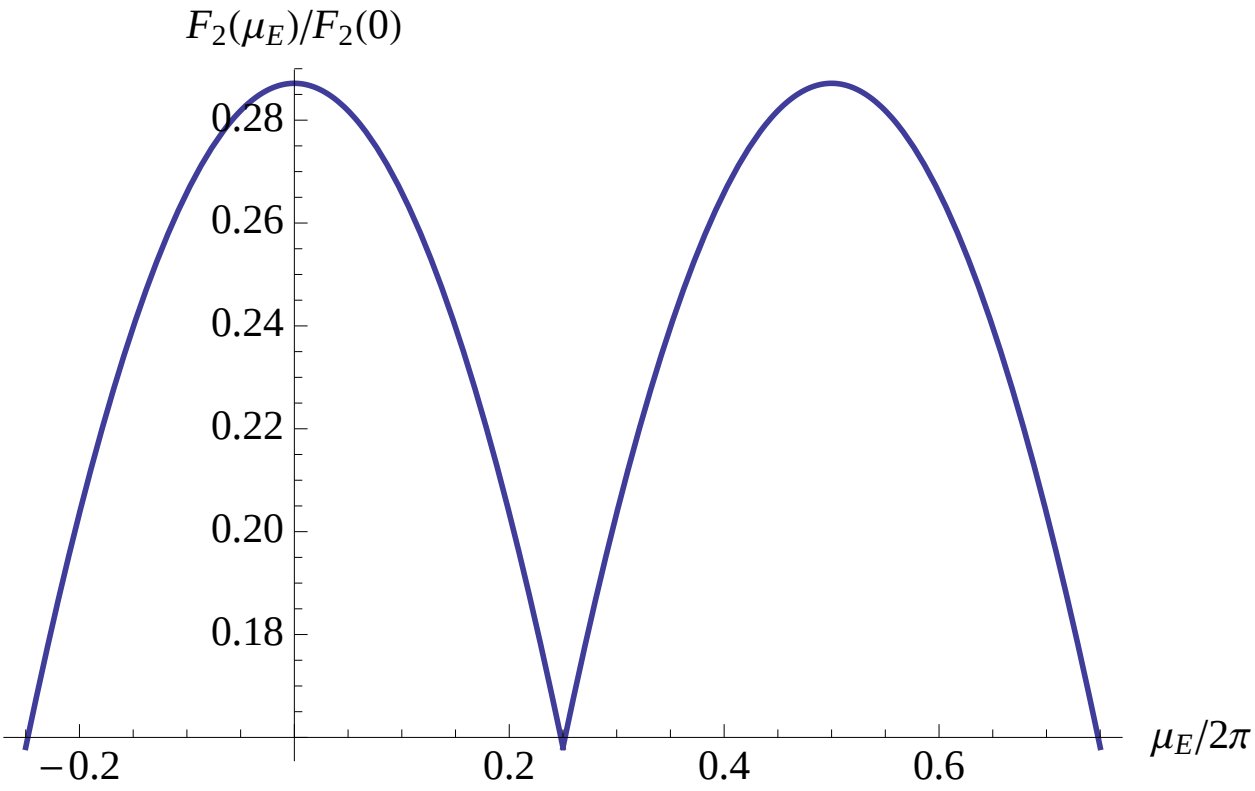

Figure 3.8: Fermion free energy $n = 2$

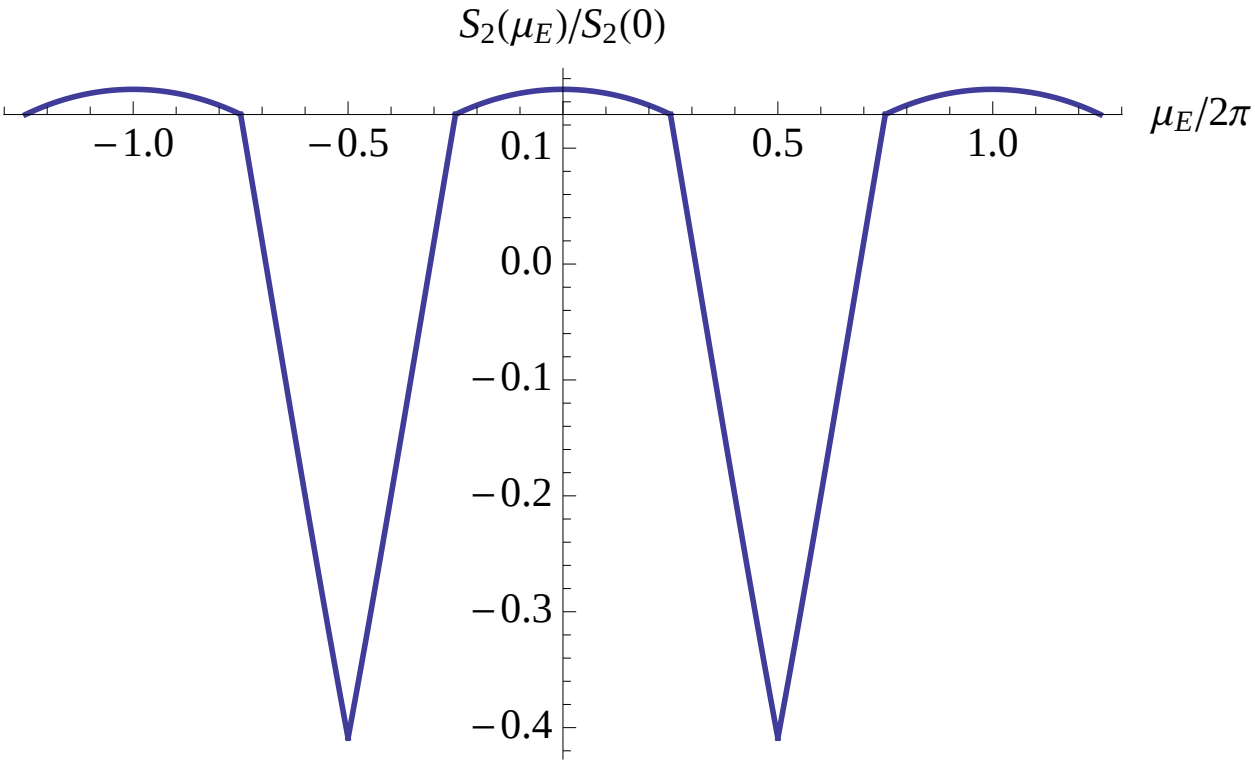

Figure 3.9: Fermion Renyi entropy $n = 2$

3.6 Appendix B: Holographic computations for $d = 2$

We now compute the holographic charged Rényi entropies for $d = 2$ using a three-dimensional bulk dual. In this case there are two interesting bulk duals: Einstein-Maxwell theory and Einstein-Chern-Simons theory.

3.6.1 Einstein-Maxwell theory

Starting with the Einstein-Maxwell action in a three-dimensional bulk

$$I_{E-M} = \frac{1}{2\ell_{\rm P}} \int d^3x \sqrt{-g} \left(\frac{2}{L^2} + \mathcal{R} - \frac{\ell_*^2}{4} F_{\mu\nu} F^{\mu\nu} \right) . \tag{3.190}$$

The charged black hole solution analogous to eq. (3.79) for this theory is [121]

$$ds^2 = -f(r) \frac{L^2}{R^2} dt^2 + \frac{dr^2}{f(r)} + r^2 d\theta^2 , \tag{3.191}$$

with

$$f(r) = \frac{r^2}{L^2} - m - \frac{q^2}{2}\log\left(\frac{r}{L\sqrt{m}}\right) . \tag{3.192}$$

With the above parametrization, the horizon radius is simply $r_H = L\sqrt{m}$. Note that the geometry is not asymptotically AdS because of the logarithmic term appearing in $f(r)$. Similar situations were considered in [122, 123, 124] and this logarithmic behaviour is the signature of broken conformal invariance, even in the UV. The solution for bulk gauge field is

$$A = -\frac{qL}{\ell_* R}\,\log\!\left(\frac{r}{L\sqrt{m}}\right) dt\,. \tag{3.193}$$

The integration constant in eq. (3.193) was chosen to ensure that $A = 0$ at the horizon. However, because of the logarithmic running of the bulk gauge field, one can not discern the chemical potential and the expectation value of the dual charge density as easily as in section 3.3 for $d \geq 3$. Following [123, 124], we arbitrarily chose a renormalization scale which will be defined by the radius $r = r_R$. Then the chemical potential is given by

$$\mu = -q\log\frac{r_H}{r_R}\,. \tag{3.194}$$

Hence we find that the chemical potential runs logarithmically with the renormalization scale.

The temperature of the black hole (3.191) is

$$\begin{aligned} T = \frac{L\,f'(r_H)}{4\pi R} &= \frac{r_H}{2\pi R L}\left(1 - \frac{L^2\,\mu^2}{4r_H^2\log[r_H/r_R]^2}\right) \\ &= T_0\left(x - \frac{\mu^2}{4x\log\left(\frac{xL}{r_R}\right)^2}\right) , \end{aligned} \tag{3.195}$$

where as before, we have introduced the parameter $x = r_H/L$. The horizon entropy is given by

$$S = 2\pi r_H = 2\pi L\,x\,. \tag{3.196}$$

The charged Rényi entropy for this solution is again determined with eq. (3.88), however, we note that in this integral, both the chemical potential and the renormalization scale r_R are

held fixed. The endpoints of the integral are again chosen such that $T(x_1, \mu, r_R) = T_0$ and $T(x_n, \mu, r_R) = T_0/n$. Given the form of eq. (3.195), the x_n can only be solved numerically for given μ (and r_R). Combining the previous results, we can write the charged Rényi entropy as follows:

$$S_n(\mu) = \frac{\pi L}{n-1}\left(2nx_1 - 2x_n + n(x_n^2 - x_1^2) + \mu(\sqrt{nx_n(nx_n-1)} - n\sqrt{x_1(x_1-1)})\right) . \tag{3.197}$$

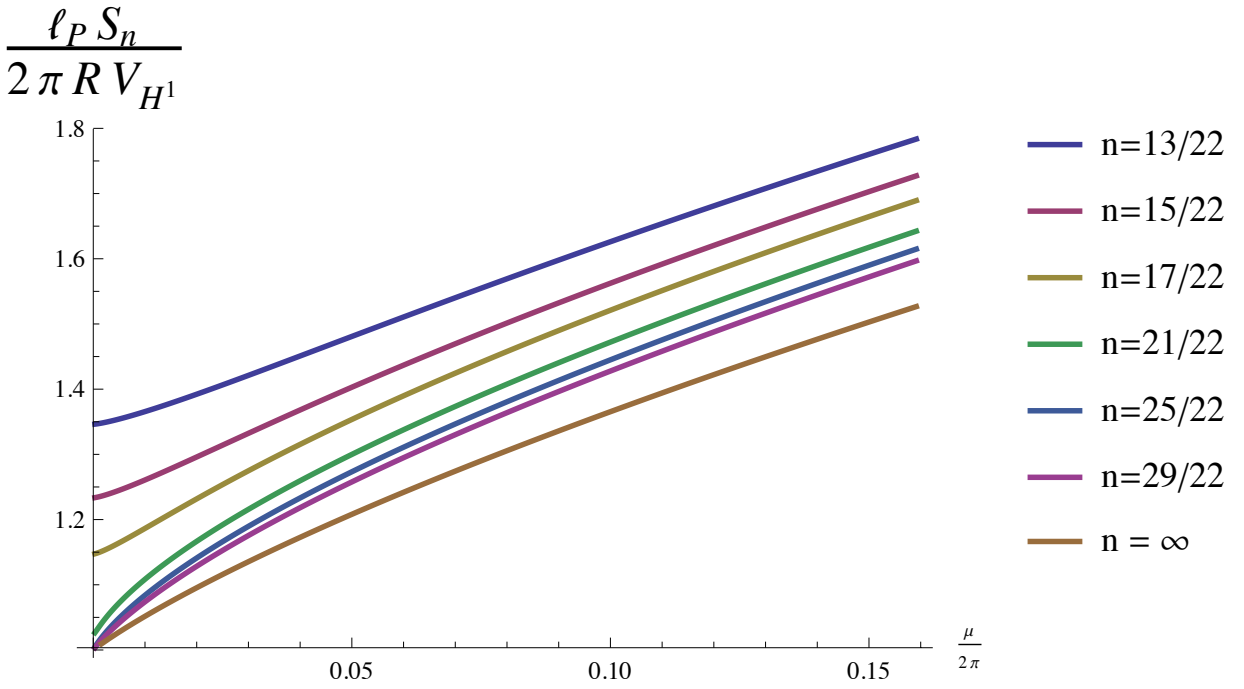

Figure 3.10: Charged Rényi entropy evaluated for the charged BTZ black hole at various values of n, setting $L = r_R = 1$.

In figure 3.10, we show the behaviour of the charge Rényi entropy as a function of μ for various values of n. For large values of μ, all of the $S_n(\mu)$ appear to increase linearly. From figure 3.11, we see that in the limit $n \to \infty$, $S_n(\mu)$ seems to approach a finite asymptotic value (which depends on μ), and we have included a plot in figure 3.10. This may be contrasted with the behaviour in eq. (3.92) for the same limit in higher dimensions. Further, the $n \to 0$ limit appears to diverge, in agreement with the analogous limit in higher dimensions, as given in eq. (3.92).

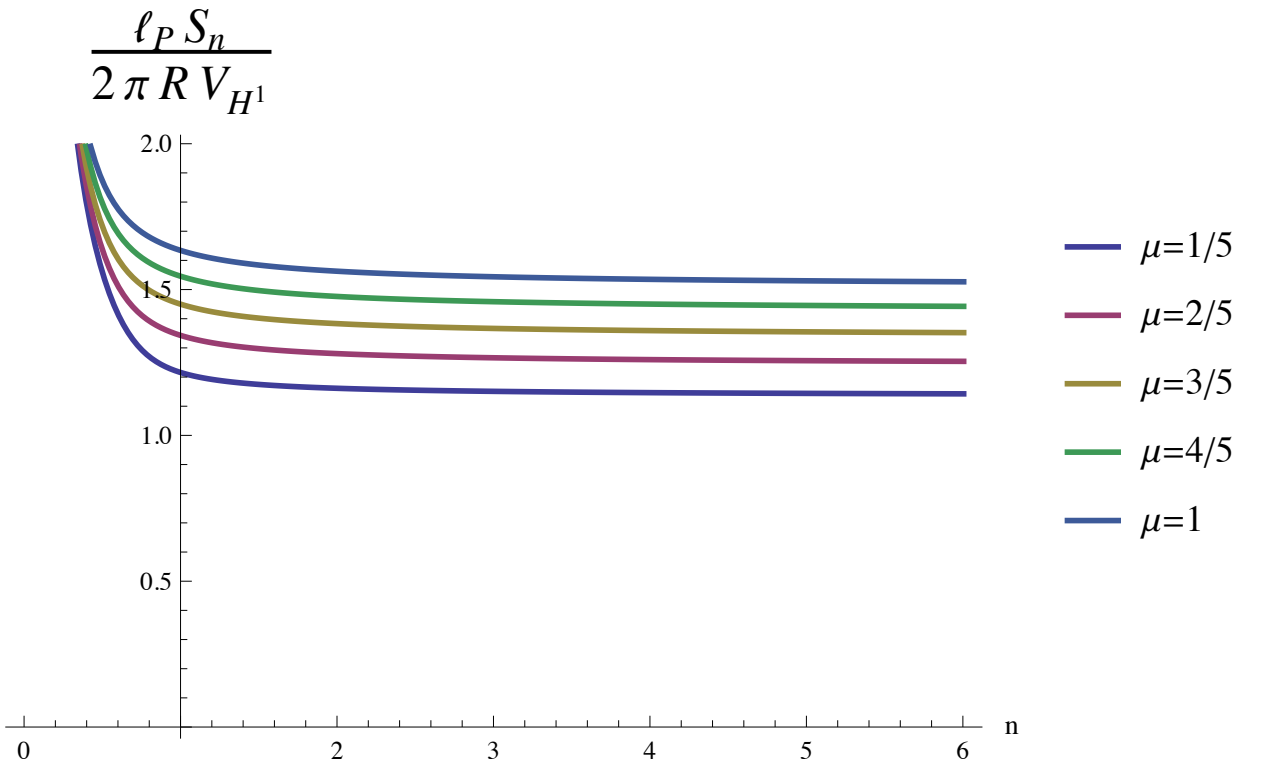

Figure 3.11: Charged Rényi entropy evaluated for the charged BTZ black hole at various values of μ, setting $L = r_R = 1$.

It is again interesting to consider imaginary chemical potentials, which is accomplished here by replacing $\mu = i\mu_{\rm E}$ and $q = iq_{\rm E}$ in the above results. The horizon radius for which $T = T_0/n$ is now given by

$$x_n = \frac{1 + \sqrt{1 - n^2 q_{\rm E}^2}}{2n} \,. \tag{3.198}$$

Clearly, we only have real solutions here when $q_{\rm E}^2 < 2/n^2$ and so the charge can only take values in a finite range. If we re-write eq. (3.198) as

$$(2n\, x_n - 1)^2 + n^2 q_{\rm E}^2 = 1 \,, \tag{3.199}$$

we see the horizon radius and the charge can be parameterized by

$$x_n = \frac{1 + \cos\phi}{2n} \,, \qquad\qquad q_{\rm E} = \frac{\sin\phi}{n} \,. \tag{3.200}$$

This is again reminiscent of the free field calculation where analytic continuation is only possible within a finite window for μ.

3.6.2 Einstein-Chern-Simons theory

We first consider the boundary duals of Einstein-Chern-Simons theory. The entropy of the charged BTZ black hole is (see e.g. (6.17) of [125])

$$S = 2\pi \left(\sqrt{\frac{c}{6}\left(L_0 - \frac{c}{24} - \frac{1}{4}q^2\right)} + \sqrt{\frac{\tilde{c}}{6}\left(\tilde{L}_0 - \frac{\tilde{c}}{24} - \frac{1}{4}q^2\right)} \right) . \tag{3.201}$$

where $L_0(\tilde{L}_0)$ and $c(\tilde{c})$ are the Virasoro generator and the central charge of the left (right) movers. Here q denotes the charge of the black hole. The expression inside the square root is independent of spectral flow. In terms of the horizon radius r_H,

$$L_0 - \frac{c}{24} - \frac{1}{4}q^2 = \frac{\pi\, r_H^2}{2\ell_{\rm P}\, L} = \tilde{L}_0 - \frac{\tilde{c}}{24} - \frac{1}{4}q^2 \,. \tag{3.202}$$

The Hawking temperature of the BTZ black hole is

$$T = \frac{r_H}{2\pi L^2} \,. \tag{3.203}$$

Using $c = 12\pi L/\ell_{\rm P}$, the entropy is the usual expression

$$S = 2\pi^2 \frac{LTc}{3} = \frac{\pi c}{3n} \,. \tag{3.204}$$

To obtain the Rényi entropy, we integrate S. However, since q cancels out, there is no dependence on the chemical potential. We note that this is in complete agreement with the free fermion results at least for sufficiently small μ_E. To be more precise, the above statement is as follows: Since the gauge potential does not couple to the metric in Chern-Simons theory, the solution of the equation of motion is a flat connection, $dF = 0$, or a constant gauge potential. Without any source term in the bulk, the gauge potential has to be zero. The charge q we mentioned above is a charge along the spatial direction θ. The result suggests that the linear term in the Rényi entropy (3.75) is not protected by a symmetry or an anomaly.

3.7 Appendix C: Holographic minutiae

In this appendix, we present various useful details of the holographic calculations, which are used in section 3.3.

3.7.1 Energy density

To evaluate the conformal weight of the twist operators using eq. (3.97), we need to evaluated the difference of energy densities: $\mathcal{E}(T_0/n, \mu) - \mathcal{E}(T_0, \mu = 0)$. Now in principle, with the introduction of appropriate boundary counterterms [126, 127], one can evaluate each of these energy densities individually. However, since we only need to determine a difference of energy densities, it is simpler to use 'background subtraction,' in which case the counterterms play no role.

To begin, we will denote the metric of a surface of constant r by $\gamma_{\mu\nu} = g_{\mu\nu} - \delta_{\mu r}\delta_{\nu r}/g^{rr}$, and the boundary hyperbolic metric (3.12) by $\hat{\gamma}$. Following [128], we write the boundary stress tensor

$$\tau_{ab} = \frac{2}{\sqrt{-\gamma}}\frac{\delta I}{\delta \gamma^{ab}} = \frac{1}{\ell_{\rm P}^{d-1}}(\gamma_{ab}K^c{}_c - K_{ab}), \tag{3.205}$$

where K_{ab} is the extrinsic curvature taken on a regulator surface at some constant radius r. To leading order as $r \to \infty$,

$$\tau_{00}(T_0/n, \mu) - \tau_{00}(T_0, \mu = 0) = \frac{(d-1)Lm}{2\ell_{\rm P}^{d-1}R^2 r^{d-2}}, \tag{3.206}$$

where m is given by (3.83). We can then evaluate the energy density of the boundary field theory with [129]

$$\begin{aligned}&\sqrt{-\hat{\gamma}}\hat{\gamma}^{00}(T_{\tau\tau}(T_0/n, \mu) - T_{\tau\tau}(T_0, \mu = 0))\\ &= \lim_{r\to\infty}\sqrt{-\gamma}\gamma^{00}(\tau_{00}(T_0/n, \mu) - \tau_{00}(T_0, \mu = 0)).\end{aligned} \tag{3.207}$$

Now using the notation $\mathcal{E} = T_{\tau\tau}$ from the main text, this equation yields the desired difference of energy densities:

$$\begin{aligned}\mathcal{E}(T_0/n, \mu) - \mathcal{E}(T_0, \mu = 0) &= \frac{(d-1)Lm}{2\ell_{\rm P}^{d-1}R^d}\\ &= \frac{(d-1)}{2R^d}\,\frac{L^{d-1}}{\ell_{\rm P}^{d-1}}\left(x_n^{d-2}(x_n^2 - 1) + \frac{q^2}{(L\,r_H)^{d-2}}\right).\end{aligned} \tag{3.208}$$

3.7.2 Charge density

In order to determine the magnetic response for our holographic model, we must evaluate the charge density $\rho(n, \mu) = \langle J_\tau \rangle$ in eq. (3.101). Of course, the standard AdS/CFT dictionary

indicates this expectation value is given by the normalizable component of the gauge field (4.21), *i.e.,* $\langle J_\tau \rangle \propto q$. However, to make precise comparisons with the expansion coefficients derived in section 3.2.3, we need the exact normalization of the current. We evaluate the latter here with a simple thermodynamic analysis.

Recall that the first law of thermodynamics of our ensemble is given by

$$d\mathcal{E} = T ds + \frac{\mu}{2\pi R} d\rho \,, \tag{3.209}$$

where $\mathcal{E}$, s and ρ denote the energy, entropy and charge densities respectively. Hence if the entropy density is held fixed, it follows that

$$\frac{\mu}{2\pi R} = \left(\frac{\partial \mathcal{E}}{\partial \rho}\right)_s \tag{3.210}$$

Now as observed above, we have $\rho(n,\mu) = \alpha\, q$ where α is some numerical factor which we aim to determine. From eq. (3.86), we can see that holding the entropy density fixed is equivalent to holding r_H constant. Hence it follows that

$$\begin{aligned} \alpha =& \frac{2\pi R}{\mu} \left(\frac{\partial \mathcal{E}}{\partial q}\right)_{r_H} \\ =& \sqrt{\frac{(d-1)(d-2)}{2}} \frac{\ell_*}{\ell_{\rm P}^{d-1} R^{d-1}} \end{aligned} \tag{3.211}$$

where up to a constant independent of q, $\mathcal{E}$ is given by eq. (3.208). Therefore, our final result for the charge density is

$$\rho(n,\mu) = \frac{(d-2) x_n^{d-2}}{4\pi\, R^{d-1}} \frac{L^{d-3} \ell_*^2}{\ell_{\rm P}^{d-1}} \mu \,. \tag{3.212}$$

3.7.3 Boundary CFT parameters

Here, we provide the values of various parameters, *i.e.,* C_V, $\hat{c}$, $\hat{e}$ and C_T, for the boundary CFT dual to the Einstein-Maxwell theory (3.78). This allows us to verify various expressions derived in section 3.2.3 for the expansion coefficients of the twist operator's conformal weight and magnetic response within the holographic framework of section 3.3.

To begin, we follow the calculation of [17] to evaluate the two-point correlator of a current dual to a bulk Maxwell field, however, we will be careful to include all of the numerical factors.

This allows us to evaluate the constant C_V appearing in eq. (3.55) for the Einstein-Maxwell theory studied in section 3.3. From [17], the bulk solution for the gauge field A, which near the AdS boundary approaches $\lim_{z\to 0} A \to \sum_i B_i(x)dx^i$, is given by

$$A(z,x) = \mathcal{N}\int d^dx' \left[\frac{z^{d-2}}{(z^2+(x-x')^2)^{d-1}}B_i(x')dx^i - z^{d-3}dz\frac{(x-x')^iB_i(x')}{(z^2+(x-x')^2)^{d-1}}\right], \quad (3.213)$$

where the normalization constant is given by

$$\mathcal{N} = \frac{\Gamma(d-1)}{\pi^{d/2}\Gamma(d/2-1)}\,. \quad (3.214)$$

This coefficient $\mathcal{N}$ is chosen to ensure that

$$\lim_{z\to 0}\mathcal{N}\frac{z^{d-2}}{(z^2+x^2)^{d-1}} = \delta^d(x)\,. \quad (3.215)$$

Now our (Euclidean) Maxwell action (3.78) is given by

$$I_{Max} = \frac{\ell_*^2}{8\ell_{\rm P}^{d-1}}\int d^dxdz\,\sqrt{G}\,G^{AC}G^{BD}\,F_{AB}F_{CD}\,, \quad (3.216)$$

where A, B range over $i = 1, \cdots d$ and z. Further, we work in Poincaré coordinates where $G_{AB} = (L^2/z^2)\,\delta_{AB}$. To extract the leading boundary contribution, we only need to consider the terms with z derivatives. That is,

$$I_{Max} = \frac{\ell_*^2L^{d-3}}{4\ell_{\rm P}^{d-1}}\int \frac{dz\,d^dx}{z^{d-3}}\,\left[(\partial_zA_i)^2 - 2\partial_iA_z\partial_zA_i + (\partial_iA_z)^2\right]\,. \quad (3.217)$$

Using the bulk equations of motion for A_i, A_z and integrating by parts, the above expression yields a boundary term at $z \to 0$:

$$\begin{aligned} I_{Max} \quad &= \lim_{z\to 0}\frac{\ell_*^2L^{d-3}}{4\ell_{\rm P}^{d-1}}\int\frac{d^dx}{z^{d-3}}\,\left[A_i\partial_zA_i - A_i\partial_iA_z\right] \\ &= \frac{(d-1)\mathcal{N}\,\ell_*^2L^{d-3}}{4\ell_{\rm P}^{d-1}}\int\int d^dx_1d^dx_2\frac{B_i(x_1)B_j(x_2)}{|x_{12}|^{2d-2}}\left(\delta_{ij} - 2\frac{x_{12}^ix_{12}^j}{|x_{12}|^2}\right), \end{aligned} \quad (3.218)$$

where the second line follows from substituting in eq. (3.213). Finally, we may differentiate this action twice with respect to the sources $B_i(x)$ to produce the two-point function of the corresponding current and we see the form matches precisely that given in eq. (3.55). Then

we may read off the central charge C_V in the boundary theory with the normalization of the bulk Maxwell term given in eq. (3.216):

$$C_V = \frac{(d-1)\mathcal{N}\,\ell_*^2 L^{d-3}}{2\ell_{\rm P}^{d-1}} = \frac{\Gamma\left(d\right)}{2\pi^{d/2}\,\Gamma\left(d/2-1\right)}\,\frac{\ell_*^2 L^{d-3}}{\ell_{\rm P}^{d-1}}\,. \tag{3.219}$$

Now eq. (3.56) relates this central charge to $(\hat{c}+\hat{e})$, the sum of the two CFT parameters which define the $\langle TJJ\rangle$ correlator (3.40). Now for the boundary CFT dual to the Einstein-Maxwell theory (3.78), this correlator does not take the most general form possible [130, 131], *i.e.,* $\hat{c}$ and $\hat{e}$ are not independent parameters. Rather one finds that

$$\hat{c} = d(d-2)\,\hat{e}\,. \tag{3.220}$$

Combining this constraint with eq. (3.56), we can also evaluate $\hat{c}$ and $\hat{e}$ for our holographic theory. In particular, we find

$$\hat{e} = \frac{\Gamma\left(\frac{d+2}{2}\right)}{2\pi^{d/2}(d-1)^2}\,C_V = \frac{(d-2)\,\Gamma(d+1)}{16\pi^d(d-1)^2}\,\frac{\ell_*^2 L^{d-3}}{\ell_{\rm P}^{d-1}} \tag{3.221}$$

and then $\hat{c}$ follows from eq. (3.220).

Finally, it is convenient to have the central charge C_T, which appears in the two-point correlator of the stress tensor (3.30), for our holographic theory. In this case, the calculation analogous to that above for the Maxwell field was carried out for the metric in [132]. Hence we can simply quote the result for C_T:

$$C_T = \frac{\Gamma(d+2)}{\pi^{d/2}(d-1)\Gamma(d/2)}\,\frac{L^{d-1}}{\ell_{\rm P}^{d-1}}\,. \tag{3.222}$$

Phase structure of the Charged Rényi entropies

The goal of Chap. 4 is to discuss the phase structure of the charged Rényi entropies in the presence of a light charged scalar field in the bulk. The charged hyperbolic black holes can also become unstable at low temperature and are generally more unstable once charge is added. Due to the fact that one has additional parameters to tune such as the charge and mass of the scalar, the entangling chemical potential and n, the phase structure is much richer. We also connect this work to the subject of holographic superconductors [84, 85]. A CFT with a light charged scalar operator is suppose to have a superconducting phase transition at finite temperature if the system is put at finite physical chemical potential. In certain limits, we can learn about the nature of this physical phase transition by studying the phase structure of the charged Rényi entropies of the ground state.

Chapter 4

Charged Rényi Entropies and Holographic Superconductors

Alexandre Belin[a,b], Ling-Yan Hung[b,c], Alexander Maloney[a,b] and Shunji Matsuura[a]

[a] *Departments of Physics and Mathematics, McGill University, Montréal, Québec, Canada*

[b] *Department of Physics, Harvard University, Cambridge, MA 02138 USA*

[c] *Department of Physics, Fudan University, Shanghai, China*

Abstract

Charged Rényi entropies were recently introduced as a measure of entanglement between different charge sectors of a theory. We investigate the phase structure of charged Rényi entropies for CFTs with a light, charged scalar operator. The charged Rényi entropies are calculated holographically via areas of charged hyperbolic black holes. These black holes can become unstable to the formation of scalar hair at sufficiently low temperature; this is the holographic superconducting instability in hyperbolic space. This implies that the Rényi entropies can be non-analytic in the Rényi parameter n. We find the onset of this instability as a function of the charge and dimension of the scalar operator. We also comment on the relation between the phase structure of these entropies and the phase structure of a holographic superconductor in flat space.

Published in Journal of High Energy Physics **1501**, 059 (2015)

4.1 Introduction

The low energy states of a quantum field theory typically exhibit a high degree of spatial entanglement. To characterize this entanglement precisely, consider a quantum field theory in state ρ, with space divided into two parts $A \cup B$. The Rényi entropies S_n are the moments of the reduced density matrix $\rho_{\rm A} = {\rm Tr}_B \rho$ for subsystem A

$$S_n = \frac{1}{1-n} \log {\rm Tr}[\rho_{\rm A}^n]. \tag{4.1}$$

The entanglement entropy S_{EE} is $S_{EE} = \lim_{n \to 1} S_n = -{\rm Tr} \rho_{\rm A} \log \rho_{\rm A}$. These entropies encode the amount of information stored in correlations between A and B, rather than in A or B separately. Entanglement entropies have played an important role in condensed matter physics [37, 35, 133, 47, 48], quantum gravity [45, 49, 72, 73, 134, 38, 39], and quantum information [135].

In many cases we are interested in theories with a conserved charge Q associated with a global symmetry, such as particle number. When Q is the integral of a local charge density one can ask how the entanglement depends on the distribution of charge between A and B. Very naively, one might expect that the entanglement between A and B should increase as charge is distributed more and more unequally between A and B. This is because one way of moving charge (say, particle number) into A from B is to create a particle-antiparticle pair, placing the particle in region A and the anti-particle in region B; particle-antiparticle pairs created from the vacuum are naturally entangled, so this process should increase the entanglement entropy. Of course, whether this naive expectation is true will depend on the details of the state and the theory.

To address this question we will follow [88] and define the charged Rényi entropy:

$$S_n(\mu) = \frac{1}{1-n} \log {\rm Tr} \left[\rho_{\rm A} \frac{e^{\mu Q_{\rm A}}}{n_{\rm A}(\mu)} \right]^n . \tag{4.2}$$

The parameter μ is known as an entanglement chemical potential, and $Q_{\rm A}$ measures the amount of charge in subsystem A; it is the integral over A of the local charge density. $n_{\rm A}(\mu) \equiv {\rm Tr}[\rho_A e^{\mu Q_{\rm A}}]$ is a normalization factor. Applications of charged Rényi entropies

include the supersymmetric Rényi entropies [94, 136] and the characterization of symmetry protected topological phases [137].

We emphasize that μ is not the physical chemical potential of the system, but rather is a formal parameter used to weight the entanglement in different charge sectors. Nevertheless, just as thermodynamic entropies can undergo phase transitions as temperatures and potentials are varied, the entanglement entropies $S_n(\mu)$ can undergo phase transitions as the Rényi parameter n and the entanglement chemical potential μ are varied. These phase transitions reflect essentially non-analytic features of the spatial entanglement structure of quantum field theory ground states.

Rényi phase transitions were investigated in [108] in the case $\mu = 0$. The authors considered large N conformal field theories which are dual to semi-classical Einstein gravity in Anti-de Sitter space plus matter. When the entangling surface ∂A is a sphere, S_n is related to the entropy of a black hole with hyperbolic event horizon. They showed that S_n is non-analytic in n if the dimension Δ of the lightest scalar operator $\mathcal{O}$ in the theory is sufficiently small. In particular, $\partial_n^2 S_n$ becomes discontinuous at some $n = n_c$, with $1 < n_c < \infty$, if

$$\frac{d-2}{2} < \Delta < \frac{d+\sqrt{d}}{2}\,. \tag{4.3}$$

Here d is the space-time dimensionality of the CFT and the first inequality is the unitarity bound. The point is that the field ϕ dual to $\mathcal{O}$ will become unstable if the black hole temperature is sufficiently small. When $n < n_c$, S_n is computed by the entropy of a Einstein gravity black hole. But when $n > n_c$ the Einstein black hole becomes unstable and the scalar operator gets a non-zero expectation value near the horizon. In this phase the entangling surface hosts a localized "impurity" operator with non-vanishing expectation value. We emphasize that this argument relies crucially on the fact that we are studying theories at large N.

Similar results have been found in purely QFT analysis [70, 71]. These authors consider the renormalization group flow of the coupling constants associated to impurity operators localized on the entangling surface. At a certain value of n, the beta functions for these couplings change sign and the system undergoes a phase transition. For example, in [70] it

was argued that the Rényi entropies of the $O(N)$ model are non-analytic at $n = 7/4$.

One consequence of this is that the replica trick – where one computes S_{EE} by computing S_n at integer values of n and analytically continuing to $n \to 1$ – must be treated with care. However, we emphasize that in the above analysis n_c was shown to be always greater than 1, and approaches 1 only as the dimension Δ approaches the unitarity bound (at which point the operator should decouple from the theory). Thus the Rényi entropies are still analytic in a finite neighbourhood of $n = 1$. So this result does not invalidate the derivation of the Ryu-Takayanagi formula by Maldacena and Lewkowycz [66], which relied only on analyticity near $n = 1$. Further relations between the Ryu-Takayanagi formula and Rényi entropies at $n \neq 1$ were discussed in [79, 81, 138].

In this paper we investigate the phase transitions of charged Rényi entropies. We consider large N CFTs with global conserved charges that are holographically dual to Einstein-Maxwell-Scalar theory in AdS. We will be interested in the charged Rényi entropies of the ground state for spherical entangling surfaces; these Rényi entropies can be computed by studying the CFT in hyperbolic space at finite temperature and charge density [67, 88]. In the bulk, the dual states are charged AdS black holes with hyperbolic event horizons [68, 88].

We will therefore study the phase structure of charged, hyperbolic black holes in AdS. In particular, we will consider instabilities where a charged scalar field – dual to a CFT operator with global charge q – condenses near the horizon. In this paper, we will find that charged entropies $S_n(\mu)$ will be non-analytic as we vary n and μ, provided the conformal dimension of the charged operator lies between

$$\frac{d-2}{2} < \Delta_c(q) < \frac{1}{2}\left(d + \sqrt{d + \frac{8(d-2)q^2\mu^2}{8\pi^2 R^2 + (d-2)\mu^2}}\right) . \tag{4.4}$$

The setup is very similar to that used in the study of holographic superconductors [84, 85, 139], the only difference being that space is hyperbolic. The qualitative features of these instabilities are similar to those in flat space. In particular, the high temperature and large chemical potential behaviour is identical to that of the flat-space holographic superconductor; in these limits the curvature of the hyperbolic spatial slice is irrelevant. Thus, even though the charged Rényi entropies under consideration probe only properties of the ground state,

they contain information about the phase structure of physical thermodynamic quantities at finite temperature. This echoes the results of [36, 140], that entanglement entropies of the ground state can be used to study phase transitions of the theory involving higher excited states.

In Section 4.2, we review the relationship between the reduced density matrix for spherical entangling surfaces and thermal density matrices in hyperbolic space. In section 4.3 we relate this to black hole entropy using AdS/CFT, and describe the phase transition using both analytic and numerical techniques. We compute the critical Rényi parameter n_c numerically using a shooting method. In Section 4.4, we discuss these results and relate them to the phase structure of the holographic superconductor in certain limits.

4.2 From entanglement entropy to thermal entropy

In a relativistic theory, an observer undergoing constant acceleration has causal access only to part of the space-time, known as the Rindler wedge, which is separated from the rest of the space-time by an event horizon. This Rindler wedge is the causal development of half-space, and a Rindler observer is in a thermal state due to the Unruh effect. From this one concludes that the reduced density matrix associated with the half-space is just the thermal density matrix on Rindler space [45]. In a conformal theory, this can be generalized to relate the reduced density matrix for a spherical region and the thermal density matrix on a hyperbolic space [67, 68]. We will now review this argument.

Consider a quantum field on a d-dimensional flat space in Euclidean signature

$$ds^2_{R^d} = dt_E^2 + dr^2 + r^2 d\Omega^2_{d-2} \tag{4.5}$$

where t_E is the Euclidean time, $d\Omega_{d-2}$ is the volume element of a unit sphere, and r is the radial coordinate. We are interested in the reduced density matrix of the $d-1$ dimensional ball of radius R centered at the origin. To compute this, we use the fact that flat space metric is conformal to $S^1 \times \mathbb{H}^{d-1}$:

$$ds^2_{R^d} = \Omega^{-2} ds^2_{S^1 \times \mathbb{H}^d} = \Omega^{-2}(d\tau_E^2 + R^2(du^2 + \sinh^2 u d\Omega^2_{d-2})) \tag{4.6}$$

where

$$\Omega = \left| 1 + \cosh\left(u + i\frac{\tau_E}{R} \right) \right| . \tag{4.7}$$

and the $S^1 \times \mathbb{H}^{d-1}$ coordinates (τ_E, u) are defined by

$$\exp\left[-\left(u + i\frac{\tau_E}{R} \right) \right] = \frac{R - (r + it_E)}{R + (r + it_E)}. \tag{4.8}$$

This conformal map has two important features. First, the $\tau_E = 0$ slice of the $S^1 \times \mathbb{H}^{d-1}$ geometry covers only the interior of the ball ($t_E = 0, r = R$); the entangling surface at ($t_E = 0, r = R$) has been mapped to the boundary of the hyperbolic space $u \to \infty$. In Lorentzian signature (taking $\tau_E = i\tau$), this coordinate patch would cover only the interior of the Causal region associated with the ball ($t = 0, r < R$). Second, from (4.8) we see that Euclidean time coordinate τ_E is periodic with period $2\pi R$. Putting this together, we see that the reduced density matrix is (up to a unitary transformation which does not enter into the trace)

$$\rho = \frac{1}{Z_1} e^{-2\pi R H_E} \tag{4.9}$$

Here $H_E = i\frac{\partial}{\partial \tau_E}$ is the Hamiltonian which generates translations in τ and Z_1 is a normalization factor. Thus the reduced density matrix for a spherical region of radius R is equivalent to the thermal density matrix on a hyperbolic space with radius R and temperature $T_0 = 1/2\pi R$. From this, one can show that the Rényi entropy (4.1) is

$$S_n = \frac{1}{n-1}(n \log Z_1 - \log Z_n), \tag{4.10}$$

where Z_n is the thermal partition function of the hyperbolic space at $T = T_0/n$.

In a theory with a global conserved charge Q, one can generalize (4.9) to

$$\rho_\mu = \frac{e^{-H_E/T_0 + \mu Q}}{Z(T_0, \mu)} . \tag{4.11}$$

where $Z(T, \mu)$ is a partition function evaluated at temperature T and chemical potential μ. The operator Q measures the charge on hyperbolic space $\mathbb{H}^{d-1}$, which – from the conformal

transformations above – simply measures the amount of charge in region A. So (4.11) is the generalized reduced density matrix introduced in (4.2).

Note that μ can be interpreted as the time component of a background gauge field B_μ which couples to the charge density, via $B_{\tau_E} = \mu/2\pi R$ [1]

$$\mu = \oint B = \int_0^{2\pi R} B_{\tau_{\rm E}} d\tau_{\rm E}\,. \tag{4.12}$$

Since the τ_E circle shrinks to zero at the entangling surface, this chemical potential introduces a magnetic flux localized at the entangling surface [88]. The charged Rényi entropies

$$S_n(\mu) = \frac{1}{1-n}\log\frac{Z(T_0/n,\mu)}{Z(T_0,\mu)^n}. \tag{4.13}$$

measure the entanglement in the (flat space, zero charge density) ground state of a theory, weighted by the charge contained in region A. In fact, using the thermodynamic identity

$$S_{\rm therm}(T,\mu) = -\left.\frac{\partial F(T,\mu)}{\partial T}\right|_\mu = \frac{\partial}{\partial T}(T\log Z(T,\mu))\big|_\mu\,. \tag{4.14}$$

this can be written in terms of the standard grand canonical ensemble thermal entropy $S_{therm}(T,\mu)$:

$$S_n(\mu) = \frac{n}{n-1}\frac{1}{T_0}\int_{T_0/n}^{T_0} S_{\rm therm}(T,\mu)\,dT\,. \tag{4.15}$$

Finally, it is important to mention the cut-off dependence of the Rényi entropy. The Rényi entropy, as well as the entanglement entropy, are divergent quantities unless we set a UV cut-off near the entangling surface. On the other hand, the thermal entropy on hyperbolic space is a divergent quantity as the volume of the hyperboloid is infinite; we must set an IR cut-off near the boundary of hyperbolic space[2]. In fact, these divergences are identical: they can be mapped into one another by the conformal transformation (4.6). We refer the reader to [67] for more details.

[1] We denote this background gauge field B to avoid confusion with the bulk dynamical A of the next section.

[2] For holographic theories, the black hole entropy of a hyperbolic horizon is also a divergent quantity and requires an IR cut-off near the boundary of AdS space.

4.3 Holographic computations

In this section we calculate charged Rényi entropies for large N CFTs which are dual to semi-classical Einstein gravity coupled to matter in AdS space. In this case $S_{therm}(T,\mu)$ is the entropy of a black hole entropy in the bulk with hyperbolic event horizon [67, 68]. The global conserved current of the boundary theory acts as a source for a bulk gauge field. We will also assume the existence of a scalar operator in the boundary theory, with dimension Δ and charge q, which is dual to a charged scalar field in the bulk. We are therefore looking for charged black holes with hyperbolic event horizons in Einstein-Maxwell-Scalar theory. These solutions are dual to the grand canonical ensemble of the boundary CFT on $\mathbb{R}\times\mathbb{H}^{d-1}$. We first describe the Einstein-Maxwell solutions and give the Rényi entropies when there is no scalar condensate. We then look for scalar instabilities for the Einstein-Maxwell black hole at the linearized level. We perform an analytic analysis of the extremal black hole, and show that instabilities do occur in this case. We then solve the Klein-Gordon equation for the scalar in the non-extremal case, using a numerical shooting method starting from the horizon. This allows us to determine the location of the phase transition in $S_n(\mu)$ as a function of Δ and q. We focus here on 3-dimensional CFT but a similar phase transition will occur in any dimension $d \geq 3$.

4.3.1 Neutral black holes and scalar instability

Before discussing the charged Rényi entropies and the related charged hyperbolic black holes, we review a few result concerning uncharged black holes. When the entangling chemical potential vanishes, the dual gravitational solutions are hyperbolic black holes

$$ds^2 = -f(r)\frac{L^2}{R^2}\,d\tau^2 + \frac{dr^2}{f(r)} + r^2\,d\mathbb{H}_2^2\,, \tag{4.16}$$

where $d\mathbb{H}_2^2 = du^2 + \sinh^2 u\,d\phi^2$ is the metric on $\mathbb{H}_2$ with unit curvature and

$$f(r) = \frac{r^2}{L^2} - 1 - \frac{M}{r} \tag{4.17}$$

In the entanglement entropy limit $n \to 1$, we recover the massless hyperbolic black hole, which is AdS_4 in Rindler coordinates. To compute the Rényi entropies, we integrate over a

range of temperatures (4.15). As n increases, the integral includes lower and lower temperatures.

We now consider a scalar field in the bulk of negative mass-squared, which is dual to an operator of dimension $\Delta < 3$ in the boundary CFT. In this case the black hole may become unstable at a certain temperature T_c (or equivalently at a certain n_c) at which the black hole undergoes a second order phase transition. This was shown in [108], although in earlier work the authors of [83] noted a similar instability for topological black holes with compact horizon (see also [141]). This effect can be understood as follows. In the extremal limit these black holes have a $AdS_2 \times \mathbb{H}_2$ near horizon geometry. Scalar fields with masses below the effective Breitenlohner-Freedman bound for the near-horizon AdS_2 (suitably corrected for the $\mathbb{H}_2$ factor) will become unstable at low temperatures. We emphasize that this happens for uncharged black holes; for AdS black holes with flat or spherical horizons, such instabilities occur only at finite chemical potential. When the scalar field is below this bound the black hole becomes unstable and will decay to a black hole solution with scalar hair. The corresponding boundary operator acquires a non-zero expectation value.

This instability implies that S_n has a phase transition as a function of n. The Rényi entropies are obtained from the thermal entropies by integrating once so $\partial_n^2 S_n$ will become discontinuous at some critical Rényi parameter n_c. In order to determine the precise value of n_c at which this transition occurs, it is necessary to study numerically the scalar wave equation in the black hole background. The results of [108] (see also [70, 71]) show that $n_c > 1$ as long Δ is above the unitarity bound. In particular, if we compute the entanglement entropy by taking $n \to 1$ then S_n is given by the Einstein black hole with vanishing scalar field. We will see that this is no longer the case for charged Rényi entropies: when $\mu \neq 0$, it is possible for n_c to be less than one.

4.3.2 Charged black hole

The Einstein-Maxwell-Scalar action with a negative cosmological constant is[3]

$$I_{E-M} = \frac{1}{2\ell_{\rm P}^2}\int d^4x\,\sqrt{-g}\left(\frac{6}{L^2}+\mathcal{R}-\frac{\ell_*^2}{4}F_{\mu\nu}F^{\mu\nu}-V(|\phi|)-\frac{1}{2}|\nabla\phi-iqA\phi|^2\right). \tag{4.18}$$

We will take the potential to be a mass term $V(|\phi|)=\frac{1}{2}m^2|\phi|^2$ which, together with boundary conditions, fixes the conformal dimension Δ of the dual CFT operator. We first consider charged hyperbolic black hole solutions with vanishing scalar field. The metric is

$$ds^2 = -f(r)\frac{L^2}{R^2}\,d\tau^2+\frac{dr^2}{f(r)}+r^2\,d\mathbb{H}_2^2\,, \tag{4.19}$$

with

$$f(r)=\frac{r^2}{L^2}-1-\frac{M}{r}+\frac{\rho^2}{r^2} \tag{4.20}$$

The time coordinate is normalized so that the boundary metric naturally is flat space in Milne coordinates: $ds^2_{CFT}=-d\tau^2+R^2d\mathbb{H}_2^2$ [67]. The bulk gauge field is

$$A=\left(\frac{2L\,\rho}{R\ell_*\,r}-\frac{\mu}{2\pi R}\right)d\tau\,. \tag{4.21}$$

We will chose our gauge so that A vanishes at the horizon $r=r_H$, so that

$$\mu = 4\pi\frac{L\,\rho}{\ell_* r_H}\,. \tag{4.22}$$

The mass parameter M is related to the horizon radius r_H by

$$M=\frac{r_H}{L^2}(r_H^2-L^2)+\frac{\rho^2}{r_H}\,. \tag{4.23}$$

We can rewrite $f(r)$ in terms of the horizon radius r_H and the chemical potential μ as

$$f(r)=\frac{(r-r_H)(16\pi^2r(r^2-L^2+rr_H+r_H^2)-r_H(\ell_*\mu)^2)}{16\pi^2L^2r^2}\,. \tag{4.24}$$

The temperature of this black hole is

$$T=\frac{T_0}{2}\,Lf'(r_H)=\frac{T_0}{2}\left[3\,\frac{r_H}{L}-\frac{L}{r_H}\left(1+\left(\frac{\mu\,\ell_*}{4\pi L}\right)^2\right)\right] \tag{4.25}$$

[3]The scale ℓ_* depends on the details of the theory. With this notation, the 4-dimensional gauge coupling is $g_4^2=2\ell_{\rm P}^2/\ell_*^2$.

where $T_0 = 1/2\pi$ and prime denotes differentiation with respect to r. The thermal entropy of the black hole is given by the Bekenstein-Hawking formula:

$$S_{therm} = \frac{2\pi}{\ell_{\rm P}^2} V_\Sigma \, r_H^2 \,, \tag{4.26}$$

where V_Σ denotes the (appropriately regulated) volume of $\mathbb{H}^2$. As noted above, the large-volume divergence of V_Σ is related to a UV divergence in the boundary theory [68]. In particular, V_Σ can be regarded as a function of R/δ, the ratio of the radius of the entangling sphere to the short-distance cut-off in the boundary theory. The leading term is

$$V_\Sigma \simeq 2\pi \, \frac{R}{\delta} + \cdots \,, \tag{4.27}$$

Hence the corresponding Rényi entropies begin with an area law contribution. When there is no scalar condensate, the charged Rényi entropies can be computed from (4.26) and (4.15):

$$S_n(\mu) \;=\; \pi V_\Sigma \left(\frac{L}{\ell_{\rm P}}\right)^2 \frac{n}{n-1} \left[\left(1 + \frac{1}{4}\left(\frac{\mu \ell_*}{2\pi L}\right)^2\right)(x_1 - x_n) + x_1^3 - x_n^3 \right] \tag{4.28}$$

with

$$x_n = \frac{1}{3n} + \sqrt{\frac{1}{9n^2} + \frac{1}{3} + \frac{1}{12}\left(\frac{\mu \ell_*}{2\pi L}\right)^2} \,. \tag{4.29}$$

4.3.3 Scalar instabilities

The Einstein-Maxwell black holes described above may become unstable at sufficiently low temperature in the presence of a scalar field. We will find the onset of the instability by solving the wave equation for the scalar on the black hole background. The endpoint of the instability will be a hairy black hole with a non-zero scalar field in the vicinity of the horizon. Thus there will be more than one classical gravitational solution that satisfies the same boundary conditions. We should then compare free energies of these saddle point configurations and determine which one is thermodynamically preferable. In general, we expect that the dynamically stable saddle point is thermodynamically preferred [142, 143]; indeed, in the holographic superconductor [85] and the constant mode analysis [108] scalar

condensate phases were found to be thermodynamically preferable. We expect that in the present case the dynamical instability analysis will agree with the thermodynamical analysis as well.

We note that the instability involves a scalar field which is not constant on $\mathbb{H}_2$, as the constant mode on $\mathbb{H}_2$ is non-normalizable. Thus the hairy black hole will not have the full hyperbolic symmetry of the Einstein-Maxwell black hole, making its explicit construction a technically difficult task. We will therefore leave the construction of hairy black hole solutions to future work; in the present paper we simply demonstrate that the black holes are unstable and find the onset of the instability.

To find the instability, we must study the Klein-Gordon equation for a charged (complex) scalar Φ on the black hole background:

$$\left((\nabla^\mu - iqA^\mu)(\nabla_\mu - iqA_\mu) - m^2\right)\Phi = 0\,. \tag{4.30}$$

It is convenient to decompose the field in eigenfunctions of the Laplacian on $\mathbb{H}_2$:

$$\Phi = \frac{\phi(r)e^{\omega\tau}Y(\sigma)}{r} \tag{4.31}$$

where $\nabla^2_{\mathbb{H}_2}Y = -\lambda Y$. For a normalizable mode on $\mathbb{H}_2$, $\lambda > 1/4$. The wave equation reduces to:

$$\left(-\left(f(r)\frac{d}{dr}\right)^2 + V(r)\right)\phi(r) \quad = 0 \tag{4.32}$$

with

$$V(r) = \frac{f(r)}{r^2}\left(\lambda + rf'(r) + r^2m^2\right) + (\omega + iqA_\tau)^2 \tag{4.33}$$

It is convenient to put equation (4.34) in Schrodinger form, by defining the tortoise coordinates r^* by $dr^* = dr/f(r)$, so that

$$\left(-\left(\frac{d}{dr^*}\right)^2 + V(r^*)\right)\phi(r^*) \quad = 0 \tag{4.34}$$

An unstable mode corresponds to a solution of this equation with $\mathrm{Re}\,\omega > 0$. We note that when $q = 0$, (4.34) is just a one dimension Schrodinger equation with potential $V(r)$,

although in general $V(r)$ will be complex. We are interested in finding the onset of this classical instability, i.e. we seek a solution with $\mathrm{Re}(\omega) = 0$.

Before performing the numerical analysis of the black hole stability, we can understand analytically when the black hole should become unstable. In the zero temperature limit, the black hole (4.19) has an $AdS_2 \times \mathbb{H}_2$ near horizon geometry. The AdS_2 and $\mathbb{H}_2$ radii are

$$L^2_{AdS_2} = \frac{2L^2_{AdS_4}}{f''(r_{ext})} \qquad L^2_{\mathbb{H}_2} = r^2_{ext} \tag{4.35}$$

where r_{ext} is the horizon radius of the extremal black hole. In addition, there is a constant electric flux on the near horizon AdS_2:

$$F = -\frac{\mu}{2\pi R r_{ext}} dvol_{AdS_2} \tag{4.36}$$

In the near horizon region, one can therefore approximate the wave equation (4.34) by

$$\left[-\left(\frac{\epsilon^2 f''(r_{ext})}{2} \partial_\epsilon \right)^2 + \epsilon^2 \frac{f''(r_{ext})}{2r^2_{ext}} (\lambda + r^2_{ext} m^2) + \left(\omega - i\epsilon \frac{q\mu}{2\pi R r_{ext}} \right)^2 \right] \phi(\epsilon) = 0 \tag{4.37}$$

where ϵ is the near-horizon radial coordinate $r = r_{ext} + \epsilon$. The solutions to (4.37) can be found analytically, and one can then determine exactly when an instability occurs. In fact, it is not necessary to even solve (4.37) explicitly to see the instability. We can simply note that near the asymptotic boundary of the near-horizon $AdS_2 \times \mathbb{H}_2$, solutions to (4.37) will behave as $\phi(\epsilon) \sim \epsilon^{-\Delta_{eff}}$, where

$$\Delta_{eff} = 1/2 + \sqrt{m^2_{eff} L^2_{AdS_2} + 1/2}, \qquad m^2_{eff} = \frac{f''(r_{ext})}{2r^2_{ext}} (\lambda + r^2_{ext} m^2) - \frac{q^2\mu^2}{4\pi^2 R^2 r^2_{ext}} \,. \tag{4.38}$$

Thus ϕ behaves like a field of mass-squared m^2_{eff} in the near-horizon AdS_2. The black hole will become unstable when the effective mass-squared falls below the AdS_2 Breitenlohner-Freedman bound, $m^2_{eff} L^2_{AdS_2} < -1/4$, i.e. when Δ_{eff} becomes complex.

We conclude that an instability will occur when

$$m^2 L^2_{AdS_4} < -\frac{f''(r_{ext})}{8} - \frac{1}{4r^2_{ext}} + \frac{2q^2\mu^2}{4\pi^2 R^2 r^2_{ext} f''(r_{ext})} \,. \tag{4.39}$$

The first term on the right hand side is the naive AdS_2 BF bound. The second term is a correction term coming from the fact that the lowest eigenvalue of a normalizable mode on

$\mathbb{H}_2$ has $\lambda = 1/4$; this effect makes the scalar more stable. The final term is a correction term coming from the charge coupling $q^2 A_\mu A^\mu$; this effect makes the scalar more unstable. Using the form of the black hole metric, we expect instabilities when

$$-\frac{9}{4} < m^2 L^2_{AdS_4} < -\frac{3}{2} + \frac{2q^2\mu^2}{8\pi^2 R^2 + \mu^2} \tag{4.40}$$

The first inequality is the usual BF bound in AdS_4.

It is straightforward to generalize this to arbitrary dimension (we will omit the details for the sake of brevity). In general, we find an instability when

$$-\frac{d^2}{4} < m^2 L^2_{AdS_{d+1}} < -\frac{d(d-1)}{4} + \frac{2(d-2)q^2\mu^2}{8\pi^2 R^2 + (d-2)\mu^2}\,. \tag{4.41}$$

In terms of conformal dimension of dual operators, this gives

$$\Delta < \frac{1}{2}\left(d + \sqrt{d + \frac{8(d-2)q^2\mu^2}{8\pi^2 R^2 + (d-2)\mu^2}}\right) \equiv \Delta_c(q) \tag{4.42}$$

We will now study the stability of the charged hyperbolic black holes by numerically solving the scalar wave equation[4]. Normalizability of the modes requires the field to be regular at the horizon; we can expand perturbatively for the field near the horizon. We then use a shooting method to obtain desired boundary conditions near the boundary of AdS_4, namely

$$\Phi(r)|_{r\to\infty} \propto r^{-\Delta} \tag{4.43}$$

In Fig. 4.1, we show the results. We show the critical value of the Rényi parameter n_c at which the phase transition occurs, as a function of μ and q for $\Delta = 2$. We see that increasing the charge makes the configuration less stable for any $\mu \neq 0$. For large enough q, increasing μ also renders the black hole less stable. However, for a neutral scalar, as we increase μ we make the black hole first more stable until some maximum value after which n_c decreases again. We will return to discuss this non-monotonic behaviour in the next section.

In Fig. 4.2, we show the value of n_c for $\mu = 5$, varying Δ and q. As expected, we see that decreasing Δ or increasing q makes the configuration less stable. From this graph, we

[4]For the remainder of this section we set $L = R = \ell_* = 1$

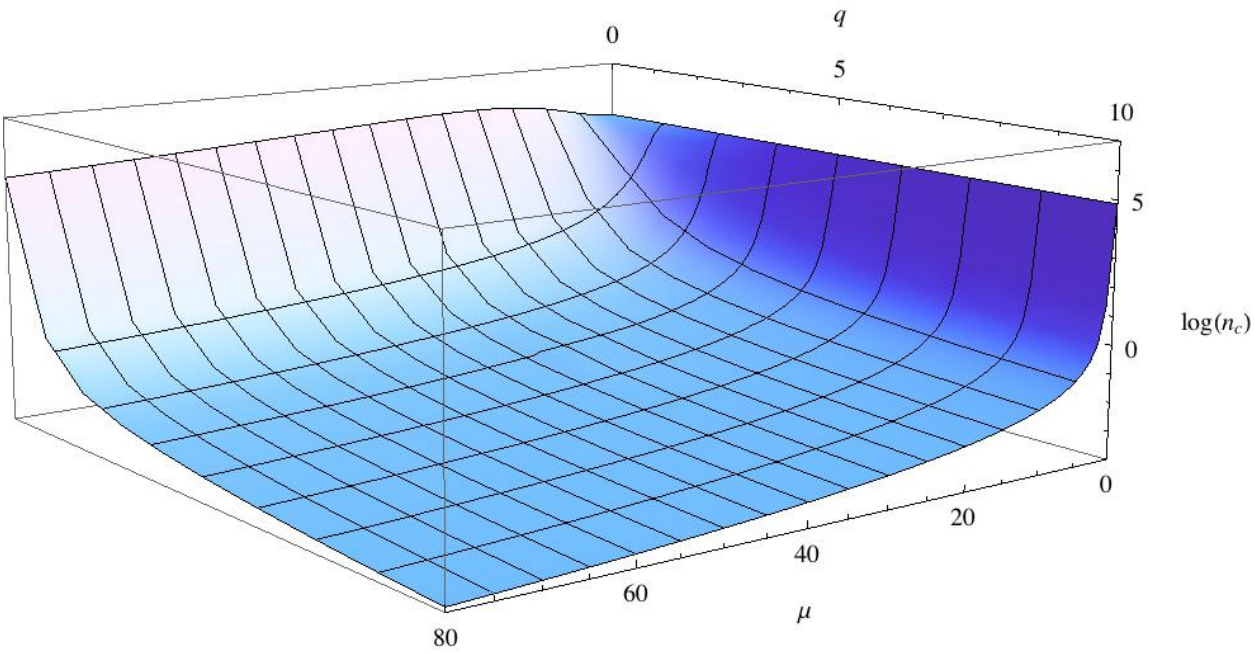

Figure 4.1: $\log n_c$ as a function of μ and q for $\Delta = 2$. Every configuration above this surface is unstable.

can determine the critical value Δ_c (for a given q) at which the instability kicks in. In Fig. 4.3, we plot the curves $\Delta(q)$ for different values of n_c and show that the curves approach the analytic value derived in (4.41) as $n_c \to \infty$. This confirms the effective mass analysis given above.

In Fig. 4.4, we show the critical chemical potential μ_c as a function of (Δ,q) with $n_c = 1$. We see that, even when $n = 1$, it is possible for the Einstein-Maxwell black hole to be unstable. When $\mu > \mu_c$, the scalar condenses even though the only remaining defect inserted at the entangling surface is a Wilson line. As we increase q and/or decrease Δ, μ_c decreases. We note, however, that $\mu = 0$ is always stable as long as Δ is above the unitarity bound, $\Delta > 1/2$.

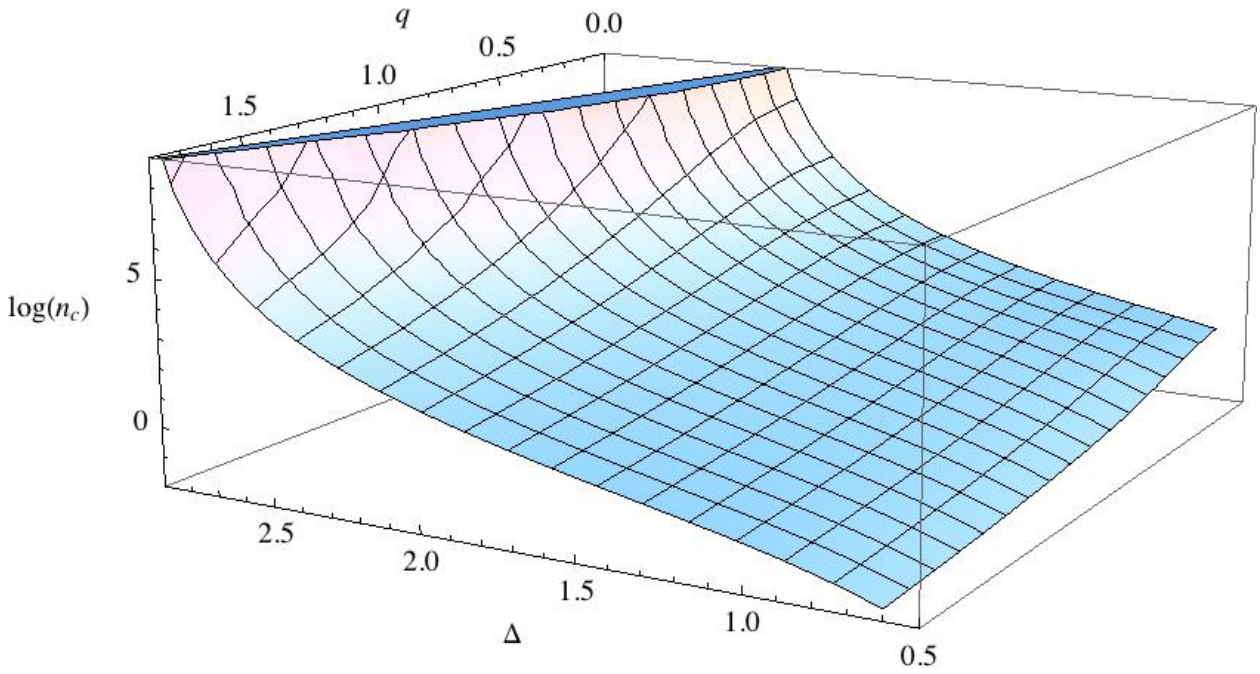

Figure 4.2: The graph of $\log n_c$ as we vary q and Δ for $\mu = 5$. Every configuration above this surface is unstable.

4.4 Discussion

We have shown that the hyperbolic charged black hole can become unstable, and investigated the onset of the instability as we vary n, μ and Δ. We now comment on our results. First, we note that for an uncharged scalar ($q = 0$), the black hole can be unstable for sufficiently small scalar mass. This is not surprising; for $\mu \neq 0$ this was already noticed in the holographic superconductor [85] for black holes with flat horizons. However, we have seen that for hyperbolic black holes increasing the chemical potential first renders the solution *more* stable until we reach a peak of stability. Beyond that point, increasing μ renders the black holes more unstable as can be seen in Fig. 4.6. This is in contrast with flat black holes, where no condensation can occur for $\mu = 0$.

In addition to the numerical method used above, one can also use a WKB method to

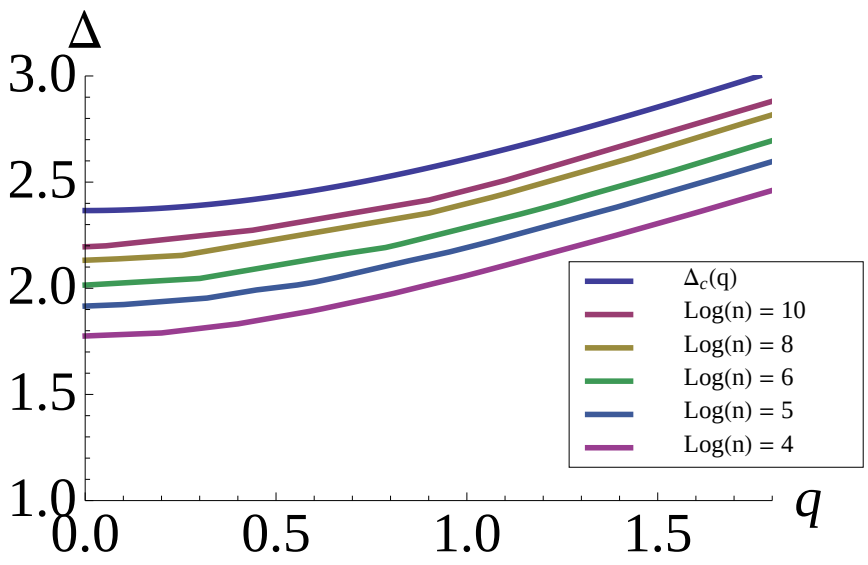

Figure 4.3: The graph of Δ as we vary q for $\mu = 5$ and different values of $\log n$. As we increase n, we get closer and closer to the analytical estimate $\Delta_c(q)$.

determine when instabilities exist and to approximate the unstable modes. We will study this in the $q = 0$ case, and use the WKB analysis to confirm the surprising behaviour described above. The number of bound states of the Schrodinger potential $V(r^*)$ can be estimated using the WKB integral:

$$N_{bound\ states} = \int \sqrt{-V(r^*)}dr^* = \int_{rh}^{r0} \frac{\sqrt{-V(r)}}{f(r)}dr \tag{4.44}$$

where we integrate from the horizon $r = r_h$ up to the zero of the potential $V(r_0) = 0$, with $r_0 > r_h$. The instability appears when $N_{bound\ states} \sim 1$. Keeping the temperature fixed and increasing μ, we find $N_{bound\ states}$ first decreases and then increases again as we increase μ. We plot of $\int \sqrt{-V(r^*)}dr^*$ against μ at $\Delta = 2$ at 10 different temperatures in Fig. 4.5 below. One can see that for a given n it decreases with μ before increasing again for sufficiently large μ, signifying that the system is more stable as μ increases at small μ, but the trend is reversed for larger values of μ. As a note of caution however, we emphasize that – in the absence of any small perturbative parameter – this WKB approximation should at best be

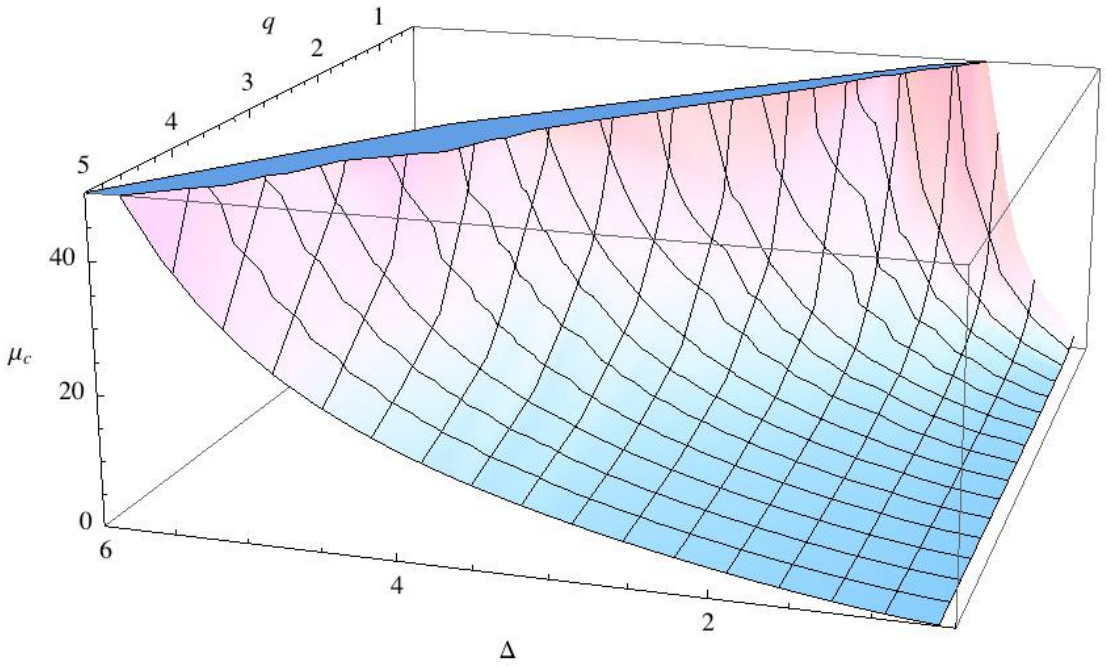

Figure 4.4: The graph of μ_c as we vary q and Δ at $n_c = 1$. Every configuration above this surface is unstable.

taken with a grain of salt, although it does reproduce the qualitative features of the numerics.

Next, we would like to comment on the large μ limit of the charged Rényi entropies. When μ becomes larger than any other scale in the problem, the critical temperature should be proportional to μ. One should note however, that the ratio T/μ remains small even in the scaling regime, meaning that the black hole continues to stay close to extremality, an observation also noted in the flatly sliced AdS charged black holes [85]. This is indeed the case as can be seen in Fig. 4.6.

It is interesting to compare the critical temperature[5] of the charged hyperbolic black hole with that of its flat counterpart – the flat holographic superconductor at finite (physical) chemical potential μ. We find a perfect match for large μ; this is to be expected, since when $\mu/R \gg 1/L$ the curvature of the horizon is small compared to the scale set by the chemical potential. This can be seen in Fig. 4.6 as well. We note that, although the gravitational

[5]We will actually compare $n_c = 1/2\pi T_c$.

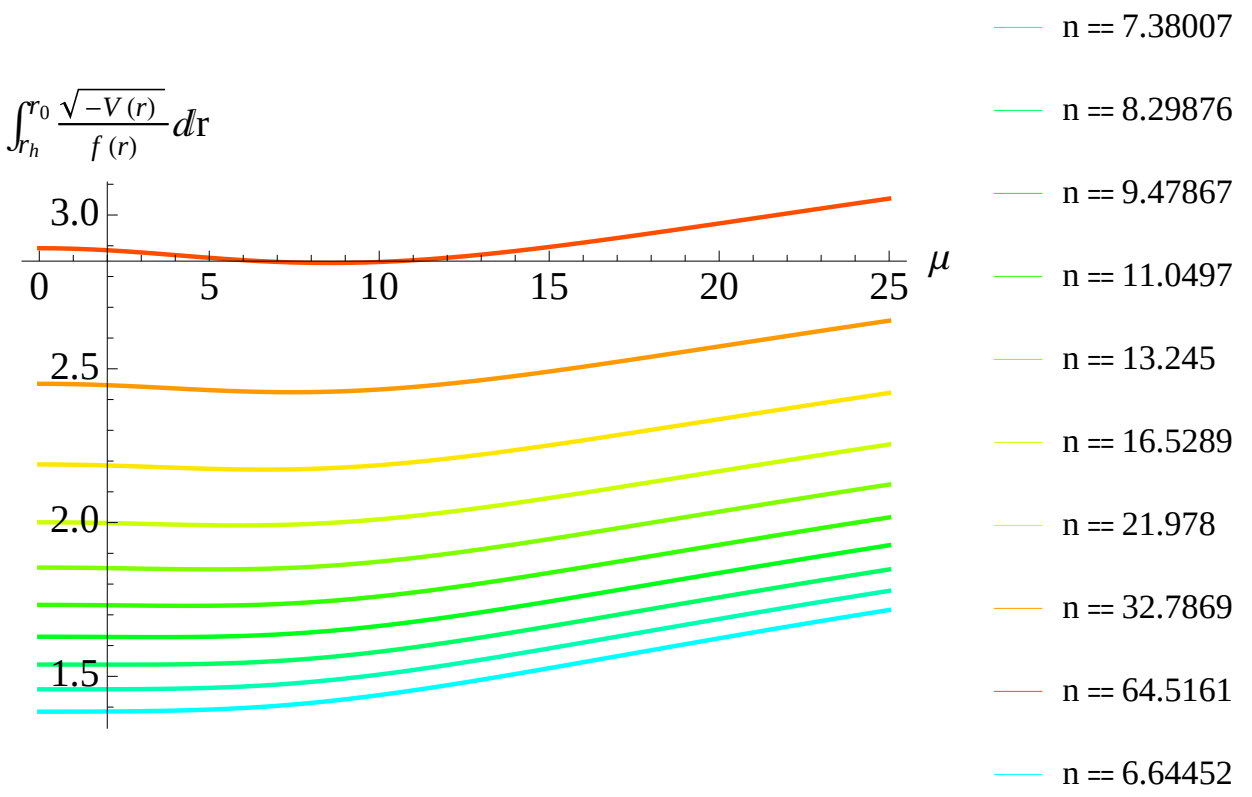

Figure 4.5: Plots of $\int_{r_h}^{r_0} \sqrt{-V(r)}/f(r)dr$ against μ at $\Delta = 2$ at 10 different temperatures.

computations for flat and hyperbolic black holes are quite similar, these quantities have very different CFT interpretations. In particular, we see that one can extract information about physical phase transitions at finite chemical potentials and temperatures (which naturally involve higher excited states) solely by considering the entanglement of the ground state.

We should comment on the difference between these two phase transitions from the CFT perspective. The superconductor lives on an infinite flat plane and boundary effects do not play any important role. However, boundary effects at the entangling surface are crucial in the phase transitions of the neutral Rényi entropies, as explained in [70]. In the phase transitions of the charged Rényi entropies, there is a qualitative difference between the neutral and the charged scalar operators. As in the case of the neutral Rényi entropies, neutral operators can be hosted on the entangling surface without breaking the $U(1)$ symmetry. Be-

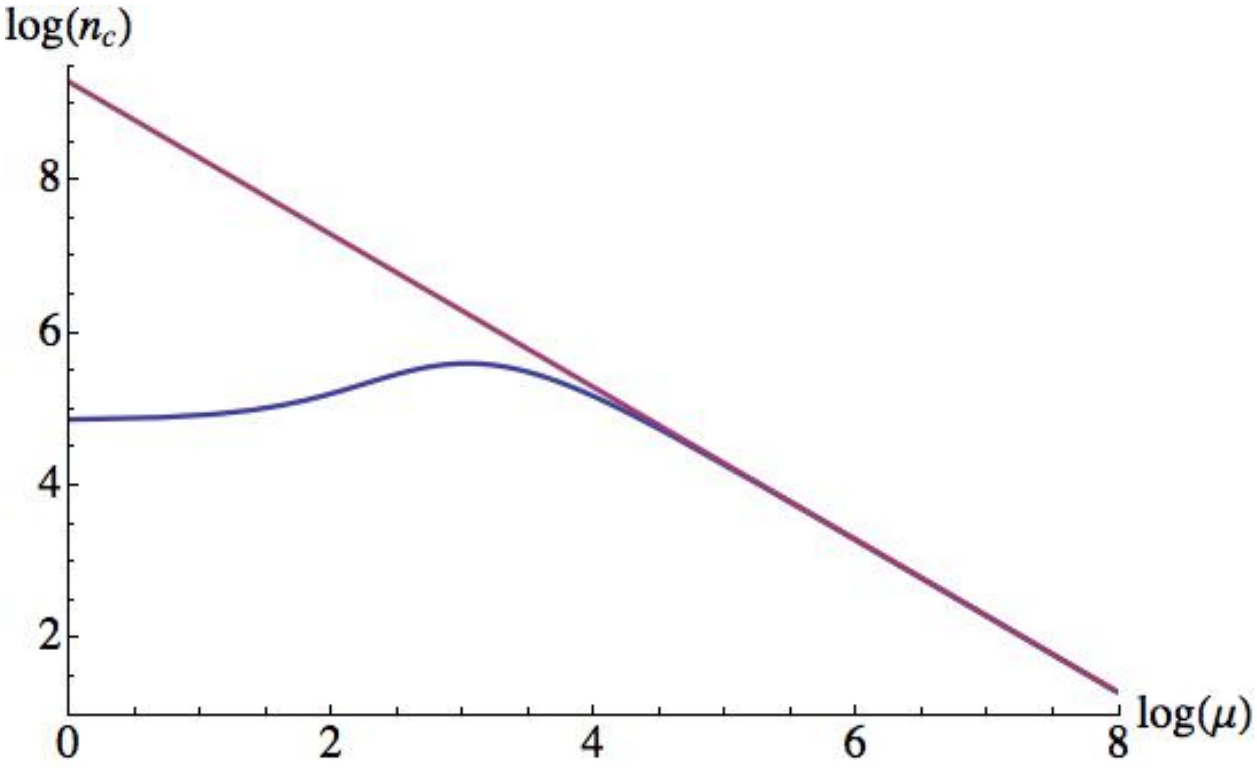

Figure 4.6: The graph of $\log n_c$ as we vary μ for $q = 0$ and $\Delta = 2$. The blue line represents the critical Rényi parameter and the red line represents the critical temperature for the field theory on flat space with physical chemical potential μ.

low the critical temperature, these localized operators induce the phase transitions. There is another instability, which is caused by the entanglement chemical potential term coupling to the entire subsystem. As in the case of the superconductors, this instability causes the scalar to condense as well[6]. These two effects may in principle compete or amplify one another. On the other hand, charged operators cannot be hosted on the entangling surface unless the $U(1)$ symmetry is spontaneously broken. Therefore, it is the entanglement chemical potential effect that causes the phase transition. This could explain the qualitative difference in the phase transitions between the $q = 0$ case and the $q \neq 0$ case (as shown in Fig.4.1). This would be interesting to investigate from the field theory point of view.

[6]Neutral scalars may condense if the conformal dimension is small enough

Let us comment also on the $n = 1$ limit. When $n = 1$ and $\mu = 0$ the conical defect operator disappears and we obtain the entanglement entropy. On the other hand, if μ is non-vanishing, then even as $n \to 1$ a defect operator – the Wilson line – remains. So a phase transition could occur even at $n \leq 1$. One might worry that a phase transition precisely at $n = 1$ would make it impossible to compute entanglement entropies as a limit of the charged Rényi entropies. However, since $\frac{\partial S_n}{\partial n}$ is still continuous (only $\frac{\partial^2 S_n}{\partial n^2}$ is discontinuous) the Rényi entropies are still smooth enough to give unique and well-defined entanglement entropies as $n \to 1$.

We note also that the Wilson line couples to the global current, so at first sight one might expect it not to effect uncharged operators. We have seen, however, that this is not the case. While uncharged operators do not directly couple to the Wilson line, they still experience its presence indirectly via couplings to other charged operators. This is manifested holographically by the fact that even neutral scalar fields in the bulk can detect changes in μ at fixed temperature indirectly, via the μ dependence of the metric.

One can also extract information about the largest eigenvalue of the charged reduced density matrix (4.11) by considering the limit $n \to \infty$. From the definition of the Rényi entropy (4.2), one can compute the eigenvalues of the charged reduced density matrix (4.11) once we know the Rényi entropy as a function of the Rényi parameter n;

$$\exp((1-n)S_n) = \int_0^{\lambda_1} d\lambda \; d(\lambda)\lambda^n \tag{4.45}$$

where λ is the eigenvalue and $d(\lambda)$ is the spectral density. λ_1 is the largest eigenvalue. In general, $d(\lambda)$ contains delta functions. In fact, if the Rényi entropy decays polynomially as $n \to \infty$, one can show that the spectral function take the following form

$$d(\lambda) = \delta(\lambda - \lambda_1)h_1(\lambda) + \Theta(\lambda - \lambda_1)h_2(\lambda), \tag{4.46}$$

where h_1 and h_2 are some functions of λ and $\Theta(\lambda - \lambda_1)$ is the Heaviside step function. There is a simple relation between the largest eigenvalue λ_1 and the $n \to \infty$ limit of the Rényi entropy (called the min-entropy)

$$S_\infty = -\log \lambda_1. \tag{4.47}$$

Below the critical temperature (when $n > n_c$) the scalar field acquires a non-zero expectation value. These hairy black holes have smaller thermal entropy than that of non-hairy black holes of the same temperature and chemical potential. Since the Rényi entropy is given by the integral of the thermal entropy (4.15), this means that the min-entropy S_∞ is always smaller than that of Einstein-Maxwell black hole

$$S_\infty(\text{Einstein-Maxwell}) > S_\infty(\text{Einstein-Maxwell-Scalar}) \tag{4.48}$$

Moreover, the critical temperature increases as one decreases the conformal dimension Δ. Therefore, as observed in [108],

$$\frac{dS_\infty(\mu, \Delta)}{d\Delta} > 0. \tag{4.49}$$

The main difference between the neutral case [108] and the charged case is that (4.49) is a strict inequality even in the case of $n_c \leq 1$, while the neutral case is not. Therefore $S_\infty(\mu, \Delta)$ is a monotonic function of Δ. The entanglement chemical potential dependence of the min-entropy is

$$\frac{dS_\infty(q \neq 0, \Delta)}{d\mu} < 0. \tag{4.50}$$

We close by recalling that the chemical potential in hyperbolic space can be interpreted as the insertion of a background Wilson line. The insertion of the Wilson line in the imaginary time direction has opposite orientation when viewed from region A as opposed to its complement B. At the same time, the ground state satisfies $S_n(A) = S_n(B)$, for all n, since the reduced density matrices of A and B have the same eigenvalues. Thus

$$S_n(\mu, A) = S_n(-\mu, B). \tag{4.51}$$

In a theory with charge conjugation invariance, this would additionally imply that $S_n(\mu, A) = S_n(-\mu, A)$, i.e. that the charged Rényi entropy is an even function of μ. This is, in particular, clearly true in the case of holographic dual of Einstein-Maxwell theory.

Acknowledgments

We are grateful to O. Dias, M. Headrick, A. Lawrence, R. Myers and A. Nicolis for useful conversations. SM acknowledges YITP, Riken, and KEK for hospitality. This research was supported by the National Science and Engineering Research Council of Canada.

Chapter 5

Discussion

In this thesis, we have discussed the analytic properties of Rényi entropies in a holographic context and showed that phase transitions in gravity translate into certain non-analyticity of the Rényi entropies in n. This addresses potential issues in the use of the replica trick and should be taken at the very least as a sign of caution in the general assumption that Rényi entropies are analytic in n. It would be interesting to understand more precisely the nature of the phase transition which is the object of some on-going work [144] as well as understand whether $1/N$ corrections render the transition smooth as in [145]. It would also be very interesting to reproduce these results from a boundary field theory calculation.

We have also introduced a new measure of entanglement that measures entanglement between different charge sectors of a theory. These charged Rényi entropies can be computed in free field theories and in strongly coupled CFTs that have a holographic dual. In the presence of a light (un)charged scalar field in the bulk, we have discussed the interesting phase structure of charged Rényi entropies as we vary the different parameters of the scalar and the entanglement chemical potential. We have used these measures of entanglement to learn about physical phase transition of systems behaving like holographic superconductors. It would be interesting to understand if one can interpret charge Rényi entropies as an entanglement of some excited state or not [146] and if so, what features does that state exhibit. It would also be very interesting to understand if one can use charged Rényi entropies

to determine Maxwell's equation in the bulk along the lines of [64, 65].

Bibliography

[1] C. Burgess and G. Moore, "The standard model," *Cambridge University Press, Cambridge* (2006) .

[2] A. Maloney and E. Witten, "Quantum Gravity Partition Functions in Three Dimensions," *JHEP* **1002** (2010) 029, arXiv:0712.0155 [hep-th].

[3] J. Bekenstein *Lett. Nuov. Cimento* **4** (1972) 737.

[4] J. Bekenstein *Phys. Rev.* **D7** (1973) 2333.

[5] J. Bekenstein *Phys. Rev.* **D9** (1974) 3292.

[6] S. Hawking *Nature* **248** (1974) 30.

[7] S. Hawking *Comm. Math. Phys.* **43** (1975) .

[8] A. Dabholkar, R. Kallosh, and A. Maloney, "A Stringy cloak for a classical singularity," *JHEP* **0412** (2004) 059, arXiv:hep-th/0410076 [hep-th].

[9] A. Strominger and C. Vafa, "Microscopic origin of the Bekenstein-Hawking entropy," *Phys.Lett.* **B379** (1996) 99–104, arXiv:hep-th/9601029 [hep-th].

[10] A. Almheiri, D. Marolf, J. Polchinski, and J. Sully, "Black Holes: Complementarity or Firewalls?," *JHEP* **1302** (2013) 062, arXiv:1207.3123 [hep-th].

[11] A. Almheiri, D. Marolf, J. Polchinski, D. Stanford, and J. Sully, "An Apologia for Firewalls," *JHEP* **1309** (2013) 018, arXiv:1304.6483 [hep-th].

[12] E. Verlinde and H. Verlinde, "Passing through the Firewall," arXiv:1306.0515 [hep-th].

[13] D. Harlow and P. Hayden, "Quantum Computation vs. Firewalls," *JHEP* **1306** (2013) 085, arXiv:1301.4504 [hep-th].

[14] K. Papadodimas and S. Raju, "Black Hole Interior in the Holographic Correspondence and the Information Paradox," *Phys.Rev.Lett.* **112** no. 5, (2014) 051301, arXiv:1310.6334 [hep-th].

[15] J. Maldacena and L. Susskind, "Cool horizons for entangled black holes," *Fortsch.Phys.* **61** (2013) 781–811, arXiv:1306.0533 [hep-th].

[16] J. M. Maldacena, "The Large N limit of superconformal field theories and supergravity," *Int.J.Theor.Phys.* **38** (1999) 1113–1133, arXiv:hep-th/9711200 [hep-th].

[17] E. Witten, "Anti-de Sitter space and holography," *Adv.Theor.Math.Phys.* **2** (1998) 253–291, arXiv:hep-th/9802150 [hep-th].

[18] O. Aharony, S. S. Gubser, J. M. Maldacena, H. Ooguri, and Y. Oz, "Large N field theories, string theory and gravity," *Phys.Rept.* **323** (2000) 183–386, arXiv:hep-th/9905111 [hep-th].

[19] E. Witten, "Anti-de Sitter space, thermal phase transition, and confinement in gauge theories," *Adv.Theor.Math.Phys.* **2** (1998) 505–532, arXiv:hep-th/9803131 [hep-th].

[20] J. L. Cardy, "Operator content of two-dimensional conformally invariant theories," *Nucl. phys. B* **270** (1986) 186.

[21] A. Strominger, "Black hole entropy from near horizon microstates," *JHEP* **9802** (1998) 009, arXiv:hep-th/9712251 [hep-th].

[22] I. R. Klebanov and E. Witten, "Superconformal field theory on three-branes at a Calabi-Yau singularity," *Nucl.Phys.* **B536** (1998) 199–218, arXiv:hep-th/9807080 [hep-th].

[23] O. Aharony, O. Bergman, D. L. Jafferis, and J. Maldacena, "N=6 superconformal Chern-Simons-matter theories, M2-branes and their gravity duals," *JHEP* **0810** (2008) 091, arXiv:0806.1218 [hep-th].

[24] M. Vasiliev, "Nonlinear equations for symmetric massless higher spin fields in (A)dS(d)," *Phys.Lett.* **B567** (2003) 139–151, arXiv:hep-th/0304049 [hep-th].

[25] M. R. Gaberdiel and R. Gopakumar, "An AdS3 Dual for Minimal Model CFTs," *Phys.Rev.* **D83** (2011) 066007, arXiv:1011.2986 [hep-th].

[26] M. R. Gaberdiel and R. Gopakumar, "Minimal Model Holography," *J.Phys.* **A46** (2013) 214002, arXiv:1207.6697 [hep-th].

[27] I. Klebanov and A. Polyakov, "AdS dual of the critical O(N) vector model," *Phys.Lett.* **B550** (2002) 213–219, arXiv:hep-th/0210114 [hep-th].

[28] E. Sezgin and P. Sundell, "Holography in 4D (super) higher spin theories and a test via cubic scalar couplings," *JHEP* **0507** (2005) 044, arXiv:hep-th/0305040 [hep-th].

[29] S. Giombi and X. Yin, "Higher Spin Gauge Theory and Holography: The Three-Point Functions," *JHEP* **1009** (2010) 115, arXiv:0912.3462 [hep-th].

[30] S. Giombi and X. Yin, "Higher Spins in AdS and Twistorial Holography," *JHEP* **1104** (2011) 086, arXiv:1004.3736 [hep-th].

[31] S. S. Gubser, "The gauge-string duality and heavy ion collisions," *Found.Phys.* **43** (2013) 140, arXiv:1103.3636 [hep-th].

[32] S. A. Hartnoll, "Lectures on holographic methods for condensed matter physics," *Class.Quant.Grav.* **26** (2009) 224002, arXiv:0903.3246 [hep-th].

[33] S. Sachdev, "Condensed Matter and AdS/CFT," *Lect.Notes Phys.* **828** (2011) 273–311, arXiv:1002.2947 [hep-th].

[34] D. Harlow, "Jerusalem Lectures on Black Holes and Quantum Information," arXiv:1409.1231 [hep-th].

[35] A. Kitaev and J. Preskill, "Topological entanglement entropy," *Phys.Rev.Lett.* **96** (2006) 110404, arXiv:hep-th/0510092 [hep-th].

[36] H. Li and F. D. M. Haldane, "Entanglement Spectrum as a Generalization of Entanglement Entropy: Identification of Topological Order in Non-Abelian Fractional Quantum Hall Effect States," *Physical Review Letters* **101** no. 1, (July, 2008) 010504, arXiv:0805.0332.

[37] M. Levin and X.-G. Wen, "Detecting topological order in a ground state wave function," *Phys. Rev. Lett.* **96** no. 110405, (2006) .

[38] M. Van Raamsdonk, "Comments on quantum gravity and entanglement," arXiv:0907.2939 [hep-th].

[39] M. Van Raamsdonk, "Building up spacetime with quantum entanglement," *Gen.Rel.Grav.* **42** (2010) 2323–2329, arXiv:1005.3035 [hep-th].

[40] E. Bianchi and R. C. Myers, "On the Architecture of Spacetime Geometry," *Class.Quant.Grav.* **31** no. 21, (2014) 214002, arXiv:1212.5183 [hep-th].

[41] R. C. Myers, R. Pourhasan, and M. Smolkin, "On Spacetime Entanglement," *JHEP* **1306** (2013) 013, arXiv:1304.2030 [hep-th].

[42] V. Balasubramanian, B. Czech, B. D. Chowdhury, and J. de Boer, "The entropy of a hole in spacetime," *JHEP* **1310** (2013) 220, arXiv:1305.0856 [hep-th].

[43] J. Callan, Curtis G. and F. Wilczek, "On geometric entropy," *Phys.Lett.* **B333** (1994) 55–61, arXiv:hep-th/9401072 [hep-th].

[44] C. Holzhey, F. Larsen, and F. Wilczek, "Geometric and renormalized entropy in conformal field theory," *Nucl.Phys.* **B424** (1994) 443–467, arXiv:hep-th/9403108 [hep-th].

[45] D. N. Kabat and M. Strassler, "A Comment on entropy and area," *Phys.Lett.* **B329** (1994) 46–52, arXiv:hep-th/9401125 [hep-th].

[46] P. Calabrese and J. Cardy, "Entanglement entropy and conformal field theory," *Journal of Physics A Mathematical General* **42** (Dec., 2009) 4005, arXiv:0905.4013 [cond-mat.stat-mech].

[47] P. Calabrese and J. L. Cardy, "Entanglement entropy and quantum field theory," *J.Stat.Mech.* **0406** (2004) P06002, arXiv:hep-th/0405152 [hep-th].

[48] P. Calabrese and J. L. Cardy, "Entanglement entropy and quantum field theory: A Non-technical introduction," *Int.J.Quant.Inf.* **4** (2006) 429, arXiv:quant-ph/0505193 [quant-ph].

[49] S. Ryu and T. Takayanagi, "Holographic derivation of entanglement entropy from AdS/CFT," *Phys.Rev.Lett.* **96** (2006) 181602, arXiv:hep-th/0603001 [hep-th].

[50] D. V. Fursaev, "Temperature and entropy of a quantum black hole and conformal anomaly," *Phys.Rev.* **D51** (1995) 5352–5355, arXiv:hep-th/9412161 [hep-th].

[51] A. Sen, "Logarithmic Corrections to Schwarzschild and Other Non-extremal Black Hole Entropy in Different Dimensions," *JHEP* **1304** (2013) 156, arXiv:1205.0971 [hep-th].

[52] S. N. Solodukhin, "Entanglement entropy of black holes," *Living Rev.Rel.* **14** (2011) 8, arXiv:1104.3712 [hep-th].

[53] L. McGough and H. Verlinde, "Bekenstein-Hawking Entropy as Topological Entanglement Entropy," *JHEP* **1311** (2013) 208, arXiv:1308.2342 [hep-th].

[54] J. M. Maldacena, "Eternal black holes in anti-de Sitter," *JHEP* **0304** (2003) 021, arXiv:hep-th/0106112 [hep-th].

[55] F. M. Haehl, T. Hartman, D. Marolf, H. Maxfield, and M. Rangamani, "Topological aspects of generalized gravitational entropy," arXiv:1412.7561 [hep-th].

[56] T. Faulkner, A. Lewkowycz, and J. Maldacena, "Quantum corrections to holographic entanglement entropy," *JHEP* **1311** (2013) 074, arXiv:1307.2892.

[57] T. Barrella, X. Dong, S. A. Hartnoll, and V. L. Martin, "Holographic entanglement beyond classical gravity," *JHEP* **1309** (2013) 109, arXiv:1306.4682 [hep-th].

[58] X. Dong, "Holographic Entanglement Entropy for General Higher Derivative Gravity," *JHEP* **1401** (2014) 044, arXiv:1310.5713 [hep-th].

[59] B. Swingle, "Entanglement renormalization and holography," *Phys. Rev. D* **86** no. 6, (Sept., 2012) 065007, arXiv:0905.1317 [cond-mat.str-el].

[60] R. C. Myers, J. Rao, and S. Sugishita, "Holographic Holes in Higher Dimensions," *JHEP* **1406** (2014) 044, arXiv:1403.3416 [hep-th].

[61] V. Balasubramanian, B. D. Chowdhury, B. Czech, J. de Boer, and M. P. Heller, "A hole-ographic spacetime," *Phys.Rev.* **D89** (2014) 086004, arXiv:1310.4204 [hep-th].

[62] M. Headrick, R. C. Myers, and J. Wien, "Holographic Holes and Differential Entropy," *JHEP* **1410** (2014) 149, arXiv:1408.4770 [hep-th].

[63] B. Czech, P. Hayden, N. Lashkari, and B. Swingle, "The Information Theoretic Interpretation of the Length of a Curve," arXiv:1410.1540 [hep-th].

[64] N. Lashkari, M. B. McDermott, and M. Van Raamsdonk, "Gravitational dynamics from entanglement 'thermodynamics'," *JHEP* **1404** (2014) 195, arXiv:1308.3716 [hep-th].

[65] T. Faulkner, M. Guica, T. Hartman, R. C. Myers, and M. Van Raamsdonk, "Gravitation from Entanglement in Holographic CFTs," *JHEP* **1403** (2014) 051, arXiv:1312.7856 [hep-th].

[66] A. Lewkowycz and J. Maldacena, "Generalized gravitational entropy," *JHEP* **1308** (2013) 090, arXiv:1304.4926 [hep-th].

[67] H. Casini, M. Huerta, and R. C. Myers, "Towards a derivation of holographic entanglement entropy," *JHEP* **1105** (2011) 036, arXiv:1102.0440 [hep-th].

[68] L.-Y. Hung, R. C. Myers, M. Smolkin, and A. Yale, "Holographic Calculations of Renyi Entropy," *JHEP* **1112** (2011) 047, arXiv:1110.1084 [hep-th].

[69] L.-Y. Hung, R. C. Myers, and M. Smolkin, "Twist operators in higher dimensions," *JHEP* **1410** (2014) 178, arXiv:1407.6429 [hep-th].

[70] M. A. Metlitski, C. A. Fuertes, and S. Sachdev, "Entanglement entropy in the O(N) model," *Phys. Rev. B* **80** no. 11, (Sept., 2009) 115122, arXiv:0904.4477 [cond-mat.stat-mech].

[71] J.-M. Stéphan, G. Misguich, and V. Pasquier, "Phase transition in the rényi-shannon entropy of luttinger liquids," *Phys. Rev. B* **84** no. 19, (2011) 195128.

[72] S. Ryu and T. Takayanagi, "Aspects of Holographic Entanglement Entropy," *JHEP* **0608** (2006) 045, arXiv:hep-th/0605073 [hep-th].

[73] T. Nishioka, S. Ryu, and T. Takayanagi, "Holographic Entanglement Entropy: An Overview," *J.Phys.* **A42** (2009) 504008, arXiv:0905.0932 [hep-th].

[74] A. Rényi, "On measures of information and entropy," *Proceedings of the 4th Berkeley Symposium on Mathematics, Statistics and Probability* **1** (U. of California Press, Berkeley, CA, 1961) 547.

[75] K. Zyczkowski, "Renyi extrapolation of Shannon entropy," *eprint arXiv:quant-ph/0305062* (May, 2003) , quant-ph/0305062.

[76] M. B. Hastings, I. González, A. B. Kallin, and R. G. Melko, "Measuring Renyi Entanglement Entropy in Quantum Monte Carlo Simulations," *Physical Review Letters* **104** no. 15, (Apr., 2010) 157201, arXiv:1001.2335 [cond-mat.str-el].

[77] P. Calabrese and A. Lefevre, "Entanglement spectrum in one-dimensional systems," *Phys. Rev. A* **78** no. 032329, (2008) .

[78] I. R. Klebanov, S. S. Pufu, S. Sachdev, and B. R. Safdi, "Renyi Entropies for Free Field Theories," *JHEP* **1204** (2012) 074, arXiv:1111.6290 [hep-th].

[79] M. Headrick, "Entanglement Renyi entropies in holographic theories," *Phys.Rev.* **D82** (2010) 126010, arXiv:1006.0047 [hep-th].

[80] T. Faulkner, "The Entanglement Renyi Entropies of Disjoint Intervals in AdS/CFT," arXiv:1303.7221 [hep-th].

[81] D. Fursaev, "Entanglement Renyi Entropies in Conformal Field Theories and Holography," *JHEP* **1205** (2012) 080, arXiv:1201.1702 [hep-th].

[82] D. A. Galante and R. C. Myers, "Holographic Renyi entropies at finite coupling," *JHEP* **1308** (2013) 063, arXiv:1305.7191 [hep-th].

[83] O. J. Dias, R. Monteiro, H. S. Reall, and J. E. Santos, "A Scalar field condensation instability of rotating anti-de Sitter black holes," *JHEP* **1011** (2010) 036, arXiv:1007.3745 [hep-th].

[84] S. A. Hartnoll, C. P. Herzog, and G. T. Horowitz, "Building a Holographic Superconductor," *Phys.Rev.Lett.* **101** (2008) 031601, arXiv:0803.3295 [hep-th].

[85] S. A. Hartnoll, C. P. Herzog, and G. T. Horowitz, "Holographic Superconductors," *JHEP* **0812** (2008) 015, arXiv:0810.1563 [hep-th].

[86] S. S. Gubser, "Colorful horizons with charge in anti-de Sitter space," *Phys.Rev.Lett.* **101** (2008) 191601, arXiv:0803.3483 [hep-th].

[87] A. Belin and A. Maloney, "A New Instability of the Topological black hole," arXiv:1412.0280 [hep-th].

[88] A. Belin, L.-Y. Hung, A. Maloney, S. Matsuura, R. C. Myers, *et al.*, "Holographic Charged Renyi Entropies," *JHEP* **1312** (2013) 059, arXiv:1310.4180 [hep-th].

[89] A. Lewkowycz and E. Perlmutter, "Universality in the geometric dependence of Renyi entropy," arXiv:1407.8171 [hep-th].

[90] A. Rényi, "On the foundations of information theory," *Rev. Int. Stat. Inst.* **33** (19861) .

[91] C. Beck and F. Schlögl, "Thermodynamics of chaotic systems," *Cambridge University Press, Cambridge,* (1993) .

[92] G. Wong, I. Klich, L. A. Pando Zayas, and D. Vaman, "Entanglement Temperature and Entanglement Entropy of Excited States," *JHEP* **1312** (2013) 020, arXiv:1305.3291 [hep-th].

[93] P. Caputa, G. Mandal, and R. Sinha, "Dynamical entanglement entropy with angular momentum and U(1) charge," *JHEP* **1311** (2013) 052, arXiv:1306.4974 [hep-th].

[94] T. Nishioka and I. Yaakov, "Supersymmetric renyi entropy," *JHEP* **1310** (2013) 155, arXiv:1306.2958 [hep-th].

[95] H. Casini, "Entropy inequalities from reflection positivity," *J.Stat.Mech.* **1008** (2010) P08019, arXiv:1004.4599 [quant-ph].

[96] B. Swingle, "Mutual information and the structure of entanglement in quantum field theory," arXiv:1010.4038 [quant-ph].

[97] A. Roberge and N. Weiss, "Gauge theories with imaginary chemical potential and the phases of qcd," *Nucl. Phys. B* **275** (1986) 734.

[98] M. G. Alford, A. Kapustin, and F. Wilczek, "Imaginary chemical potential and finite fermion density on the lattice," *Phys.Rev.* **D59** (1999) 054502, arXiv:hep-lat/9807039 [hep-lat].

[99] E. Witten, "Constraints on Supersymmetry Breaking," *Nucl.Phys.* **B202** (1982) 253.

[100] R. C. Myers and A. Sinha, "Seeing a c-theorem with holography," *Phys.Rev.* **D82** (2010) 046006, arXiv:1006.1263 [hep-th].

[101] R. C. Myers and A. Sinha, "Holographic c-theorems in arbitrary dimensions," *JHEP* **1101** (2011) 125, arXiv:1011.5819 [hep-th].

[102] E. Perlmutter, "A universal feature of cft renyi entropy," *JHEP* **1403** (2014) 117, arXiv:1308.1083 [hep-th].

[103] H. Osborn and A. Petkou, "Implications of conformal invariance in field theories for general dimensions," *Annals Phys.* **231** (1994) 311–362, arXiv:hep-th/9307010 [hep-th].

[104] T. Takayanagi, "unpublished,".

[105] H. Casini and M. Huerta, "Entanglement entropy in free quantum field theory," *J.Phys.* **A42** (2009) 504007, arXiv:0905.2562 [hep-th].

[106] H. Casini, C. D. Fosco, and M. Huerta, "Entanglement and alpha entropies for a massive Dirac field in two dimensions," *Journal of Statistical Mechanics: Theory and Experiment* **7** (July, 2005) 7, cond-mat/0505563.

[107] T. Azeyanagi, T. Nishioka, and T. Takayanagi, "Near Extremal Black Hole Entropy as Entanglement Entropy via AdS(2)/CFT(1)," *Phys.Rev.* **D77** (2008) 064005, arXiv:0710.2956 [hep-th].

[108] A. Belin, A. Maloney, and S. Matsuura, "Holographic Phases of Renyi Entropies," *JHEP* **1312** (2013) 050, arXiv:1306.2640 [hep-th].

[109] R.-G. Cai and A. Wang, "Thermodynamics and stability of hyperbolic charged black holes," *Phys.Rev.* **D70** (2004) 064013, arXiv:hep-th/0406057 [hep-th].

[110] M. Cvetic, S. Nojiri, and S. D. Odintsov, "Black hole thermodynamics and negative entropy in de Sitter and anti-de Sitter Einstein-Gauss-Bonnet gravity," *Nucl.Phys.* **B628** (2002) 295–330, arXiv:hep-th/0112045 [hep-th].

[111] X.-H. Ge, Y. Matsuo, F.-W. Shu, S.-J. Sin, and T. Tsukioka, "Viscosity Bound, Causality Violation and Instability with Stringy Correction and Charge," *JHEP* **0810** (2008) 009, arXiv:0808.2354 [hep-th].

[112] D. Anninos and G. Pastras, "Thermodynamics of the Maxwell-Gauss-Bonnet anti-de Sitter Black Hole with Higher Derivative Gauge Corrections," *JHEP* **0907** (2009) 030, arXiv:0807.3478 [hep-th].

[113] A. Belin, A. Maloney, S. Matsuura, R. C. Myers, T. Sierens, and L.-Y. Hung, "Holographic rotating rényi entropies," *In preparation* .

[114] A. Grigor'yan and M. Noguchi, "The heat kernet on hyperbolic space," *Bull. London Math. Soc.* **30** (1998) 643.

[115] A. Grigor'yan, "Upper bounds on a complete non compact manifold," *J. Funct. Anal.* **127** (1995) 363.

[116] E. M. A. Debiard, B. Gaveau, "Theoreme de comparison in geometrie rimannienne," *Publ. Res. Inst. Math. Sci. Kyoto* **12** (1976) 391.

[117] R. Camporesi and A. Higuchi, "Spectral functions and zeta functions in hyperbolic spaces," *J. Math. Phys.* **35** (1994) 4217.

[118] R. Camporesi *Commun. Math. Phys.* **148** (1992) 283.

[119] R. Camporesi, "Harmonic analysis and propagators on homogeneous spaces," *Phys. Rept.* **196** (1990) 1.

[120] R. Camporesi, "The spinor heat kernel in maximally symmetric spaces," *Commun. Math. Phys.* **148** (1992) 283.

[121] C. Martinez, C. Teitelboim, and J. Zanelli, "Charged rotating black hole in three space-time dimensions," *Phys.Rev.* **D61** (2000) 104013, arXiv:hep-th/9912259 [hep-th].

[122] I. R. Klebanov and E. Witten, "AdS / CFT correspondence and symmetry breaking," *Nucl.Phys.* **B556** (1999) 89–114, arXiv:hep-th/9905104 [hep-th].

[123] L.-Y. Hung and A. Sinha, "Holographic quantum liquids in 1+1 dimensions," *JHEP* **1001** (2010) 114, arXiv:0909.3526 [hep-th].

[124] A. Ejaz, H. Gohar, H. Lin, K. Saifullah, and S.-T. Yau, "Quantum tunneling from three-dimensional black holes," *Phys.Lett.* **B726** (2013) 827–833, arXiv:1306.6380 [hep-th].

[125] P. Kraus, "Lectures on black holes and the AdS(3) / CFT(2) correspondence," *Lect.Notes Phys.* **755** (2008) 193–247, arXiv:hep-th/0609074 [hep-th].

[126] V. Balasubramanian and P. Kraus, "A Stress tensor for Anti-de Sitter gravity," *Commun.Math.Phys.* **208** (1999) 413–428, arXiv:hep-th/9902121 [hep-th].

[127] R. Emparan, C. V. Johnson, and R. C. Myers, "Surface terms as counterterms in the AdS / CFT correspondence," *Phys.Rev.* **D60** (1999) 104001, arXiv:hep-th/9903238 [hep-th].

[128] J. D. Brown and J. York, James W., "Quasilocal energy and conserved charges derived from the gravitational action," *Phys.Rev.* **D47** (1993) 1407–1419, arXiv:gr-qc/9209012 [gr-qc].

[129] R. C. Myers, "Stress tensors and Casimir energies in the AdS / CFT correspondence," *Phys.Rev.* **D60** (1999) 046002, arXiv:hep-th/9903203 [hep-th].

[130] D. M. Hofman and J. Maldacena, "Conformal collider physics: Energy and charge correlations," *JHEP* **0805** (2008) 012, arXiv:0803.1467 [hep-th].

[131] D. Chowdhury, S. Raju, S. Sachdev, A. Singh, and P. Strack, "Multipoint correlators of conformal field theories: implications for quantum critical transport," *Phys. Rev. B* **87** (2013) 085138, 1210.5247 [hep-th].

[132] A. Buchel, J. Escobedo, R. C. Myers, M. F. Paulos, A. Sinha, *et al.*, "Holographic GB gravity in arbitrary dimensions," *JHEP* **1003** (2010) 111, arXiv:0911.4257 [hep-th].

[133] A. Hamma, R. Ionicioiu, and P. Zanardi, "Ground state entanglement and geometric entropy in the Kitaev model [rapid communication]," *Physics Letters A* **337** (Mar., 2005) 22–28, quant-ph/0406202.

[134] T. Takayanagi, "Entanglement Entropy from a Holographic Viewpoint," *Class.Quant.Grav.* **29** (2012) 153001, arXiv:1204.2450 [gr-qc].

[135] R. Horodecki, P. Horodecki, M. Horodecki, and K. Horodecki, "Quantum entanglement," *Rev.Mod.Phys.* **81** (2009) 865–942, arXiv:quant-ph/0702225 [quant-ph].

[136] T. Nishioka, "The Gravity Dual of Supersymmetric Renyi Entropy," *JHEP* **1407** (2014) 061, arXiv:1401.6764 [hep-th].

[137] L.-Y. Hung, S. Ryu, S. Matsuura, and X.-G. Wen, "Charged topological entanglement entropy," *To appear* (2015) .

[138] G. Pastras and D. Manolopoulos, "Charged Renyi entropies in CFTs with Einstein-Gauss-Bonnet holographic duals," *JHEP* **1411** (2014) 007, arXiv:1404.1309 [hep-th].

[139] S. S. Gubser, "Breaking an Abelian gauge symmetry near a black hole horizon," *Phys.Rev.* **D78** (2008) 065034, arXiv:0801.2977 [hep-th].

[140] T. H. Hsieh and L. Fu, "Bulk Entanglement Spectrum Reveals Quantum Criticality within a Topological State," *Physical Review Letters* **113** no. 10, (Sept., 2014) 106801, arXiv:1305.1949 [cond-mat.str-el].

[141] C. Martinez, R. Troncoso, and J. Zanelli, "Exact black hole solution with a minimally coupled scalar field," *Phys.Rev.* **D70** (2004) 084035, arXiv:hep-th/0406111 [hep-th].

[142] S. S. Gubser and I. Mitra, "Instability of charged black holes in Anti-de Sitter space," arXiv:hep-th/0009126 [hep-th].

[143] S. S. Gubser and I. Mitra, "The Evolution of unstable black holes in anti-de Sitter space," *JHEP* **0108** (2001) 018, arXiv:hep-th/0011127 [hep-th].

[144] A. Belin, X. Dong, and A. Maloney, "work in progress,".

[145] D. Anninos, S. A. Hartnoll, and N. Iqbal, "Holography and the Coleman-Mermin-Wagner theorem," *Phys.Rev.* **D82** (2010) 066008, arXiv:1005.1973 [hep-th].

[146] A. Belin, R. C. Myers, and T. Sierens, "work in progress,".